Supplement B to "Evaluated kinetic and photochemical data for atmospheric chemistry: Volume VII - Criegee intermediates":

Detailed data sheets for the thermal and photochemical reactions of stabilized Criegee intermediates, prepared by the IUPAC Task Group on Atmospheric Chemical Kinetic Data Evaluation. The data sheets are also available at http://iupac.pole-ether.fr/ (access date: May 2020), where a guide to data sheet format and evalution methods is also provided.

Contents

B1. Data sheets for thermal reactions of C_1 species

CGI_1: $CH_2OO + SO_2$

Last evaluated: May 2020; Last change in preferred values: May 2020

$CH_2OO + SO_2 \rightarrow$ products

Rate coefficient data

k/cm^3 molecule^{-1} s^{-1}	Temp./K	Reference	Technique/Comments
Absolute Rate Coefficients			
$(3.9 \pm 0.7) \times 10^{-11}$	298	Welz et al., 2012	PLP-PIMS(a)
$(4.1 \pm 0.3) \times 10^{-11}$	295	Sheps, 2013	PLP-UVA (b)
$(3.42 \pm 0.42) \times 10^{-11}$	295	Stone et al., 2014	PLP-LIF/PIMS (c)
$(3.80 \pm 0.04) \times 10^{-11}$	293	Chhantyal-Pun et al., 2015	PLP-CRDS (d)
$(3.64 \pm 0.10) \times 10^{-11}$ (51 Torr)	295	Liu et al., 2014	PLP-LIF(e)
$(3.37 \pm 0.25) \times 10^{-11}$ (100 Torr)			
$(3.43 \pm 0.09) \times 10^{-11}$ (152 Torr)			
$(3.44 \pm 0.15) \times 10^{-11}$ (200 Torr)			
$(3.52 \pm 0.11) \times 10^{-11}$ (30.1 Torr)	298	Huang et al., 2015	PLP-UVA (f)
$(3.57 \pm 0.02) \times 10^{-11}$ (100.2 Torr)			
$(3.70 \pm 0.09) \times 10^{-11}$ (199.7 Torr)			
$(3.30 \pm 0.15) \times 10^{-11}$ (755.6 Torr)			
$(3.3 \pm 0.9) \times 10^{-11}$	295	Berndt et al., 2017	Free-Jet FR-CIMS (g)
$(3.74 \pm 0.43) \times 10^{-11}$	295	Howes et al., 2018	PLP-PIMS (h)
$(3.87 \pm 0.45) \times 10^{-11}$	295		PLP-UVA (h)
$(3.6 \pm 0.1) \times 10^{-11}$	295	Qiu and Tonokura, 2019	PLP-IR (i)

Comments

(a) CH_2OO was produced by the reaction of $CH_2I + O_2$. CH_2I was generated by 248-nm laser photolysis of diiodomethane, CH_2I_2, at 298 K and 4 torr total pressure in a large excess of O_2. The reacting mixture was monitored by tunable synchrotron photoionization mass spectrometry, which allowed characterisation of the PIMS for CH_2OO and its reaction products over the region 9.5 – 11.5 eV, and time-resolved direct detection of CH_2OO at m/z = 46 amu. The first order decay CH_2OO in the presence of excess known concentrations of SO_2 was used to determine the rate constants. The uncertainty limits are 95 %, based on unweighted linear fit of [SO_2] dependence of decay lifetimes.

(b) CH_2OO prepared by PLP (266 nm) of CH_2I_2 in O_2/Ar mixtures at 5.1 Torr pressure. CH_2OO kinetics observed by time-resolved UV absorption in the $\tilde{B}$ (1A′) ← $\tilde{X}$(1A′) electronic spectrum in presence of excess SO_2.

(c) Photolysis of CH_2I_2-O_2-N_2 mixtures. in the presence of excess SO_2, under pseudo-first-order conditions. Kinetics of $CH_2OO + SO_2$ reaction were followed by time-resolved monitoring of HCHO products by laser-induced fluorescence (LIF) spectroscopy (pressure range: 50 – 450 Torr), and also by direct detection of CH_2OO by photo-ionisation mass spectrometry (PIMS) at 1.5 Torr pressure. Rate coefficients for $CH_2OO + SO_2$ were independent of pressure between 1.5 - 450 Torr, and cited values of k are average values in this range. The uncertainty limits are 1σ errors from fitting data.

(d) Cavity ring-down spectroscopy was used to perform kinetic measurements at 293 K under low pressure (7 to 30 Torr) conditions, for reactions of CH_2OO generated by (248 nm) laser photolysis of CH_2I_2 in the presence of O_2. The cited *k* value for the $CH_2OO + SO_2$ reaction was determined from pseudo first order decay constants, obtained by fitting decay curves at different [SO_2], accounting for contribution from self-reaction of CH_2OO and unimolecular decay. *k* was independent of pressure up to 30 Torr. An upper limit for the unimolecular CH_2OO loss rate coefficient of (11.6 ± 8.0) s^{-1} was deduced from the analysis. An SO_2 catalysed CH_2OO isomerization or intersystem crossing is proposed to occur with a rate coefficient of (3.53 ± 0.32) × 10^{-11} cm^3 $molecule^{-1}$ s^{-1}.

(e) CH_2OO generated by 351nm laser flash photolysis of CH_2I/O_2 mixtures is accompanied by significant amounts of HO, observed by time resolved LIF. At least two different processes formed HO; a second, slower process appeared to be associated with the decay of CH_2OO. Using the HO signals as a proxy for the [CH_2OO] concentration in the presence of excess SO_2 the rate constant for the reaction of SO_2 with CH_2OO could be determined under pseudo first order conditions. *k* showed no pressure dependence over the range of 50−200 Torr, the average value was (3.53 ± 0.29) × 10^{-11} cm^3 $molecule^{-1}$ s^{-1}.

(f) CH_2OO prepared by PLP (266 nm) of CH_2I_2 in O_2/N_2 mixtures at 30 - 755 Torr total pressure and 298 K. CH_2OO kinetics observed by time-resolved UV absorption spectrum in the $\tilde{B}$ (1A′) ← $\tilde{X}$(1A′) electronic transition in presence of excess SO_2. CH_2OO was monitored by UV absorption at 340 nm, corresponding to the maximum in the $\tilde{B}$ (1A′) ← $\tilde{X}$(1A′) electronic transition. A mean value of $k = (3.56 \pm 0.11) \times 10^{-11}$ cm^3 $molecule^{-1}$ s^{-1}, was reported, with no significant pressure dependence of *k* in the experimental pressure range.

(g) CH_2OO (formaldehyde oxide) was produced by the $O_3 + C_2H_4$ reaction in air in a free-jet flow reactor at 1 bar and 295 ± 2 K. CH_2OO was detected as $CH_2OO\text{-}H^+$ using CI-APi-TOF mass spectrometry. *k* was determined from the relative suppression of the steady state concentration of the protonated species as a function of [SO_2].

(h) CH_2OO generated by laser flash photolysis (LF) of CH_2I_2/O_2 and its concentration monitored by photoionization mass spectrometry (PIMS). PIMS has been used to determine the rate coefficient for the reaction of CH_2OO with SO_2 at 295 K and 2 Torr (He). Additional LFP experiments were performed monitoring CH_2OO by time resolved broadband UV absorption spectroscopy at 295 K and 50 Torr (N_2). The rate coefficients determined at 295 ± 2 K in both experimental systems are in excellent agreement.

(i) CH_2OO was produced by the 266 nm laser photolysis of $CH_2I_2\text{-}O_2\text{-}N_2$ mixtures at 295 ± 3 K and 7.7 Torr. The time-resolved decay kinetics of CH_2OO were followed by mid-IR continuous-wave quantum cascade laser spectroscopy in the ν_4 band at 1274 cm^{-1}, under pseudo-first order conditions in the presence of excess [SO_2]. The tabulated value of *k* was determined from the dependence of the first-order decay constant on [SO_2].

Preferred Values

Parameter	Value	T/K
k /cm^3 $molecule^{-1}$ s^{-1}	3.7×10^{-11}	298
Reliability		
$\Delta \log k$	± 0.05	298

Comments on Preferred Values

The efficient and rapid production of CH_2OO in the photolysis of CH_2I_2/O_2 mixtures has been shown to be due to the reaction of CH_2I photofragment with O_2. The results from several laboratories using different spectroscopic techniques, including use of HO-LIF as a spectroscopic marker (Liu et al., 2014), to detect and make time-resolved measurements of decay of [CH_2OO], or use of LIF (Stone et al, 2014) to follow formation of product HCHO, are in good agreement. The rate constants for CH_2OO reaction with SO_2 show no significant pressure dependence over the range 3 to 1000 mbar (Huang et al., 2015). The rate coefficient is much larger than was deduced from earlier relative rate studies (e.g. see Johnson and Marston, 2008). Although the temperature dependence has not been investigated it is likely to be close to zero. The recommended temperature and pressure independent value of *k* is an unweighted mean of the values reported by Welz et al. (2012), Sheps (2013), Liu et al. (2014), Stone et al. (2014), Chhantyal-Pun et al. (2015) (excluding the low [SO_2] results), Huang et al. (2015), Howes et al. (2018) and Qiu and Tonokura (2019).

All these studies utilized the same photochemical source of CH_2OO. This source provides a high yield of stabilised CH_2OO and has been well characterized (Welz et al., 2012; Stone et al., 2013; Chhantyal-Pun et al., 2015). The less direct determination of Berndt et al. (2017), using the ethene + O_3 reaction as the CH_2OO source, and reported relative rate studies (Berndt et al., 2014; Newland et al., 2015), all yield results for the kinetics that are consistent with the direct laser photolysis measurements of *k*. Thus, the recommendation is valid for application in atmospheric modelling of CH_2OO reactions produced in ozone + alkene reactions.

Cox and Penkett (1972) proposed that oxidation of SO_2 to H_2SO_4 aerosols in the presence of ozone + alkene, occurred as a result of its reaction with carbonyl oxide (Criegee) intermediates to form SO_3 molecules, which then reacted with water to produce H_2SO_4 aerosol particles. Many experimental studies of ozone + alkene reactions have subsequently confirmed the importance of this process, and it is generally assumed that the CH_2OO + SO_2 reaction predominantly forms HCHO + SO_3. The theoretical investigation of Vereecken et al. (2012) re-examined the potential energy surface of the reaction, explicitly examining the open shell biradical structures than can be formed following barrierless formation of a chemically-activated secondary ozonide in the initial CH_2OO + SO_2 encounter. The subsequent mechanism involved rearrangement to a singlet biradical intermediate, $HC(O)OS(O)O^{\cdot}$. Under atmospheric conditions, this was calculated to dissociate mainly to form HCHO + SO_3 (68 %), this being the dissociation channel with the lowest barrier. Alternative channels involving formation of SO_2 and a bis-oxy diradical, $CH_2(O^{\cdot})O^{\cdot}$ (17 %), and H-elimination to form the very stable formylsulfinic acid, HC(=O)OS(=O)OH (15 %), were also calculated for atmospheric conditions, using RRKM methods. The results are consistent with reported product observations, i.e. formation of HCHO and/or SO_3, (Welz et al., 2012; Stone et al., 2014), regeneration of SO_2 with an oxygen exchange between the sCI and SO_2 moieties (Hatakeyama et al., 1984, 1986), and kinetic anomalies at high [SO_2], (Chhantyal-Pun et al., 2015). Until quantitative experimental product channel data become available, we recommend that the reaction predominantly forms HCHO and SO_3.

References

Berndt, T., Voigtlander, J., Stratmann, F., Junninen, H., Mauldin III, R.L., Sipila, M., Kulmala,. M., and Herrmann, H.: Phys. Chem. Chem. Phys., 16, 19130, 2014.

Chhantyal-Pun, R., Davey, A., Shallcross, D.E., Percival, C.J., Orr-Ewing, A.J.: Phys. Chem. Chem. Phys., 17, 3617, 2015.

Cox, R. A. and Penkett, S. A.: J. Chem. Soc., Faraday Trans. 1, 68, 1735, 1972.

Hatakeyama, S., Kobayashi, H. and Akimoto, H.: J. Phys. Chem., 88, 4736, 1984.

Hatakeyama, S., Kobayashi, H., Lin, Z. Y., Takagi, H. and Akimoto, H.: J. Phys. Chem., 90, 4131, 1986.

Howes, N. U. M., Mir, Z. S., Blitz, M. A., Hardman, S., Lewis, T. R., Stone, D., and Seakins, P. W., Phys. Chem. Chem. Phys., 20, 22218, 2018.
Huang, H-L, Chao, W., and Lin, J Jr.-M.: PNAS, 112, 10857, 2015.
Johnson, D. and Marston, G.: Chem. Soc. Rev., 37, 699, 2008.
Liu, Y., Bayes, K. D. and Sander, S. P.: J. Phys. Chem. A 118, 741, 2014.
Newland, M. J., Rickard, A. R., Alam, M. S., Vereecken, L., Munoz, A., Rodenas, M., and Bloss, W. J.: Phys. Chem. Chem. Phys., 17, 4076, 2015.
Qiu, J. and Tonokura, K.: Chem. Phys. Lett. X, 2, 100019, 2019.
Sheps, L.: J. Phys. Chem. Lett., 4, 4201, 2013.
Stone, D., Blitz, M., Daubney, L., Ingham, T. and Seakins, P.: Phys. Chem. Chem. Phys., 15, 19119, 2013.
Stone, D., Blitz, M., Daubney, L., Howes, N. U. M. and Seakins, P.: Phys. Chem. Chem. Phys., 16, 1139, 2014.
Vereecken, L., Harder, H. and Novelli, A.: Phys. Chem. Chem. Phys., 14, 14682, 2012.
Welz, O, Savee, J. D. Osborn, D. L., Vasu, S. S., Percival, C. J., Shallcross, D. E. and Taatjes, C. A.: Science, 335, 204, 2012.

CGI_2: $CH_2OO + NO_2$
Last evaluated: May 2020; Last change in preferred values: June 2018

$CH_2OO + NO_2 \rightarrow$ products

Rate coefficient data

k/cm^3 molecule^{-1} s^{-1}	Temp./K	Reference	Technique/Comments
Absolute Rate Coefficients			
$(7^{+3}_{-2}) \times 10^{-12}$	298	Welz et al., 2012	PLP-PIMS (a)
$(1.5 \pm 0.5) \times 10^{-12}$	295	Stone et al., 2014	PLP-LIF/PIMS (b)
$(4.4 \pm 0.2) \times 10^{-12}$	295	Qiu and Tonokura, 2019	PLP-IR (c)
$(1.0 \pm 0.2) \times 10^{-12}$	298	Luo et al., 2019	PLP-IR (d)
Relative Rate Coefficients			
$(5.2 \pm 1.5) \times 10^{-13}$	298	Manzanares et al., 1987	RR-AFT-UVscat (e)
$\sim 7.8 \times 10^{-11}$	297	Ouyang et al., 2013	RR-LP-UVvis (f)

Comments

(a) CH_2OO was produced by the reaction of $CH_2I + O_2$. CH_2I was generated by 248-nm laser photolysis of diiodomethane, CH_2I_2, at 298 K and 4 torr total pressure in a large excess of O_2. The reacting mixture was monitored by tunable synchrotron photoionization mass spectrometry, which allowed characterisation of the PIMS for CH_2OO and its reaction products over the region 9.5 – 11.5 eV, and time-resolved direct detection of CH_2OO at m/z = 46 amu. The first order decay CH_2OO in the presence of excess known concentrations of NO_2 was used to determine the rate constants. The asymmetrical uncertainty limits are 95 %, based on un-weighted linear fit of [NO_2] dependence of decay lifetimes.

(b) Laser photolysis at 248 nm of CH_2I_2-O_2-N_2 mixtures was used to produce CH_2OO in the presence of excess NO_2 at 295 K. Kinetics of CH_2OO were followed by time-resolved monitoring of HCHO reaction products by laser-induced fluorescence (LIF), under pseudo-first-order conditions. k was found to be independent of pressure over range 25 – 300 Torr, and the cited value is an average of the values in this range. The uncertainty limits are 1σ errors from fitting kinetic data. Yield of HCHO is 100 % of CH_2OO reacted.

(c) CH_2OO was produced by the 266 nm laser photolysis of CH_2I_2-O_2-N_2 mixtures at 295 ± 3 K and 10.6 Torr. The time-resolved decay kinetics of CH_2OO were followed by mid-IR continuous-wave quantum cascade laser spectroscopy in the ν_4 band at 1274 cm^{-1}, under pseudo-first order conditions in the presence of excess [NO_2]. The tabulated value of k was determined from the dependence of the first-order decay constant on [NO_2].

(d) CH_2OO was produced by the 248 nm laser photolysis of CH_2I_2-O_2 mixtures at 298 K and 5.9 – 9.7 Torr. The time-resolved decay kinetics of CH_2OO were followed by mid-IR continuous-wave quantum cascade laser spectroscopy using high-resolution features in the 880-932 cm^{-1} region, corresponding to the O-O stretching band. Experiments were carried out under pseudo-first order conditions in the presence of excess [NO_2], measured by UV absorption at 340 nm. The tabulated value of k was determined from the dependence of the first-order decay constant on [NO_2].

(e) Flow system involving C_2H_4-O_3-SO_2-H_2O mixtures in which H_2SO_4 particle concentrations were monitored by scattered UV light, as described by Suto et al. (1985). Relative rate coefficients obtained from the dependencies of the aerosol formation on the concentrations of O_3, SO_2, and H_2O, and the inclusion of the effect of added NO_2 on the formation of the H_2SO_4 aerosol. The

resultant measured value of $k(CH_2OO + NO_2)/k(CH_2OO + SO_2) = (1.4 \pm 0.4) \times 10^{-2}$ is placed on an absolute basis using $k(CH_2OO + SO_2) = 3.7 \times 10^{-11}$ cm^3 molecule^{-1} s^{-1} (IUPAC, current recommendation).

(f) Photolysis of CH_2I_2-O_2-N_2-NO_2 mixtures at 348 nm in continuous flow conditions at 760 Torr pressure. Simultaneous measurement of products NO_3 and $[N_2O_5+NO_2]$ was made using cavity-enhanced absorption spectroscopy at 663 nm. Analysis of these data as function of $[NO_2]$ allowed evaluation of the rate constant ratio: $k_d(CH_2OO)/k(CH_2OO + NO_2) = (6.4 \pm 1.7) \times 10^{12}$ molecule cm^{-3}, where k_d is the total loss rate constant for competing first order processes. Assuming the competing kinetics is dominated by the reaction of CH_2OO with water gave the rate constant ratio: $k(CH_2OO + H_2O)/k(CH_2OO + NO_2) = 3.6 \times 10^{-6}$ (error ± 40%). The tabulated approximate value of $k(CH_2OO + NO_2)$ is based on using $k(CH_2OO + H_2O) = 2.8 \times 10^{-16}$ cm^3 molecule^{-1} s^{-1} (IUPAC, current recommendation).

Preferred Values

Parameter	Value	T/K
k /cm^3 molecule^{-1} s^{-1}	3×10^{-12}	298
Reliability		
$\Delta \log k$	± 0.5	298

Comments on Preferred Values

There are four absolute studies of the $CH_2OO + NO_2$ reaction kinetics, three based on the removal kinetics of CH_2OO (Welz et al., 2012; Qiu and Tonokura, 2019; Luo et al., 2019), and one less direct study, based the formation kinetics of the product, HCHO (Stone et al., 2014). The results of these studies are not in good agreement, with the reported values of k covering a range of a factor of seven. The preferred value of k is the geometric mean of the three values based on observation of CH_2OO removal, with wide uncertainty limits that encompass the reported range. Given that the three studies employ the same chemical system, and two the same method of detection, the origin of the large disagreement is unclear, and further studies are therefore required to allow the uncertainty limits to be reduced. The absolute rate coefficient reported by Stone et al. (2014) lies within the recommended range, although the interpretation of their results may be complicated by HCHO not being a direct product of the reaction. Neither of the relative rate studies has a well-defined reference reaction and they are not taken into account.

Decomposition of the cyclic ozonide formed in the initial $CH_2OO + NO_2$ encounter, to HCHO + NO_3, was proposed to be the major product-forming channel, as indicated by the experiments of Stone et al. (2014) and Ouyang et al., (2013). However, the experimental work reported by Taatjes et al. (2013) and Caravan et al. (2017) did not detect NO_3 in low-pressure photo-ionization experiments, placing an upper limit of 30 % on the NO_3 yield. Their observation of a product mass equivalent to the sCI + NO_2 adduct suggests that addition is the main product pathway. A multi-reference theoretical study by Vereecken and Nguyen (2017) predicted formation of the nitromethyl-peroxy radical adduct, in agreement with these latter experimental studies, with HCHO formed from its subsequent chemistry.

References

Caravan, R. L., Khan, M. A. H., Rotavera, B., Papajak, E., Antonov, I. O., Chen, M.-W., Au, K., Chao, W., Osborn, D. L., Lin, J. J.-M., Percival, C. J., Shallcross, D. E. and C. A. Taatjes: Faraday Discuss., 200, 313, 2017.

Luo, P.-L. Chung, C.-A. and Lee, Y.-P.: Phys. Chem. Chem. Phys., 21, 17578, 2019.

Manzanares, E. R., Suto, M. and Lee, L. C.: unpublished data, 1987.

Ouyang, B., McLeod, M.W., Jones, R. L., and Bloss, W. J.: Phys. Chem. Chem. Phys., 15, 17070, 2013.

Qiu, J. and Tonokura, K.: Chem. Phys. Lett. X, 2, 100019, 2019.

Stone, D., Blitz, M., Daubney, L., Howes, N. U. M. and Seakins, P.: Phys. Chem. Chem. Phys., 16, 1139, 2014.

Suto, M., Manzanares, E. R. and Lee, L. C.: Environ. Sci. Technol., 19, 815, 1985.

Taatjes, C. A. , Welz, C. A.; Eskola, A. J. , Savee, J. D. , Scheer, A. M., Shallcross, D. E., Rotavera, B., Lee, E. P. F., Dyke, J. M., Mok, D. K. W., Osborn, D. L. and Percival, C. J.: Science, 340, 171, 2013.

Vereecken, L. and Nguyen, H. M. T., Int. J. Chem. Kinet., 49, 752, 2017.

Welz, O, Savee, J. D. Osborn, D. L., Vasu, S. S., Percival, C. J., Shallcross, D. E. and Taatjes, C. A.: Science, 335, 204, 2012.

CGI_3: CH_2OO + NO

Last evaluated: June 2015; Last change in preferred values: June 2015

CH_2OO + NO → products

Rate coefficient data

k/cm^3 molecule^{-1} s^{-1}	Temp./K	Reference	Technique/Comments
Absolute Rate Coefficients			
$< 6 \times 10^{-14}$	298	Welz et al., 2012	PLP-PIMS (a)
$< 2 \times 10^{-13}$	295	Stone et al., 2014	PLP-LIF/PIMS (b)

Comments

(a) CH_2OO was produced by the reaction of $CH_2I + O_2$. CH_2I was generated by 248-nm laser photolysis of di-iodomethane, CH_2I_2, at 298 K and 4 Torr total pressure in a large excess of O_2. The reacting mixture was monitored by tunable synchrotron photo-ionization mass spectrometry, which allowed characterisation of the PIMS for CH_2OO and its reaction products over the region 9.5 – 11.5 eV. Time-resolved direct detection of CH_2OO at m/z = 46 amu. The first order decay CH_2OO in the presence of 5×10^{15} molecule cm^{-3} NO was unaffected, leading to the cited upper limit for *k*, based on the assumption that a 25 % increase on the decay constant could be detected.

(b) Laser photolysis at 248 nm of CH_2I_2-O_2-N_2 mixtures was used to produce CH_2OO in the presence of excess NO (0.36 - 1.7) $\times 10^{15}$ molec.cm^{-3}. Kinetics of CH_2OO followed by time-resolved monitoring of HCHO reaction products by laser-induced fluorescence (LIF), which exhibited exponential growth (1st order kinetics) on two timescales. The fast HCHO production is assigned to the reaction of CH_2IO_2 with NO and the slower growth due to CH_2OO reactions. The upper limit for *k* was based on the observation of no effect of [NO] on the slow growth curves, assuming the HCHO production was due to the reaction with NO.

Preferred Values

Parameter	Value	T/K
k /cm^3 molecule^{-1} s^{-1}	$< 6 \times 10^{-14}$	298

Comments on Preferred Values

The only studies of the reaction kinetics are those of Welz et al. (2012) and of Stone et al. (2014), who both reported upper limits for *k*. These results are consistent but the preferred upper limit is the lower value from Welz et al. (2012), as their monitoring of [CH_2OO] is more direct and the possible interferences are less. Since no clear reaction has been observed, the products under atmospheric conditions are not known. Theoretical calculations (Vereeken et al., 2012) using DFT methods found the CH_2OO + NO reaction to show a barrier at all levels of theory employed. The lowest entrance transition state was found for the formation of a cyclic adduct with a nitrogen-centered radical, with a barrier calculated at 5.8 kcal mol^{-1}. The estimated rate coefficient, 1.7×10^{-18} cm^3 molecule^{-1} s^{-1}, is well below the experimental value of Welz et al. (2012).

References

Stone, D., Blitz, M., Daubney, L., Howes, N. U. M. and Seakins, P.: Phys. Chem. Chem. Phys., 16, 1139, 2014.

Vereeken, L., Harder, H. amd Novelli, A.: Phys. Chem. Chem. Phys., 14, 14682, 2012.

Welz, O, Savee, J. D. Osborn, D. L., Vasu, S. S., Percival, C. J., Shallcross, D. E. and Taatjes, C. A.: Science, 335, 204, 2012.

CGI_4: $CH_2OO + H_2O/(H_2O)_2$
Last evaluated: May 2020; Last change in preferred values: February 2020

$$CH_2OO + H_2O \rightarrow HOCH_2OOH \quad (1a)$$
$$\rightarrow HCHO + H_2O_2 \quad (1b)$$
$$\rightarrow HC(O)OH + H_2O \quad (1c)$$

$$CH_2OO + (H_2O)_2 \rightarrow HOCH_2OOH + H_2O \quad (2a)$$
$$\rightarrow HCHO + H_2O_2 + H_2O \quad (2b)$$
$$\rightarrow HC(O)OH + 2H_2O \quad (2c)$$

Rate coefficient data

k/cm^3 molecule^{-1} s^{-1}	Temp./K	Reference	Technique/Comments
Absolute Rate Coefficients			
$k_1 < 4.0 \times 10^{-15}$	298	Welz et al., 2012	PLP-PIMS(a)
$k_1 < 9 \times 10^{-17}$	295	Stone et al., 2014	PLP-LIF/PIMS (b)
$k_1 = (3.2 \pm 1.2) \times 10^{-16}$	297	Berndt et al., 2015	Free-Jet FR-TOF-MS (c)
$k_2 = (6.5 \pm 0.8) \times 10^{-12}$	298	Chao et al., 2015	PLP-UVAS(d)
$k_2 = (4.2 \pm 1.2) \times 10^{-12}$	294	Lewis et al., 2015	PLP-LP-UVAS (e)
$k_2 = (7.4 \pm 0.6) \times 10^{-12}$	298	Smith et al., 2015	PLP-LP-UVAS (f)
$k_2 = 8.72 \times 10^{-18} \exp[(4076 \pm 302)/T]$	283-324		
$k_1 = (2.4 \pm 1.6) \times 10^{-16}$	293	Sheps et al., 2017	TR-BB-CEAS/PIMS (g)
$k_2 = (6.6 \pm 0.7) \times 10^{-16}$	293		
Relative Rate Coefficients			
$k_1 = (8.5 \pm 3.7) \times 10^{-15}$	298	Suto et al., 1985	RR-AFT-UVscat (h)
$k_1 = (1.1 \pm 0.4) \times 10^{-17}$	297	Ouyang et al., 2013	RR-LP-UVvis (i)
$k_2 = (1.07 \pm 0.04) \times 10^{-11}$	293	Berndt et al., 2014	RR-AFT-CIMS(ToF) (j)
$k_1 = (9.3 \pm 2.6) \times 10^{-16}$	298	Newland et al., 2015	RR-FTIR/UVAS/UVF (k)
$k_2 = (5.2 \pm 6.7) \times 10^{-13}$	298		
Branching ratios			
$k_{1a}/k_1 = 0.73$	295	Nguyen et al., 2016	(l)
$k_{1b}/k_1 = 0.06$	295		
$k_{1c}/k_1 = 0.21$	295		
$k_{2a}/k_2 = 0.40$	295		
$k_{2b}/k_2 = 0.06$	295		
$k_{2c}/k_2 = 0.54$	295		
$k_{2a}/k_2 = 0.55 \pm 0.15$	293	Sheps et al., 2017	TR-BB-CEAS/PIMS (g)
$k_{2b}/k_2 = 0.40 \pm 0.10$	293		
$k_{2c}/k_2 = < 0.10$	293		

Comments

(a) CH_2OO was produced by the reaction of $CH_2I + O_2$. CH_2I was generated by 248 nm laser photolysis of di-iodomethane, CH_2I_2, at 298 K and 4 torr, in a large excess of O_2. The reacting mixture was monitored by tunable synchrotron photoionization mass spectrometry, which allowed characterisation of the PIMS for CH_2OO and its reaction products over the region 9.5 – 11.5 eV. Time-resolved direct detection of [CH_2OO] decay at m/z = 46. The first order decay of CH_2OO in the presence of excess known concentrations of H_2O was used to determine the rate constants, at a

total pressure of 4.5 Torr. The upper limit determined on the basis of absence of any effect of $[H_2O] = 3 \times 10^{16}$ molecule cm^{-3}

(b) Photolysis of CH_2I_2-O_2-N_2 mixtures. in the presence of excess H_2O, under pseudo-first-order conditions. Kinetics of $CH_2OO + H_2O$ reaction were followed by time-resolved monitoring of HCHO product by laser-induced fluorescence (LIF) spectroscopy (pressure range: 50 – 450 Torr). Rate coefficients for $CH_2OO + H_2O$ was investigated at 200 Torr, using up to $[H_2O] = 1.7 \times 10^{17}$ molecule cm^{-3}. The cited value of k is an upper limit based on the lack of significant effect of $[H_2O]$ and the assumption that HCHO detected is derived solely from reaction with H_2O.

(c) The rate coefficients of the bimolecular reaction of CH_2OO with the water monomer have been experimentally determined at T = (297 ± 1) K and at atmospheric pressure by using a free-jet flow system. CH_2OO was produced by the reaction of ozone with C_2H_4, and $[CH_2OO]$ was measured indirectly by titrating with excess SO_2 and detection of product H_2SO_4 after 7.5 s reaction time. Low water concentrations of $[H_2O] < 10^{15}$ molecule cm^{-3} and, as a consequence, very low water dimer concentrations of $[(H_2O)_2] = 2.5 \times 10^9$ molecule cm^{-3} (Scribano et al., 2006) permitted the separation of reaction (1) from reaction (2). The cited rate coefficient k_1 was determined by fitting a parameterized expression for the $[H_2O]$ dependence of the ratio $[H_2SO_4]/[C_2H_4]$, assuming k_{uni} = 0.19 s^{-1}, and appropriate uncertainty in the parameters.

(d) CH_2OO prepared by PLP (266 nm) of CH_2I_2 in O_2/Ar mixtures at 5.1 Torr pressure. CH_2OO kinetics observed by time-resolved UV absorption in the $\tilde{B}$ (1A′) ← $\tilde{X}$(1A′) electronic transition, measured over range 280-600 nm using a CCD or a photodiode (at 350 ± 5 nm), in the absence and presence of H_2O (RH = 3 % to 80 %). Rate constants extracted by fitting plots of k_{obs} vs RH or $[(H_2O)_2]$, calculated using K_p (298) = 0.0501 bar^{-1} at 298 K where P_{sat} = 23.8 torr. Uncertainty on $[(H_2O)_2]$ was estimated to be ± 12 %. Incorporation of the monomer reaction into the fit gave $k_1 < 1.5 \times 10^{-15}$ cm^3 $molecule^{-1}$ s^{-1}.

(e) CH_2OO prepared by PLP (266 nm) of CH_2I_2 in O_2/Ar mixtures at 5.1 Torr pressure. CH_2OO kinetics, observed by time-resolved UV absorption in the $\tilde{B}$ (1A′) ← $\tilde{X}$(1A′) electronic transition between 350 – 420 nm, were first order in the presence and absence of H_2O, independent of total pressure. However, dependence of the first-order decay constant on $[H_2O]$ in the range 0 to 25 × 10^{16} molecule cm^{-3} was fitted best by a quadratic function, indicating that CH_2OO was reacting predominantly with the water dimer. The cited rate coefficient, k_2, was calculated using the parameterisation of Scribano et al. (2006) to calculate $[(H_2O)_2]$, i.e. K_p (298) = 0.0579 bar^{-1} at 294 K.

(f) CH_2OO prepared by PLP (248 nm) of CH_2I_2 in N_2/O_2 at 5.1 Torr pressure. CH_2OO was observed by time-resolved of UV absorption at 340 nm. The kinetics of the reaction of CH_2OO with water vapor was measured as a function of $[H_2O]$ at temperatures from 283 to 324 K. The observed first-order decay constant increased quadratically with $[H_2O]$, consistent with dominant reaction with the water dimer. The dimer concentrations were calculated using the T-dependent equilibrium constant for water dimerization, K_{eq}(T) of Ruscic (2013), with values of k_2 derived from the variation of the first-order decay constant with $[(H_2O)_2]$. They report an activation energy of -(8.1 ± 0.6) kcal mol^{-1}, from the variation of k_2 over the studied temperature range, and this forms the basis of the Arrhenius expression tabulated above.

(g) CH_2OO prepared by PLP (248, 266 or 351nm) of CH_2I_2 in O_2/He or O_2/N_2 at 30–100 Torr pressure. The experiments were probed using either time-resolved broadband cavity-enhanced absorption spectroscopy (TR-BB-CEAS) or photoionization mass spectrometry (PIMS). Values of k_1 and k_2 obtained from variation of observed first-order decay constants in experiments performed over a range of $[H_2O]$, using a simplified mechanism in which CH_2OO was removed by reactions (1), (2) and background loss process. Product identification and quantification using PIMS allowed channel contributions to be determined for reaction (2).

(h) Flow system involving C_2H_4-O_3-SO_2-H_2O mixtures in which H_2SO_4 aerosol concentrations were monitored by scattered UV light. Relative rate coefficients obtained from the dependencies of the

aerosol formation on the concentrations of O_3, SO_2, and H_2O. The relative rate constant reported was $k_1/k(CH_2OO + SO_2) = (2.3 \pm 1.0) \times 10^{-4}$. The value of k_1 tabulated above is based on $k(CH_2OO + SO_2) = 3.7 \times 10^{-11}$ cm^3 molecule^{-1} s^{-1} (IUPAC, current recommendation).

(i) Photolysis of CH_2I_2-O_2-N_2-NO_2 mixtures at 348 nm in continuous flow conditions at 760 Torr pressure. CH_2OO produced in this system was allowed to react with NO_2. Simultaneous measurement of products NO_3 and $[N_2O_5+NO_2]$ was made at 663 nm. Analysis of these data as function of $[NO_2]$ allowed evaluation of the rate constant ratio: $k_d(CH_2OO)/k(CH_2OO + NO_2) = (6.4 \pm 1.7) \times 10^{12}$ molecule cm^{-3}, where k_d is the total loss rate constant for competing first order processes. Assuming the competing kinetics is dominated by the reaction of Criegee radicals with water gave the rate constant ratio: $k(CH_2OO + H_2O)/k(CH_2OO + NO_2) = 3.6 \times 10^{-6}$ (error ± 40%). The value of k_1 tabulated above is based on $k(CH_2OO + NO_2) = 3 \times 10^{-12}$ cm^3 molecule^{-1} s^{-1} (IUPAC, current recommendation).

(j) CH_2OO produced from $O_3 + C_2H_4$ reaction in atmospheric pressure flow tube at 293 ± 0.5 K. H_2SO_4 formation from the reaction $CH_2OO + SO_2$ as a function of RH (= 2% to 50%) for close to atmospheric conditions, was measured using NO_3^--CI-APi-TOF-MS. The uncertainty in the $[H_2SO_4]$ estimated to be ± 45%. Second-order kinetics with regard to water vapour concentration indicates a preferred reaction of CH_2OO with the water dimer. The relative rate coefficient $k_2/k(CH_2OO + SO_2) = 0.29 \pm 0.01$, based on K_p calculated using the parameterisation of Scribano et al. (2006). Measurements at the lowest relative humidity (RH ~2%) yield an upper limit of the rate coefficient ratio $k_{uni}/k(CH_2OO + SO_2) = 2.4 \times 10^{11}$ molecule cm^{-3}, where k_{uni} is the total first order loss coefficient for CH_2OO in the absence of water dimer. Combining $k_2/k(CH_2OO + SO_2) = 0.29 \pm 0.01$ with $k(CH_2OO + SO_2) = 3.7 \times 10^{-11}$ (IUPAC, current recommendation) gives the tabulated value of k_2 above.

(k) The removal of SO_2 in the presence of ethene-ozone systems was measured as a function of humidity in EUPHORE simulation chamber, under atmospheric boundary layer conditions. SO_2 and O_3 abundance were measured using conventional fluorescence and UV absorption monitors, respectively; alkene abundance was determined via FTIR spectroscopy. SO_2 removal decreased with increasing relative humidity (1.5 – 21%) confirming a significant reaction for CH_2OO with H_2O. The observed SO_2 removal kinetics are consistent with the relative rate constant, $k_1/k(CH_2OO + SO_2) = (3.3 \pm 1.1) \times 10^{-5}$, if removal is due solely to reaction (1). An expanded analysis considering removal by both reactions (1) and (2) yielded $k_1/k(CH_2OO + SO_2) = (2.5 \pm 0.7) \times 10^{-5}$ and $k_2/k(CH_2OO + SO_2) = (1.4 \pm 1.8) \times 10^{-2}$. The values of k_1 and k_2 tabulated above are based on $k(CH_2OO + SO_2) = 3.7 \times 10^{-11}$ cm^3 molecule^{-1} s^{-1} (IUPAC, current recommendation).

(l) Products formed from the ozonolysis of isoprene investigated in the multi-instrumented Caltech dual 24m^3 teflon chamber at atmospheric pressure. CH_2OO reported to dominate the population of stabilized Criegee intermediates formed, and their bimolecular reactivity. $HOCH_2OOH$, $HC(O)OH$ and H_2O_2 were quantified with a triple-quadrupole chemical ionization mass spectrometer (CIMS) using CF_3O^- as an ionization reagent. The product channel contributions for reactions (1) and (2) were determined from from the observed product distribution, and its dependence on $[H_2O]$, by simulations of the system using a detailed chemical mechanism, with $k_1 = 9.0 \times 10^{-16}$ cm^3 molecule^{-1} s^{-1} and $k_2 = 8.0 \times 10^{-13}$ cm^3 molecule^{-1} s^{-1}.

Preferred Values

Parameter	Value	T/K
k_1 /cm^3 molecule^{-1} s^{-1}	2.8×10^{-16}	298
k_2 /cm^3 molecule^{-1} s^{-1}	6.4×10^{-12}	298
k_2 /cm^3 molecule^{-1} s^{-1}	$7.35 \times 10^{-18} \exp(4076/T)$	280-325
Reliability		
$\Delta \log k_1$	± 0.3	298
$\Delta \log k_2$	± 0.2	298
$\Delta (E_2/R)$	± 500 K	280-325

Comments on Preferred Values

An important discovery arising from the direct studies of CH_2OO reaction with water vapour was the quadratic dependence of the pseudo-first order rate constant for loss of CH_2OO on $[H_2O]$. This is consistent with the predominant reaction being with the water dimer (k_2). The reaction with monomeric water molecules (k_1) is slow, and probably less important under atmospheric conditions. This conclusion is supported by recent relative rate studies, although there remain inconsistencies in results obtained in different laboratories. The most recent study of Smith et al. (2015) reports a strong negative temperature dependence for the reaction of CH_2OO with the water dimer, also consistent with dimer reaction. Their reported (negative) activation energy forms the basis of the preferred value of E_2/R.

Because of the observed quadratic dependence of the rate on $[H_2O]$ only those experimental studies which employed conditions of high enough $[H_2O]$ provide $[(H_2O)_2]$ sufficient to compete with monomer reaction and other loss reactions of CH_2OO. The preferred value of k_2 at 298 K is the mean of the values from the direct kinetic studies of Chao et al. (2015), Smith et al (2015) and Sheps et al. (2017) (corrected to 298 K using the preferred value of E_2/R); and is also consistent with the direct kinetic determination of Lewis et al. (2015) within the assigned uncertainty. These results at room temperature are in very good agreement, considering the experimental uncertainty arising mainly from uncertainty in $[H_2O]$ which propagates by a factor of two in calculating $[(H_2O)_2]$. Support for these high values of k_2 comes from the relative rate study of Berndt et al. (2014). The preferred value of k_1 at 298 K is the mean of the absolute values reported by Berndt et al. (2015) and Sheps et al. (2017), which are in good agreement. Most other kinetic studies take no account of the dimer reaction and only provide upper limits pertaining to k_1. The relative rate study of Newland et al. (2015) considers the possibility of a significant reaction with water dimer, but only provides an indeterminate value for $k_2/k(CH_2OO + SO_2)$. The reported relative rate constant ratio $k_1/k(CH_2OO + SO_2) = (2.5 \pm 0.7) \times 10^{-5}$ at 298 K in their expanded analysis, implies the contribution of k_1 to the overall rate of CH_2OO loss too small to detect at $[H_2O]$ used in the experiments of Welz et al. (2012).

Work of Neeb et al. (1997) shows that the reaction of the CH_2OO Criegee intermediate with H_2O leads initially to hydroxymethyl hydroperoxide ($HOCH_2OOH$). Estimates using quantum chemistry calculations of the rate coefficient for reaction of CH_2OO with water vapour dimer forming $HOCH_2OOH$ product (Ryzhkov and Ariya, 2004), are of similar order of magnitude to the experimental values. $HOCH_2OOH$ is expected to be formed chemically activated, and is either subsequently thermalized or decomposes to form HCHO and H_2O_2 or HC(O)OH and H_2O. In their study of the ozonolysis of isoprene, from which CH_2OO is believed to be the dominant sCI formed, Nguyen et al. (2016) were able to derive the product channel contributions tabulated above for reactions (1) and (2). However, there is some disagreement with those subsequently reported for

reaction (2) by Sheps et al. (2017), in which CH_2OO was produced by photolysis of CH_2I_2/O_2. Although both studies report an important contribution from channel (2a), forming $HOCH_2OOH$, they provide contradictory conclusions for the contributions of the HCHO and HC(O)OH forming channels (2b) and (2c). Further studies are required before firm recommendations can be made.

References

Berndt, T., Voigtlander, J., Stratmann, F., Junninen, H., Mauldin III, R.L., Sipila, M., Kulmala,. M., and Herrmann, H., Phys. Chem. Chem. Phys., 16, 19130, 2014.

Berndt, T., Kaethner, R., Voigtländer, J., Stratmann, F., Pfeifle, M., Reichle, P., Sipilä, M., Kulmala, M. and Olzmann, M.: Phys. Chem. Chem. Phys., 17, 19862, 2015.

Chao, W., Hsieh, J-T., Chang, C-H., Lin, Jim Jr-M., Science, 347, 751-754, 2015.

Lewis, T.R., Blitz, M.A., Heard, D.E., and Seakins, P.W., Phys. Chem. Chem. Phys., 17 4859, 2015.

Neeb, P., Sauer, F., Horie, O. and Moortgat, G. K., Atmos. Environ., 31, 1417,1997.

Newland, M. J., Rickard, A. R., Alam, M. S., Vereecken, L., Munoz, A., Rodenas, M., and Bloss, W. J.: Phys. Chem. Chem. Phys., 17, 4076, 2015.

Nguyen, T. B., Tyndall, G. S., Crounse, J. D., Teng, A. P., Bates, K. H., Schwantes, R. H., Coggon, M. M., Zhang, L., Feiner, P., Milller, D. O., Skog, K. M., Rivera-Rios, J. C., Dorris, M., Olson, K. F., Koss, A., Wild, R. J., Brown, S. S., Goldstein, A. H., de Gouw, J. A., Brune, W. H., Keutsch, F. N., Seinfeld, J, H. and Wennberg, P. O.: Phys. Chem. Chem. Phys., 18, 10241, 2016.

Ouyang, B., McLeod, M. W., Jones, R. L., and Bloss, W. J.: Phys. Chem. Chem. Phys., 15, 17070, 2013.

Ruscic, B.: J. Phys. Chem. A, 117(46), 11940, 2013.

Ryzhkov, A. B., and Ariya, P. A.: Phys. Chem. Chem. Phys., 6, 5042, 2004.

Scribano, Y., Goldman, N., Saykally, R. J., and Leforestier, C.: J. Phys. Chem. A, 110, 5411, 2006.

Sheps, L., Rotavera, B., Eskola, A. J., Osborn, D. L., Taatjes, C. A., Au, K., Shallcross, D. E., Khan, M. A. H., and Percival, C. J: Phys. Chem. Chem. Phys., 19, 21970, doi: 10.1039/c7cp03265j, 2017.

Smith, M.C., Chang, C-H., Chao, Wen., Lin, L-C., Takahashi, K., Boering, K.A. and Lin, Jim Jr-M.: J Phys. Chem. Lett., 6, 2708, 2015.

Stone, D., Blitz, M., Daubney, L., Howes, N. U. M., and Seakins, P.: Phys. Chem. Chem. Phys., 16, 1139, 2014.

Suto, M., Manzanares, E. R. and Lee, L. C.: Environ. Sci. Technol., 19, 815, 1985.

Welz, O, Savee, J. D. Osborn, D. L., Vasu, S. S., Percival, C. J., Shallcross, D. E. and Taatjes, C. A.: Science, 335, 204, 2012.

CGI_5: $CH_2OO + CH_2OO$

Last evaluated: June 2015; Last change in preferred values: June 2015

$CH_2OO + CH_2OO \rightarrow HCHO + HCHO + O_2(^1\Delta_g)$

Rate coefficient data

k/cm^3 molecule^{-1} s^{-1}	Temp./K	Reference	Technique/Comments
Absolute Rate Coefficients			
$(4 \pm 2) \times 10^{-10}$	343	Su et al., 2014	PLP-FTIR (a)
$(6.0 \pm 2.1) \times 10^{-11}$	297	Buras et al, 2014	PLP-UVA (b)
$(8 \pm 4) \times 10^{-11}$	295	Ting et al, 2014a	PLP-UVA (c)
$(7.35 \pm 0.63) \times 10^{-11}$	293	Chhantyal-Pun et al., 2015	PLP-CRDS (d)

Comments

(a) CH_2OO was produced by the reaction of $CH_2I + O_2$, following 355 nm laser photolysis of CH_2I_2 (4×10^{13} cm^{-3}) in a large excess of O_2. CH_2OO was detected by time-resolved step scan FTIR spectroscopy using absorption coefficients determined in their investigation of the IR spectrum of CH_2OO (Su et al., 2013). Rate coefficients ($(3.1 \pm 0.1) \times 10^{-10}$ and $(4.5 \pm 0.2) \times 10^{-10}$ cm^3 molecule^{-1} s^{-1} respectively) were determined at pressures of 10 and 90 Torr. Kinetic modelling of experimental decay profiles yielded the cited value of k_1, which has an estimated uncertainty of a factor of 2. Fitting also yielded a value of $k(CH_2OO + I) = (4 \pm 2) \times 10^{-11}$ cm^3 molecule^{-1}s^{-1}.

(b) CH_2OO was produced by the reaction of $CH_2I + O_2 \rightarrow CH_2OO + I$ following 355 nm laser photolysis of CH_2I_2 in a large excess of O_2. CH_2OO kinetics was followed by time resolved absorption at 375 nm in the B $\leftarrow$ X transition and the atomic I co-product followed by probing the 1315.246 nm F = 3 $^2P_{1/2} \leftarrow$ F = 4 $^2P_{3/2}$ atomic transition. $[CH_2OO]_0$ determined by fitting simultaneous decay of [I] and $[CH_2OO]$, allowing a determination of the self-reaction rate coefficient, k_{self} with an uncertainty of ±35%. The absorption cross section of CH_2OO at the UV probe wavelength (λ = 375 nm) was derived as $(6.2 \pm 2.2) \times 10^{-18}$ cm^2 molecule^{-1}, which is consistent with the results of Ting et al (2014b) which form the basis of the IUPAC recommended value (see data sheet P33).

(c) CH_2OO was prepared by pulsed 248 nm photolysis of CH_2I_2/O_2 mixtures in the pressure range 7.6–779 Torr. Transient absorption spectra were recorded using a gated intensified CCD camera (1 ms gate width) to monitor simultaneously CH_2I_2, CH_2OO, CH_2I, and IO. The decay of CH_2OO was second order and various reactions, including the self-reaction and the reaction of CH_2OO + I, contributed to decay. The rate coefficients were determined with a detailed mechanism to model the observed temporal dependences of observed species. The fitted value of k ranged from $(8.2 – 12.0) \times 10^{-11}$ cm^3 molecule^{-1}s^{-1}, with the cited value an average of N_2 and O_2 bath-gas results. The error limits are 1 σ. The yield of CH_2OO from $CH_2I + O_2$ was found to have a pressure dependence; for air at 1 atm., the yield of approximately 30 % is about twice previous estimates.

(d) Cavity ring-down spectroscopy was used to perform kinetic measurements at 293 K under low pressure (7 to 30 Torr) conditions, for reactions of CH_2OO generated by (248 nm) laser photolysis of CH_2I_2 in the presence of O_2, and monitored by a probe laser at 355 nm. Decay of $[CH_2OO]$, from initial concentrations in the range $2.5 – 5.0 \times 10^{12}$ molecule cm^{-3}, was second order. The rate

coefficient, k = (7.35 ± 0.63) × 10^{-11} cm^3 $molecule^{-1}s^{-1}$, was derived from the measured CH_2OO decay rates, using an absorption cross-section reported previously.

Preferred Values

Parameter	Value	T/K
k /cm^3 $molecule^{-1}$ s^{-1}	7.4×10^{-11}	298
Reliability		
$\Delta \log k$	± 0.1	298

Comments on Preferred Values

The occurrence of a rapid self-reaction of CH_2OO was discovered during the search for infrared spectroscopic features of CH_2OO, using the reaction of CH_2I with O_2 as a source (Su et al., 2013), when high concentrations of CH_2OO were required to observe the weak IR absorptions. However, the results of Su et al. (2014) are a factor of 10 higher, than the subsequent studies using UV detection. The reported rate coefficient values of Buras et al. (2014), Ting et al. (2014a) and Chhantyal-Pun et al. (2015), who all used time resolved UV absorption spectroscopy to determine CH_2OO kinetics, are in agreement within the error limits. These are quite significant in the former two studies, which used simulations with a complex kinetic scheme to extract the rate coefficient of interest. The data quality and analysis methods in the CRDS experiments provided more precise measurements of the kinetics and are the basis of our recommendation. The values of k appear to be independent of pressure.

References

Buras, Z. J., Elsamra, R. M. and Green, W. H.: J. Phys. Chem. Lett., 5, 2224, 2014.

Chhantyal-Pun, R., Davey, A., Shallcross, D.E., Percival, C.J. and Orr-Ewing, A.J.: Phys. Chem. Chem. Phys., 17, 3617, 2015.

Su, Y-T., Huang, Y-H., Witek, H. and Lee, Y-P.: Science, 340, 174, 2013.

Su, Y-T., Lin, H-Y., Putikam, R., Matsui, H., Lin, M.C., and Lee, Y-P.: Nature Chemistry, 6, 477, 2014.

Ting, W-L, Chen, Y-H., Lee, Y-F, Matsui, H., Lee, Y-P. and Lin, J Jr -M.: J. Chem. Phys., 141, 104308, 2014a.

Ting, W-L, Chen, Y-H., Chao, W., Smith, M.C. and Lin, J Jr -M.: Phys. Chem. Chem. Phys., 16, 10438, 2014b.

CGI_6: $CH_2OO + I$

Last evaluated: November 2016; Last change in preferred values: November 2016

$$CH_2OO + I \rightarrow HCHO + IO \quad (1)$$
$$\rightarrow CH_2I + O_2 \quad (2)$$
$$CH_2OO + I + M \rightarrow ICH_2OO + M \quad (3)$$

Rate coefficient data ($k = k_1 + k_2 + k_3$)

k/cm^3 molecule^{-1} s^{-1}	Temp./K	Reference	Technique/Comments
Absolute Rate Coefficients			
$(4 \pm 2) \times 10^{-11}$	343	Su et al., 2014	PLP-FTIR (a)
$< 1 \times 10^{-11}$	297	Buras et al., 2014	PLP-UVA (b)
$k_1 = 9.0 \times 10^{-12}$	295	Ting et al., 2014	PLP-UVA (c)
$< 5 \times 10^{-12}$	293	Chhantyal-Pun et al., 2015	PLP-CRDS (d)

Comments

(a) CH_2OO was produced by the reaction of $CH_2I + O_2$, following 355nm laser photolysis of CH_2I_2 in a large excess of O_2. CH_2OO was detected by time-resolved step scan FTIR spectroscopy using absorption coefficients determined in their investigation of the IR spectrum of CH_2OO (Su et al., 2013). Kinetic modelling to fit the experimental decay profiles yielded a value of $k(CH_2OO + I) = (4 \pm 2) \times 10^{-11}$ cm^3 molecule^{-1}s^{-1}.

(b) CH_2OO was produced by the reaction of $CH_2I + O_2 \rightarrow CH_2OO + I$ following 355 nm laser photolysis of CH_2I_2 in a large excess of O_2. CH_2OO kinetics was followed by time resolved absorption at 375 nm in the B $\leftarrow$ X transition and the atomic I co-product followed by probing the 1315.246 nm F = 3 $^2P_{1/2} \leftarrow$ F = 4 $^2P_{3/2}$ atomic transition. $[CH_2OO]_0$ determined by fitting simultaneous decay of [I] and $[CH_2OO]$, allowing a determination of the self-reaction rate coefficient, k_{self} with an uncertainty of ± 35%, and an upper limit for $k(CH_2OO + I)$.

(c) CH_2OO was prepared by pulsed 248 nm photolysis of CH_2I_2/O_2 mixtures in the pressure range 10–798 mbar. Transient absorption spectra were recorded using a gated intensified CCD camera to monitor simultaneously CH_2I_2, CH_2OO, CH_2I, and IO in the reaction system. The decay of CH_2OO was second order and various channels, including the self-reaction and the reaction of $CH_2OO + I$, contributing to decay. The rate coefficients were determined with a detailed mechanism to model the observed temporal dependences of observed species. The fitted value for formation of IO was independent of pressure. The yield of CH_2OO from $CH_2I + O_2$ was found to have a pressure dependence due to pressure stabilisation of ICH_2OO^* adduct formed in the alternative channel (3); for air at 1 atm., the yield of CH_2OO was approximately 30 %, which is about twice previous estimates.

(d) Cavity ring-down spectroscopy was used to perform kinetic measurements at 293 K under low pressure (7 to 30 Torr) conditions, for reactions of CH_2OO generated by (248-nm) laser photolysis of CH_2I_2 in the presence of O_2, and monitored by a probe laser at 355 nm. $[CH_2OO]_0 \sim 2.5 - 5.0 \times 10^{12}$ molecule cm^{-3}. Decay was essentially second order and dominated by the self-reaction of CH_2OO. Estimation of the upper limit of rate coefficient for the reaction $CH_2OO + I$ was obtained by numerical simulation of decay traces at lowest pressure, where there was minimal contribution from pressure dependent reactions, e.g. $CH_2OO + I$ (+ M) $\rightarrow ICH_2OO$ (+ M). The upper limit values cited are based on the value where the goodness of fit to experimental data starts to deteriorate.

Preferred Values

Parameter	Value	T/K
k_1 /cm^3 molecule^{-1} s^{-1}	9.0×10^{-12}	298
Reliability		
$\Delta \log k$	± 0.3	298

Comments on Preferred Values

When the reaction of CH_2I with O_2 is used as a source of CH_2OO, secondary chemistry results, requiring simulations with a complex kinetic scheme to extract the rate coefficients of interest. The reported upper limit values of k reported by Buras et al. (2014) and Chhantyal-Pun, et al. (2015) and the value of Ting et al. (2014), who all used time-resolved UV absorption spectroscopy to determine CH_2OO kinetics, are consistent within the error limits. The value reported by Su et al. (2014) using the less sensitive IR detection to monitor CH_2OO kinetics is higher and has substantial error limits. The results of Ting et al. (2014) give a specific rate constant for the IO producing channel (k_1), which is the basis of the recommendation. The value of k_1 appears to be independent of pressure.

References

Buras, Z. J., Elsamra, R. M. and Green, W. H.: J. Phys. Chem. Lett., 5, 2224, 2014.

Chhantyal-Pun, R., Davey, A., Shallcross, D.E., Percival, C.J. and Orr-Ewing, A.J.: Phys. Chem. Chem. Phys., 17, 3617, 2015.

Su, Y-T., Huang, Y-H., Witek, H. and Lee, Y-P.: Science, 340, 174, 2013.

Su, Y-T., L, Lin, H-Y., Putikam, R., Matsui, H., Lin, M.C., and Lee, Y-P.: Nature Chem., 6, 477, 2014.

Ting, W-L, Chen, Y-H., Lee, Y-F, Matsui, H., Lee, Y-P. and Lin, J Jr -M.: J. Chem. Phys., 141, 104308, 2014.

CGI_7: $CH_2OO + CH_3CHO$

Last evaluated: June 2015; Last change in preferred values: June 2015

$CH_2OO + CH_3CHO \rightarrow$ products

Rate coefficient data

k/cm^3 molecule^{-1} s^{-1}	Temp./K	Reference	Technique/Comments
Absolute Rate Coefficients			
$(9.5 \pm 0.7) \times 10^{-13}$ (4 Torr)	293	Taatjes et al., 2012	PLP-PIMS (a)
$(1.48 \pm 0.04) \times 10^{-12}$ (25 Torr)	295	Stone et al., 2014	PLP-LIF/PIMS (b)
$\sim 2.2 \times 10^{-12}$ (50 Torr)			
$(1.7 \pm 0.5) \times 10^{-12}$ (760 Torr)	297	Berndt et al., 2015	Free-Jet FR-TOF-MS (c)
Relative Rate Coefficients			
$\sim 2.5 \times 10^{-12}$ (730 Torr)	295	Horie et al., 1999	Static system/FTIR (d)

Comments

(a) CH_2OO was produced by the reaction of $CH_2I + O_2$. CH_2I was generated by 248-nm laser photolysis of di-iodomethane, CH_2I_2, at 293 K and 4 Torr total pressure in a large excess of O_2. The reacting mixture was monitored by tunable synchrotron photoionization mass spectrometry, which allowed characterisation of the PIMS for CH_2OO and its reaction products over the region 9.5 – 11.5 eV. Time-resolved direct detection of CH_2OO at m/z = 46 amu. The measured decay constant of CH_2OO, which was linearly dependent on (excess) concentrations of acetaldehyde (up to 3.6×10^{14} molecule cm^{-3}), was used to determine the rate coefficient. The uncertainty limits are 95 %. No secondary ozonide was observed in the reaction products for $CH_2OO + CH_3CHO$ under reaction conditions, but $CH_3C(O)OH$ was identified as a product, probably formed by decomposition of secondary ozonide.

(b) Photolysis of CH_2I_2-O_2-N_2 mixtures in the presence of excess acetaldehyde (0.2 to 1.0×10^{15} molecule cm^{-3}), under pseudo-first-order conditions. Kinetics of $CH_2OO + CH_3CHO$ reaction were followed by time-resolved monitoring of HCHO product by laser-induced fluorescence (LIF) spectroscopy. $CH_2OO + CH_3CHO$ reaction rates were determined by fitting the single exponential growth of the fluorescence signal for different [CH_3CHO], and rate coefficients derived from a bimolecular plot at each total pressure (range: 25 – 300 Torr). The HCHO yields decreased with pressure indicating stabilisation of the initially formed ozonide.

(c) Rate coefficients for the bimolecular reaction of CH_2OO with acetaldehyde have been experimentally determined at 1 bar and (297±1) K by using a free-jet flow system. CH_2OO was produced by the $O_3 + C_2H_4$ reaction and [CH_2OO] was measured indirectly by titrating with excess SO_2 and measurement of product H_2SO_4 by ToF-CIMS. k was determined by non-linear regression fitting a parameterized expression for the [CH_3CHO] dependence of the ratio [H_2SO_4]/[C_2H_4], assuming $k_{uni} = 0.19$ s^{-1}, and appropriate uncertainty in the parameters. The value cited is close to the high-pressure limit calculated by Stone et al. (2014) from their direct measurements.

(d) Ozonolysis of ethene studied in the presence of CH_3CHO. The relative rates of CH_2OO reaction with CH_3CHO and CF_3COCF_3 determined at 730 Torr in synthetic air using FT-IR spectroscopy to monitor the decay of CF_3COCF_3 and production of the secondary ozonide (methyl-1,2,4-trioxolane) from the reaction with CH_3CHO, leading to $k(CH_2OO+CF_3COCF_3)/k(CH_2OO+CH_3CHO) \approx 13$. The cited value of k is calculated using the pressure independent value for $k(CH_2OO+CF_3COCF_3) = 3.2 \times 10^{-11}$ cm^3 molecule^{-1} s^{-1} (IUPAC, current recommendation).

Preferred Values

Parameter	Value	T/K
k_0 / cm^3 molecule^{-1} s^{-1}	1.6×10^{-29} [M]	298
k_∞ /cm^3 molecule^{-1} s^{-1}	1.7×10^{-12}	298
Reliability		
$\Delta \log k_0$	± 0.2	298
$\Delta \log k_\infty$	± 0.2	298

Comments on Preferred Values

The determinations of the rate coefficient for this reaction indicate that the reaction of CH_2OO with CH_3CHO is pressure dependent. This is assigned to pressure quenching (k_q) of the initially formed ozonide, which otherwise decomposes to HCHO (k_d). Stone et al. (2014) presented a Stern-Volmer analysis of the pressure dependence of the HCHO yields, corrected for any HCHO production from CH_2I_2 in the source chemistry. The Stern–Volmer plot gave an intercept of 1.19 ± 0.39 and slope (k_q/k_d) of $(1.09 \pm 0.08) \times 10^{-18}$ cm^3. Assuming an intercept of 1, the estimated yield of HCHO of 88 % at 4 Torr, and a yield of 4 % at 730 Torr, reconciling the results of Taatjes et al. (2012) and Horie et al. (1999). Taatjes et al. also observed acetic acid as a product at low pressure.

Stone et al. (2014) used the results of Taatjes et al. at 4 Torr ($k = 9.5 \times 10^{-13}$ cm^3 molecule^{-1} s^{-1}) with their own results at 25 Torr and at 50 Torr, together with the determination of k_q/k_d from the Stern–Volmer plot ($(1.09 \pm 0.08) \times 10^{-18}$ cm^3), to obtain estimates for the low and high pressure limits defining the pressure dependence of k over the atmospheric range, using a simple Lindemann-Hinshelwood mechanism for chemical activation. These form the basis of our 298 K preferred values, with k_∞ applying at pressures above about 100 Torr. The preferred value of k_∞ is also supported by the atmospheric pressure rate coefficient reported subsequently by Berndt et al. (2015).

References

Berndt, T., Kaethner, R., Voigtlander, J., Stratmann, F., Pfeifler, M, Reichler, P., Sipila, M., Kulmala, M., and Olzmann, M.: Phys. Chem. Chem. Phys., 17, 19862, 2015.

Horie, O., Schafer, C. and G. K. Moortgat: Int. J. Chem. Kinet., 31, 261, 1999.

Stone, D., Blitz, M., Daubney, L., Howes, N. U. M. and Seakins, P.: Phys. Chem. Chem. Phys., 16, 1139, 2014.

Taatjes, C. A., Welz, O, Eskola, A. J., Savee, J. D., Osborn, D. L., Lee, E. P. F., Dyke, J.M., Mok, D. W. K., Shallcross, D. E. and Percival, C. J.: Phys. Chem. Chem. Phys., 14, 10391, 2012.

CGI_8: $CH_2OO + CH_3C(O)CH_3$
Last evaluated: May 2018; Last change in preferred values: May 2018

$CH_2OO + CH_3C(O)CH_3 \rightarrow$ products

Rate coefficient data

k/cm^3 molecule^{-1} s^{-1}	Temp./K	Reference	Technique/Comments
Absolute Rate Coefficients			
$(2.3 \pm 0.3) \times 10^{-13}$ (4 Torr)	293	Taatjes et al., 2012	PLP-PIMS (a)
$(3.4 \pm 0.9) \times 10^{-13}$ (760 Torr)	297	Berndt et al., 2015	Free-Jet FR-TOF-MS (b)

Comments

(a) CH_2OO was produced by the reaction of $CH_2I + O_2$. CH_2I was generated by 248-nm laser photolysis of diiodomethane, CH_2I_2, at 293 K and 4 Torr total pressure in a large excess of O_2. The reacting mixture was monitored by tunable synchrotron photoionization mass spectrometry, which allowed characterisation of the PIMS for CH_2OO and its reaction products over the region 9.5 – 11.5 eV, and time-resolved direct detection of CH_2OO at m/z = 46 amu. The first order decay CH_2OO in the presence of excess known concentrations of acetone was used to determine the rate constants. The uncertainty limits are 95%. The secondary ozonide (3,3-dimethyl-1,2,4-trioxalane) was identified as a reaction product from its PIMS aided by quantum chemical calculations.

(b) Rate coefficients for the bimolecular reaction of CH_2OO with acetone have been experimentally determined at 1 bar and (297±1) K by using a free-jet flow system. CH_2OO was produced by the $O_3 + C_2H_4$ reaction and $[CH_2OO]$ was measured indirectly by titrating with excess SO_2 and measurement of product H_2SO_4 by ToF-CIMS. k was determined by non-linear regression fitting a parameterized expression for the $[CH_3C(O)CH_3]$ dependence of the ratio $[H_2SO_4]/[C_2H_4]$, assuming $k_{uni} = 0.19$ s^{-1}, and appropriate uncertainty in the parameters.

Preferred Values

Parameter	Value	T/K
k /cm^3 molecule^{-1} s^{-1}	3.4×10^{-13}	298
Reliability		
$\Delta \log k$	± 0.3	298

Comments on Preferred Values

The value of k reported by Berndt et al. (2015) at 1 bar is somewhat higher than that reported by Taatjes et al. (2012) at 4 Torr pressure, which was probably influenced by fall-off behaviour, as demonstrated for the $CH_2OO + CH_3CHO$ reaction by Stone et al. (2014). The rate measurements appear to be precise and consistent with the emerging reactivity pattern for CH_2OO reactivity. The recommendation applies to 1 bar pressure and probably corresponds to the high-pressure limit.

References

Berndt, T., Kaethner, R., Voigtlander, J., Stratmann, F., Pfeifler, M, Reichler, P., Sipila, M., Kulmala, M., and Olzmann, M.: Phys. Chem. Chem. Phys., 17, 19862, 2015.

Stone, D., Blitz, M., Daubney, L., Howes, N. U. M. and Seakins, P.: Phys. Chem. Chem. Phys., 16, 1139, 2014.

Taatjes, C. A., Welz, O, Eskola, A. J., Savee, J. D., Osborn, D. L., Lee, E. P. F., Dyke, J.M., Mok, D. W. K., Shallcross, D. E. and Percival, C. J.: Phys. Chem. Chem. Phys., 14, 10391, 2012.

CGI_9: $CH_2OO + CF_3C(O)CF_3$

Last evaluated: June 2015; Last change in preferred values: June 2015

$CH_2OO + CF_3C(O)CF_3 \rightarrow$ products

Rate coefficient data

k/cm^3 molecule^{-1} s^{-1}	Temp./K	Reference	Technique/Comments
Absolute Rate Coefficients			
$(3.0 \pm 0.3) \times 10^{-11}$	293	Taatjes et al., 2012	PLP-PIMS (a)
$(3.33 \pm 0.27) \times 10^{-11}$	295	Liu et al., 2014	PLP-LIF (b)

Comments

(a) CH_2OO was produced by the reaction of $CH_2I + O_2$. CH_2I was generated by 248-nm laser photolysis of diiodomethane, CH_2I_2, at 293 K and 4 torr total pressure in a large excess of O_2. The reacting mixture was monitored by tunable synchrotron photoionization mass spectrometry, which allowed characterisation of the PIMS for CH_2OO and its reaction products over the region 9.5 – 11.5 eV, and time-resolved direct detection of CH_2OO at m/z = 46 amu. The measured decay constant of CH_2OO, linearly dependent on known (excess) concentrations of hexafluoracetone ($0.01 – 1.0 \times 10^{14}$ molecule cm^{-3}), was used to determine the rate constant. The uncertainty limits are 95%.

(b) CH_2OO molecule generated by 351-nm laser flash photolysis of CH_2I/O_2 mixtures is accompanied by significant amounts of OH, observed by time resolved LIF. At least two different processes formed OH; a second, slower process appeared to be associated with the decay of CH_2OO. Using the OH signals as a proxy for the [CH_2OO] concentration in the presence of excess hexafluoroacetone the rate constant could be determined under pseudo first order conditions. k showed no pressure dependence over the range of 50−200 Torr, and the average value was $(3.33 \pm 0.27) \times 10^{-11}$ cm^3 molecule^{-1} s^{-1}.

Preferred Values

Parameter	Value	T/K
k /cm^3 molecule^{-1} s^{-1}	3.2×10^{-11}	298
Reliability		
$\Delta \log k$	± 0.1	298

Comments on Preferred Values

The rate constants for CH_2OO reaction with $CF_3C(O)CF_3$ appear to be accurately determined. The rate coefficient is larger than was measured for unsubstituted carbonyl compounds using a similar technique and is independent of pressure. Although the temperature dependence has not been investigated it is likely to be weak. The recommended temperature and pressure independent value is an unweighted mean of the values reported by Welz et al. (2012) and Liu et al. (2014). The products of this reaction were secondary ozonides, together with the products of ozonide decomposition.

References

Liu, Y., Bayes, K. D. and Sander, S. P.: J. Phys. Chem. A, 118, 741, 2014.
Taatjes, C. A., Welz, O, Eskola, A. J., Savee, J. D., Osborn, D. L., Lee, E. P. F., Dyke, J.M., Mok, D. W. K., Shallcross, D. E. and Percival, C. J.: Phys. Chem. Chem. Phys., 14, 10391, 2012.

CGI_11: CH_2OO + HC(O)OH

Last evaluated: May 2020; Last change in preferred values: May 2015

CH_2OO + HC(O)OH → products

Rate coefficient data

k/cm^3 molecule^{-1} s^{-1}	Temp./K	Reference	Technique/Comments
Absolute Rate Coefficients			
$(1.1 \pm 0.1) \times 10^{-10}$	298	Welz et al., 2014	PLP-PIMS (a)
$(1.1 \pm 0.1) \times 10^{-10}$	298		CEA/UVS (a)
$(1.14 \pm 0.06) \times 10^{-10}$	293	Chhantyal-Pun et al., 2018	PLP-CRDS (b)
Relative Rate Coefficients			
3.9×10^{-12}	293	Neeb et al., 1997	Static system/FTIR (c)

Comments

(a) CH_2OO was produced by the reaction of $CH_2I + O_2$. CH_2I was generated by 248-nm laser photolysis of diiodomethane, CH_2I_2, at 298 K and 4 Torr total pressure in a large excess of O_2. Two complementary techniques were used for time resolved detection of CH_2OO following its formation: multiplexed synchrotron photoionization mass spectrometry (MPIMS), and cavity enhanced broadband UV spectroscopy. The decay constant of CH_2OO was determined by fitting a single exponential to the decay curves for each acid concentration, and a linear dependence of the decay constant on [HCOOH] (up to 8×10^{12} molecule cm^{-3}) was observed, yielding the bimolecular rate coefficient. The uncertainty limits are 95%, based on unweighted linear fit to decay lifetime plots.

(b) CH_2OO was produced by 355 nm laser photolysis of diiodomethane in the presence of HC(O)OH, O_2 and N_2 at a total pressure of 13 mbar; and characterized by cavity ringdown ultraviolet absorption spectroscopy. Experiments were carried out under pseudo-first order conditions, with excess concentrations of HC(O)OH, and k was derived from the linear dependence of the decay constant on [HC(O)OH].

(c) The ozonolysis of ethene in the presence of H_2O (up to 0.18 % v/v) in air was investigated in a static chamber experiment at 293 K and 973 mbar, with FTIR analysis. The formation and removal of $HOCH_2OOH$ and HC(O)OH was investigated. Simulations of the system yielded the reported rate coefficient ratio, $k/k(CH_2OO + H_2O) = 14000$. The tabulated value of k is placed on an absolute basis using this ratio and $k(CH_2OO + H_2O) = 2.8 \times 10^{-16}$ cm^3 molecule^{-1} s^{-1} (IUPAC, current recommendation). However, it is noted that the dominant competing reaction would have been with $(H_2O)_2$ at the high end of the $[H_2O]$ range studied, consistent with a considerably higher value of k.

Preferred Values

Parameter	Value	T/K
k /cm^3 molecule^{-1} s^{-1}	1.1×10^{-10}	298
Reliability		
$\Delta \log k$	± 0.1	298

Comments on Preferred Values

The values of the rate coefficients obtained by two independent direct experimental techniques by Welz et al. (2014) and Chhantyal-Pun et al. (2018) give confidence that the reaction kinetics are well determined. The cited relative rate determination, using $CH_2OO + H_2O$ as a reference reaction, is uncertain because of the influence of the water dimer on the kinetics. The extremely rapid rates of the reactions of CH_2OO with organic acids contrasts with the slower rates for reaction with aliphatic carbonyl compounds, and is orders of magnitude larger than earlier estimates based on ozonolysis experiments. These results are consistent with quantum calculations (Aplincourt and Ruiz-Lopez, 2000) which suggest that the reaction of CH_2OO with acids proceeds through a barrierless association channel forming a hydroperoxymethylester of the acid, with no pre-reaction complex identified.

References

Aplincourt, P. and Ruiz-Lopez, M. F.: J. Phys. Chem., A,104, 380, 2000.

Chhantyal-Pun, R., Rotavera, B., McGillen, M. R., Khan, M. A. H., Eskola, A. J., Caravan, R. L., Blacker, L., Tew, D. P., Osborn, D. L., Percival, C. J., Shallcross, D. E. and Orr-Ewing A. J.: ACS Earth Space Chem., 2, 833, 2018.

Neeb, P., Sauer, F., Horie, O. and Moortgat, G. K.: Atmos. Environ, 31, 1417, 1997.

Welz, O, Eskola, A. J., Sheps, L., Rotavera, B., Savee, J. D., Scheer, M., D. Osborn, D. L., Lowe, D., Booth, M., Xiao, P., Khan, M. A. H., Percival, C. J., Shallcross, D. E. and Taatjes, C. A.: Angew. Chemie Int. Ed., 53, 4347, 2014.

CGI_10: $CH_2OO + CH_3C(O)OH$
Last evaluated: May 2020; Last change in preferred values: May 2020

$CH_2OO + CH_3C(O)OH \rightarrow$ products

Rate coefficient data

k/cm^3 molecule^{-1} s^{-1}	Temp./K	Reference	Technique/Comments
Absolute Rate Coefficients			
$(1.3 \pm 0.1) \times 10^{-10}$	298	Welz et al., 2014	PLP-PIMS (a)
$(1.2 \pm 0.1) \times 10^{-10}$	298		CEA/UVS (a)
$(1.25 \pm 0.30) \times 10^{-10}$	295	Berndt et al., 2017	Free-Jet FR-CIMS (b)
$(1.47 \pm 0.09) \times 10^{-10}$	293	Chhantyal-Pun et al., 2018	PLP-CRDS (c)

Comments

(a) CH_2OO was produced by the reaction of $CH_2I + O_2$. CH_2I was generated by 248-nm laser photolysis of diiodomethane, CH_2I_2, at 298 K and 4 Torr total pressure in a large excess of O_2. The reacting mixture was monitored by multiplexed synchrotron photoionization mass spectrometry (MPIMS), which allowed time resolved detection CH_2OO and its reaction products over the region 9.5 – 11.5 eV. Time-resolved direct detection of CH_2OO at m/z = 46 amu. The measured decay constant of CH_2OO which was linearly dependent on (excess) concentrations of acetic acid (up to 3.6×10^{14} molecule cm^{-3}) was used to determine the rate coefficient. The uncertainty limits are 95%, based on an unweighted linear fit to decay lifetime plots. No mass signal for adducts from the reaction products for $CH_2OO + CH_3C(O)OH$ was identified.

(b) CH_2OO was produced by the $O_3 + C_2H_4$ reaction in air in a free-jet flow reactor at 1 bar and 295 ± 2 K. CH_2OO was detected as CH_2OO-H^+ using CI-APi-TOF mass spectrometry. k was determined from the relative suppression of the steady state concentration of the protonated species as a function of $[CH_3C(O)OH]$.

(c) CH_2OO was produced by 355 nm laser photolysis of diiodomethane in the presence of $CH_3C(O)OH$, O_2 and N_2 at a total pressure of 13 mbar; and characterized by cavity ringdown ultraviolet absorption spectroscopy. Experiments were carried out under pseudo-first order conditions, with excess concentrations of $CH_3C(O)OH$, and k was derived from the linear dependence of the decay constant on $[CH_3C(O)OH]$.

Preferred Values

Parameter	Value	T/K
k /cm^3 molecule^{-1} s^{-1}	1.3×10^{-10}	298
Reliability		
$\Delta \log k$	± 0.1	298

Comments on Preferred Values

The values of *k* obtained by Welz et al. (2014) and Chhantyal-Pun et al. (2018), using two independent experimental techniques, and with CH_2OO produced from CH_2I_2 photolysis, give confidence that the reaction is very rapid and that the kinetics are well determined. The determination of *k* reported by Berndt et al. (2017), with CH_2OO produced from the O_3 + ethene reaction at atmospheric pressure, is less direct but yields a value of *k* that is in very good agreement with laser photolysis studies. The preferred value of *k* is based on the average of the determinations reported in the three studies.

The extremely rapid rates of the reactions of CH_2OO with organic acids contrasts with the slower rates for reaction with aliphatic carbonyl compounds. These results are consistent with quantum calculations which suggest that the reaction of CH_2OO with acids proceeds through a barrierless association channel forming a hydroperoxymethylester of the acid, with no pre-reaction complex identified.

References

Berndt, T., Herrmann, H. and Kurtén, T.: J. Am. Chem. Soc., 139, 13387, 2017.

Chhantyal-Pun, R., Rotavera, B., McGillen, M. R., Khan, M. A. H., Eskola, A. J., Caravan, R. L., Blacker, L., Tew, D. P., Osborn, D. L., Percival, C. J., Shallcross, D. E. and Orr-Ewing A. J.: ACS Earth Space Chem., 2, 833, 2018.

Welz, O, Eskola, A. J., Sheps, L., Rotavera, B., Savee, J. D., Scheer, M., D. Osborn, D. L., Lowe, D., Booth, M., Xiao, P., Khan, M. A. H., Percival, C. J., Shallcross, D. E. and Taatjes, C. A.: Angew. Chemie Int. Ed., 53, 4347, 2014.

CGI_23: $CH_2OO + CF_3C(O)OH$
Last evaluated: July 2017; Last change in preferred values: July 2017

$CH_2OO + CF_3C(O)OH \rightarrow$ products

Rate coefficient data

k/cm^3 molecule^{-1} s^{-1}	Temp./K	Reference	Technique/Comments
Absolute Rate Coefficients			
$(3.4 \pm 0.3) \times 10^{-10}$	294	Chhantyal-Pun et al., 2017	PLP-CRDS (a)
$3.8 \times 10^{-18}\ T^2 \exp[(1620 \pm 180)/T] + 2.5 \times 10^{-10}$	240-340		

Comments

(a) CH_2OO was produced by the reaction of $CH_2I + O_2$. CH_2I was generated by 248-nm laser photolysis of diiodomethane, CH_2I_2. Time-resolved direct detection of CH_2OO by CRDS at 355 nm in the temperature range 240 – 340 K. The measured decay constant of CH_2OO, which was linearly dependent on (excess) concentrations of trifluoroacetic acid (up to 3.6×10^{14} molecule cm^{-3}), was used to determine the rate coefficient. The uncertainty limits are 95%. The rate coefficients were independent of pressure over the range 13 – 130 mbar and H/D substitution had no effect on k at all temperatures in the range studied.

Preferred Values

Parameter	Value	T/K
k /cm^3 molecule^{-1} s^{-1}	3.3×10^{-10}	298
k /cm^3 molecule^{-1} s^{-1}	$3.8 \times 10^{-18}\ T^2 \exp(1620/T) + 2.5 \times 10^{-10}$	240-340
Reliability		
$\Delta \log k$	± 0.2	298
$\Delta E/R$	± 500	240-340

Comments on Preferred Values

The reaction of CH_2OO with trifluoroacetic acid at 294 K is extremely rapid, as found for reactions with other carboxylic acids (see data sheets CGI_10 and CGI_11). The rate coefficient decreases with increasing temperature in the range 240-340 K, and exceeds the estimates for collision-limited values. This suggests rate enhancement by capture mechanisms, attributable to the large permanent dipole moments of the two reactants. However, the observed temperature dependence is steeper than predicted by a simple dipole capture model with computed dipole moments. A different model involving competitive stabilization of a pre-reactive complex, binding the two reactants by two H-bonds, is proposed to explain the temperature dependence. This model was used in computational studies to describe the temperature dependence of the CH_2OO + HCOOH reaction (Long et al., 2009), which predicts an overall T-dependence of the form,

$$k = AT^2 \exp\left(\frac{\Delta H}{RT}\right) + k_d$$

where the first term describes the complex-forming reaction, and k_d is the rate coefficient for the direct (non complex-forming) reaction, approximated to be temperature-independent. The recommended parameters for CH_2OO + $CF_3C(O)OH$ are based on a fit to the experimental data, as reported by Chhantyal-Pun et al. (2017) using this model.

References

Chhantyal-Pun, R., McGillen, M. R., Beames, J. M., Khan, M. A. H., Percival, C. J., Shallcross, D. E., and Orr-Ewing, A. J.: Angew. Chem. Int. Ed., 56, 9044, 2017.

Long, B., Cheng, J. R., Tan, X. F., Zhang, W. J.: J. Mol. Struct. Theochem., 916, 159, 2009.

CGI_12: $CH_2OO + M$
Last evaluated: May 2020; Last change in preferred values: July 2019

$$CH_2OO + M \rightarrow H_2 + CO_2 + M \quad (1)$$
$$\rightarrow H + H + CO_2 + M \quad (2)$$
$$\rightarrow H + HOCO + M \quad (3)$$
$$\rightarrow H_2O + CO + M \quad (4)$$
$$\rightarrow HO + HCO + M \quad (5)$$

Rate coefficient data ($k = k_1 + k_2 + k_3 + k_4 + k_5$)

k/ s^{-1}	Temp./ K	Reference	Technique/Comments
Absolute Rate Coefficients			
< 120	295	Liu et al., 2014	LIF (HO product) (a)
< 11.6 ± 8.0	293	Chhantyal-Pun et al., 2015	PLP-CRDS (b)
0.19 ± 0.07 (1 bar)	297	Berndt et al., 2015	Free-Jet FR-TOF-MS (c)
$1.1^{+1.5}_{-1.1} \times 10^{-3}$ (1 bar)	298	Stone et al. 2018	PLP-UVA/LIF (d)
$k_0 = 3.2 \times 10^{-4} (T/298)^{-5.81} \exp(-12770/T)$ [M]	450-650		
$k_\infty = 1.4 \times 10^{13} (T/298)^{0.06} \exp(-10010/T)$	450-650		
Relative Rate Coefficients			
< 19.2 ± 5.1	297	Ouyang et al., 2013	(e)
≤ 8.9	293	Berndt et al., 2014	(f)
0.23 ± 0.12	293	Berndt et al., 2015	APFT-ToFMS/FTIR (f),(g)

Comments

(a) CH_2OO molecule generated by 351 nm laser flash photolysis of CH_2I/O_2 mixtures is accompanied by formation of significant amounts of HO, observed by time resolved LIF. At least two different processes formed HO; a second, slower process appeared to be associated with the decay of CH_2OO. Using the HO signals as a proxy for the [CH_2OO] concentration, in the absence of added reactant (SO_2 or $CF_3C(O)CF_3$) the inferred decomposition lifetime of CH_2OO was ~8 ms, corresponding to the cited upper limit for k.

(b) Cavity ring-down spectroscopy was used to perform kinetic measurements at 293 K under low pressure (10 to 30 Torr) conditions, for reactions of CH_2OO generated by (248 nm) laser photolysis of CH_2I_2 in the presence of O_2.and SO_2. The upper limit value of k tabulated above was determined from analysis of pseudo-first order decay constants at low [SO_2], following correction for removal via self-reaction and a proposed SO_2 catalysed CH_2OO isomerization.

(c) The rate coefficients of the unimolecular decomposition of CH_2OO, and its bimolecular reaction with the water monomer were determined at T = (297 ± 1) K and at atmospheric pressure by using a free-jet flow system. CH_2OO was produced by the reaction of ozone with C_2H_4, and [CH_2OO] was measured indirectly by titrating with excess SO_2 and detection of product H_2SO_4 after different reaction times in the range 1.1–7.5 s. Time-resolved experiments yielded the cited rate coefficient, $k = (0.19 \pm 0.07)$ s^{-1}. Additional experiments with a longer reaction time of 39.5 s were carried out in the atmospheric pressure flow tube IfT-LFT to determine k under steady-state conditions. The cited value, $k = (0.23 \pm 0.12)$ s^{-1}, includes a correction for wall loss, $k_{wall} = 0.034$ s^{-1}.

(d) Decomposition kinetics of stabilised CH_2OO and CD_2OO Criegee intermediates have been investigated as a function of temperature (450–650 K) and pressure 2.6 – 395 mbar, using flash photolysis coupled with time-resolved cavity-enhanced broadband UV absorption spectroscopy.

Production of HO radicals following CH_2OO decomposition was also monitored using LIF, with results indicating direct production of HO in the v = 0 and v = 1 states in low yields. Measurements of *k* were also made using time-resolved LIF of HO (v = 1) to monitor CH_2OO decay kinetics. Decomposition of CD_2OO was observed to be faster than CH_2OO under equivalent conditions Master equation calculations enabled fitting of the barriers for the decomposition of CH_2OO and CD_2OO to the experimental data. The low- and high-pressure limit rate coefficients are as tabulated above, with fitted F_c = 0.447. The median uncertainty was ~12% over the range of experimental conditions used. Extrapolation to atmospheric conditions yields k(298 K, 760 Torr) = $1.1^{+1.5}_{-1.1} \times 10^{-3}$ s^{-1}. For CD_2OO, the rate coefficients are $k_0 = 5.2 \times 10^{-5}(T/298)^{-5.28}\exp(-11\,610/T)$ cm^3 $molecule^{-1}$ s^{-1} and $k_\infty = 1.2 \times 10^{13}(T/298) \times 0.06 \exp(-9800/T)$ s^{-1}, with overall error of ~6% over the present range of temperature and pressure. The extrapolated k(298 K, 760 Torr) = $5.5^{+9}_{-5.5} \times 10^{-3}$ s^{-1}. The master equation calculations for CH_2OO indicate decomposition yields of 63.7% for $H_2 + CO_2$, 36.0% for $H_2O + CO$ and 0.3% for HO + HCO with no significant dependence on temperature between 400 and 1200 K or pressure between 1 and 3000 Torr.

(e) Photolysis of $CH_2I_2 – O_2 – N_2$- NO_2 mixtures at 348 nm in continuous flow conditions at 760 Torr pressure. Simultaneous measurement of products NO_3 and $[N_2O_5+NO_2]$ was made in a dual channel BB-CEAS at 663 nm. Analysis of these data as function of $[NO_2]$ allowed evaluation of the rate constant ratio: $k_I/k(CH_2OO + NO_2) = (6.4 \pm 1.7) \times 10^{12}$ molecule cm^{-3}, where k_I is the total loss rate constant for competing first order processes. Using $k(CH_2OO + NO_2) = 3 \times 10^{-12}$ cm^3 $molecule^{-1}$ s^{-1} (IUPAC, current recommendation) gives the tabulated value of k_I above, as an upper limit of *k* for thermal decomposition.

(f) CH_2OO produced from $O_3 + C_2H_4$ reaction at atmospheric pressure at 293 ± 0.5 K. H_2SO_4 formation from the reaction $CH_2OO + SO_2$ as a function of RH (= 2% to 50%) for close to atmospheric conditions, was measured using NO_3^-–CI–APi–TOF MS. The uncertainty in the $[H_2SO_4]$ estimated to be ± 45%. Measurements at the lowest relative humidity (RH ~2%) yield the rate coefficient ratio $k_I/k(CH_2OO + SO_2) \leq 2.4 \times 10^{11}$ molecule cm^{-3}, where k_I is the total first order loss coefficient for CH_2OO in the absence of water. Combining this ratio with $k(CH_2OO + SO_2) = 3.7 \times 10^{-11}$ (IUPAC, current recommendation) gives the upper limit value of *k* tabulated above.

(g) Analysis of data for steady state conditions from atmospheric pressure flow tube (IfT-LFT) at (293 ± 0.5) K with residence time = 39.5 s.

Preferred Values

Parameter	Value	T/K
k_0 /s^{-1}	$3.2 \times 10^{-4} (T/298)^{-5.81} \exp(-12770/T)$ [M]	450-650
k_∞ /s^{-1}	$1.4 \times 10^{13}(T/298)^{0.06} \exp(-10010/T)$	450-650
F_c	0.447	
k /s^{-1}	1×10^{-3} (1 bar)	298
Reliability		
$\Delta \log k$ (1 bar)	± 1.0	298
$\Delta (E_0/R)$	± 500	450-650
$\Delta (E_\infty/R)$	± 500	450-650

Comments on Preferred Values

The values of k derived from most of the experiments carried out at ambient temperature are upper limits because they relate to the total first order loss process, including thermal decomposition. The lowest value from direct studies at room temperature, using $CH_2I + O_2$ reaction as a source of CH_2OO, is that reported by Chhantyal-Pun et al. (2015), who presented evidence for an SO_2 catalysed CH_2OO isomerization, which gives rise to non-linear dependence of the decay constant of CH_2OO with $[SO_2]$. The occurrence of this process, together with the non-linearity due to presence of the self-reaction at high $[CH_2OO]$, leads to systematic inaccuracies in the measurement and assignment of the first order loss by slow thermal decomposition. However, Berndt et al. (2015) reported the lowest absolute determination of k, obtained from experiments using ozonolysis of ethene as a source of CH_2OO. That value of k agrees with those obtained in the same study relative to the $CH_2OO + SO_2$ reaction, also using ozonolysis of ethene as the CH_2OO source (Berndt et al., 2015).

The more recent measurements of Stone at al. (2018) indicate that the rate constant for decomposition of CH_2OO observed directly at higher temperatures exhibits pressure dependence typical of classic unimolecular decomposition of small molecules, i.e. fall-off behavior which can be fitted with the Troe formalism, modified to account for background losses. A global fit using data at all temperatures and pressures was performed to determine $k(p,T)$, described by the basic Troe formalism. We adopt their values of k_0, k_∞ and F_c in our recommendation, as given above for 450-650 K in the table of preferred values.

Extrapolation to room temperature using the parameters reported by Stone et al. (2018) gives: $k = 1.1^{+1.5}_{-1.1} \times 10^{-3}$ s^{-1} at 1 bar and 298 K, a value substantially lower than suggested from all room temperature experiments carried out previously. Reflecting that the room temperature values may have contributions from first-order loss processes other than decomposition, our preferred value of k at 1 bar and 298 K is tentatively based on the results of this extrapolation, but with wide reliability limits to reflect the uncertainties in the extrapolation procedure.

Olzmann et al. (1997) estimated k to be 0.33 s^{-1} at 1 bar and 298 K, using electronic structure calculations. Although in some conflict with the much lower value of k obtained by extrapolation of the high temperature results of Stone et al. (2018), this value, and those reported in the experimental study of Berndt et al. (2015), nevertheless confirm that unimolecular decomposition of CH_2OO is unimportant under atmospheric conditions, compared with removal by bimolecular reactions (particularly reaction with $(H_2O)_2$).

Many experimental product studies have reported evidence for unimolecular decomposition of CH_2OO, formed from alkene ozonolysis, including formation of HO radicals and other products identified in channels (1)-(5) listed above (e.g. see data sheet Ox_VOC5). However, the thermal stability of stabilized CH_2OO discussed above indicates that this is likely a result of prompt unimolecular decomposition of the chemically activated Criegee intermediate, $[CH_2OO]^*$.

References

Berndt, T., Voigtlander, J., Stratmann, F., Junninen, H., Mauldin III, R.L., Sipila, M., Kulmala,. M., and Herrmann, H.: Phys. Chem. Chem. Phys., 16, 19130, 2014.

Berndt, T., Kaethner, R., Voigtländer, J., Stratmann, F., Pfeifle, M., Reichle, P., Sipilä, M., Kulmala, M., Olzmann, M.: Phys. Chem. Chem. Phys., 17(30), 19862, 2015.

Chhantyal-Pun, R., Davey, A., Shallcross, D.E., Percival, C.J. and Orr-Ewing, A.J.: Phys. Chem. Chem. Phys., 17, 3617, 2015.

Liu, Y., Bayes, K. D. and Sander, S. P.: J. Phys. Chem. A 118, 741, 2014.

Olzmann, M., Kraka, E., Kremer, D., Gutbrod, R., and Andersson, S.: J. Phys. Chem. A, 101, 9421, 1997.

Ouyang, B., McLeod, M.W., Jones, R. L., and Bloss, W. J.: Phys. Chem. Chem. Phys., 15, 17070, 2013.

Stone, D. Au, K., Sime, S., Medeiros, D. J., Blitz, M., Seakins, P. W, Decker, Z., Sheps, L.: Phys. Chem. Chem. Phys., 20, 24940, 2018.

B2. Data sheets for thermal reactions of C_2 species

CGI_15: CH_3CHOO (*Z*- and *E*-) + SO_2

Last evaluated: May 2020; Last change in preferred values: May 2020

CH_3CHOO (*Z*- and *E*-) + SO_2 → products

Rate coefficient data

k/cm^3 molecule^{-1} s^{-1}	Temp./K	Reference	Technique/Comments
Absolute Rate Coefficients			
$k_{(Z\text{-})} = (2.4 \pm 0.3) \times 10^{-11}$	298	Taatjes et al., 2013	PLP-PIMS (a)
$k_{(E\text{-})} = (6.7 \pm 1.0) \times 10^{-11}$	298		
$k_{(Z\text{-})} = (2.9 \pm 0.3) \times 10^{-11}$	293	Sheps et al., 2014	PLP-CEUVA (b)
$k_{(E\text{-})} = (2.2 \pm 0.2) \times 10^{-10}$	293		
$(2.0 \pm 0.3) \times 10^{-11}$	295	Smith et al., 2014	PLP-CEUVA (c)
$(1.7 \pm 0.3) \times 10^{-11}$	295	Howes et al., 2018	PLP-PIMS (d)
$k_{(Z\text{-})} = (2.5 \pm 0.2) \times 10^{-11}$	298	Zhou et al., 2019	PLP-LIF (HO product) (e)

Comments

(a) CH_3CHOO was produced by the reaction of $CH_3CHI + O_2$. CH_3CHI was generated by 248-nm laser photolysis of 1,1-diiodoethane, $CH_3CH_2I_2$, at 298 K and 4 Torr, in a large excess of O_2. The reacting mixture was monitored by PIMS. Both *Z*- and *E*- conformers of CH_3CHOO are produced, which could be distinguished by the difference in their ionisation energies. It was demonstrated that *E*-CH_3CHOO is substantially more reactive toward SO_2 than is *Z*-CH_3CHOO. SO_3 production was observed, with a rise–time correlated with the decay-time of CH_3CHOO, showing it to be a primary product of the reaction. The first order decay of *Z*- and *E*-CH_3CHOO in the presence of excess SO_2 was measured. Linear fits to the first order decay constants vs. [SO_2] plots were used to determine $k_{(Z\text{-})}$ and $k_{(E\text{-})}$ for *Z*- and *E*-CH_3CHOO, respectively.

(b) CH_3CHOO prepared by PLP (266 nm) of CH_3CHI_2 in O_2/Ar mixtures at 5 - 20 Torr pressure. CH_3CHOO kinetics observed by recording the time-resolved UV absorption spectrum in the region 300 – 450 nm, corresponding to the $\tilde{B}$ (1A′) ← $\tilde{X}$(1A′) electronic transition. IO (formed from secondary chemistry) was also detected. Absorption features due to *Z*- and *E*- conformers of CH_3CHOO could be distinguished by their differing reactivities, reflected in their characteristic time dependencies, allowing conformer-specific rate coefficients to be determined. The pseudo-first order decay plots in presence of varying excess [SO_2] gave the cited values of $k_{(Z\text{-})}$ and $k_{(E\text{-})}$ for *Z*- and *E*-CH_3CHOO.

(c) CH_3CHOO prepared by PLP (266 nm) of CH_3CHI_2 in O_2/Ar mixtures and measured by wavelength-resolved transient absorption in a flow cell at 295 K and 15–100 Torr pressure (N_2). k was determined from plots of first order decay constant vs. [SO_2]. The absorption data quality did not allow distinction between the reactivity of *Z*- and *E*-conformers, but earlier work of Taatjes et al. (*Z*-:*E*- = 9:1) and Sheps et al. (*Z*-:*E*- = 3:1) suggests that the *Z*- conformer is dominant.

(d) CH_3CHOO generated by 248 nm laser photolysis of CH_3CHI_2 in the presence of O_2. The PIMS system used in this study was unable to differentiate between the reactivity of *Z*- and *E*-conformers

of CH_3CHOO, but earlier work of Taatjes et al. (*Z*-:*E*- = 9:1) and Sheps et al. (*Z*-:*E*- = 3:1) suggests that the *Z*- conformer is dominant.

(e) CH_3CHOO produced from 248 nm laser photolysis of CH_3CHI_2 in the presence of O_2, at 298 K at pressures in the range 10-100 Torr (Ar). The decay kinetics of *Z*-CH_3CHOO ($k_{(Z\text{-})}$) were monitored using HO as a marker species (LIF), making the assumption that the observed formation of HO is due to the thermal decomposition of *Z*-CH_3CHOO, with [HO] controlled by its rapid removal in the system (e.g. via reaction with CH_3CHI_2). Experiments were carried out under pseudo-first order conditions in the presence of excess [SO_2]. The tabulated value of $k_{(Z\text{-})}$ was determined from the dependence of the first-order decay constant on [SO_2].

Preferred Values

Parameter	Value	T/K
$k_{(Z\text{-})}$/cm^3 molecule^{-1} s^{-1}	2.6×10^{-11}	298
$k_{(E\text{-})}$/cm^3 molecule^{-1} s^{-1}	1.4×10^{-10}	298
Reliability		
$\Delta \log k_{(Z\text{-})}$	± 0.1	298
$\Delta \log k_{(E\text{-})}$	± 0.3	298

Comments on Preferred Values

CH_3CHOO has two possible conformers: *E*- and *Z*-CH_3CHOO, which differ in the orientation of the C-O-O group. This leads to conformer-dependent reactivity. Computational studies indicate that *Z*-CH_3CHOO is significantly less reactive than *E*-CH_3CHOO towards, e.g. H_2O (Anglada et al., 2011). Calculations place the *Z*- conformer ~15 kJ mol^{-1} lower in energy than *E*- CH_3CHOO (Kuwata et al., 2010), reflecting the zwitterionic character of the C–O bond. The barrier to interconversion of these conformers is substantial, ~160 kJ mol^{-1}, and consequently *Z*- and *E*-CH_3CHOO act as distinct chemical species at atmospheric temperatures.

The five studies of the reaction with SO_2 used the same source of acetaldehyde oxide, i.e. reaction of CH_3CHI with O_2, which produces both conformers of CH_3CHOO together with iodine atoms. The signal:noise characteristics of the spectra needed to define conformer differences is marginal so the parameter distinction is not well defined in the case of acetaldehyde oxide. Moreover, there is uncertainty in the relative amounts of the two conformers formed in the source chemistry. Nevertheless, the results for the rate coefficient for reaction of predominantly *Z*-CH_3CHOO with SO_2 are in good agreement, considering the uncertainties (quoted error limits were 1σ). The result of Sheps et al. (2014) for $k_{(E\text{-})}$ is a factor of ~3 higher than that obtained by Taatjes et al. (2013), and both determinations are significantly larger than their determinations of $k_{(Z\text{-})}$, and that of Zhou et al. (2019). The difference between these rate coefficients probably reflects the sensitivity and selectivity of the detection techniques; the decay data for *E*-CH_3CHOO using the UV spectroscopy method appears superior in quality to the PIMS but there is some uncertainty in the relative UV cross sections and initial yields of the two conformers, both of which are required to extract conformer-specific rate coefficients. The observed higher reactivity of the *E*-CH_3CHOO is consistent with theoretical predictions for the reactivity of the two conformers referred to above, and the preferred value of $k_{(E\text{-})}$ is the mean of the two reported values, which carries an uncertainty of a factor of 2. The preferred value of $k_{(Z\text{-})}$ is based on an unweighted mean of the determinations of Taatjes et al. (2013), Sheps et al. (2014) and Zhou et al. (2019), which are in good agreement.

Quantum chemical studies predict that the reactions of the CH_3CHOO conformers with SO_2 proceed via initial barrierless formation of chemically-activated cyclic secondary ozonides (Vereecken et al. 2012). As discussed for the $CH_2OO + SO_2$ reaction (data sheet CGI_1), the chemically-activated C_2 secondary ozonides are expected to isomerise and decompose mainly to form $CH_3CHO + SO_3$, and this is consistent with the results of direct kinetics studies at low pressures (Taatjes et al., 2013; Howes et al., 2018). At higher pressures, collisional stabilization of the secondary ozonides may be important (Vereecken et al. 2012), and further studies are required to characterize their onward reactions. Until additional theoretical and quantitative experimental product channel data become available, we recommend that the reaction predominantly forms CH_3CHO and SO_3.

References

Anglada, J. M., González, J. and Torrent-Sucarrat, M.: Phys., Chem. Chem. Phys. 13, 13034, 2011.

Kuwata, K. T., Hermes, M. R., Carlson, M. J. and Zogg, C. K.: J. Phys. Chem. A, 114, 9192, 2010.

Sheps, L., Scully, A. M., and Au, K.: Phys. Chem. Chem. Phys., 16, 19941, 2014.

Smith, M. C., Ting, W. L., Chang, C. H., Takahashi, K., Boering, K. A. and Lin, J. J. M.: J. Chem. Phys., 141, 074302, 2014.

Howes, N. U. M., Mir, Z. S., Blitz, M. A., Hardman, S., Lewis, T. R., Stone, D., and Seakins, P. W., Phys. Chem. Chem. Phys., 20, 22218, 2018.

Taatjes, C. A., Welz, O.; Eskola, A. J., Savee, J. D., Scheer, A. M., Shallcross, D. E., Rotavera, B., Lee, E. P. F., Dyke, J. M., Mok, D. K. W., Osborn, D. L., and Percival, C. J.: Science, 340, 177, 2013.

Vereecken, L., Harder, H. and Novelli, A.: Phys. Chem. Chem. Phys., 14, 14682, 2012.

Zhou, X., Liu, Y., Dong, W. and Yang, X.: J. Phys. Chem. Lett., 10(17), 4817, 2019.

CGI_16: CH_3CHOO (*Z*- and *E*-) + $H_2O/(H_2O)_2$
Last evaluated: February 2020; Last change in preferred values: February 2020

CH_3CHOO (*Z*- and *E*-) + $H_2O \rightarrow$ products (1)
CH_3CHOO (*Z*- and *E*-) + $(H_2O)_2 \rightarrow$ products (2)

Rate coefficient data

k/cm^3 molecule^{-1} s^{-1}	Temp./K	Reference	Technique/Comments
Absolute Rate Coefficients			
$k_{1(Z\text{-})} < 4 \times 10^{-15}$	298	Taatjes et al., 2013	PLP-PIMS (a)
$k_{1(E\text{-})} = (1.0 \pm 0.4) \times 10^{-14}$	298		
$k_{1(Z\text{-})} < 2 \times 10^{-16}$	293	Sheps et al., 2014	CE-UVAS (b)
$k_{1(E\text{-})} = (2.4 \pm 0.4) \times 10^{-14}$	293		
$k_{1(E\text{-})} = (1.31 \pm 0.26) \times 10^{-14}$	298	Lin et al., 2016	PLP-UVAS (c)
$k_{1(E\text{-})} = 1.11 \times 10^{-14} \exp[(50 \pm 644)/T]$	288-328		
$k_{2(E\text{-})} = (4.40 \pm 0.29) \times 10^{-11}$	298		
$k_{2(E\text{-})} = 5.21 \times 10^{-20} \exp[(6125 \pm 332)/T]$	288-328		
Relative Rate Coefficients			
$k_{1(E\text{-})} = (2.0 \pm 0.6) \times 10^{-14}$	293	Berndt et al., 2014	FT/CI-APi-TOF MS (d)
$k_{1(E\text{-})} = (4.9 \pm 4.3) \times 10^{-14}$	296-302	Newland et al., 2015	RR-FTIR/UVA/UV-F (e)

Comments

(a) CH_3CHOO was produced by the reaction of $CH_3CHI + O_2$. CH_3CHI was generated by 248-nm laser photolysis of 1,1-diiodoethane, $CH_3CH_2I_2$, at 298 K and 4 torr, in a large excess of O_2. The reacting mixture was monitored by tunable synchrotron photoionization mass spectrometry, which allowed characterisation of the PIMS. Both conformers of CH_3CHOO (*Z*- and *E*-) are produced in this process, and they could be distinguished by the difference in their ionisation energies. The first order decay of CH_3CHOO in the presence of excess known concentrations of H_2O up to 2.4×10^{16} molecule cm^{-3}, was used to determine the rate constants. It was demonstrated that decay of *Z*-CH_3CHOO was independent of the presence of H_2O at this concentration, allowing only the upper limit of $k_{1(Z\text{-})}$ to be determined. On the other hand decay of *E*-CH_3CHOO increased monotonically with $[H_2O]$, allowing $k_{1(E\text{-})}$ to be determined with some confidence.

(b) CH_3CHOO prepared by PLP (266 nm) of CH_3CHI_2 in O_2/Ar mixtures at 5 - 20 Torr pressure. The UV absorption spectrum of CH_3CHOO in the region 300 – 450 nm, corresponding to the $\tilde{B}$ (1A′) ← $\tilde{X}$(1A′) electronic transition was determined in this work, using time-resolved cavity enhanced absorption spectroscopy. Absorption features due to *Z*- and *E*- conformers of CH_3CHOO could be distinguished by their differing reactivities - reflected in characteristic time-dependences. IO (formed from secondary chemistry) was also detected. CH_3CHOO kinetics were investigated by recording the time-dependence of components due to *Z*- and *E*- conformers, and fitting the observed growth and decay curves. This allowed conformer-specific rate coefficients to be determined. The first-order decay rate of *Z*-CH_3CHOO, 160 ± 25 s^{-1}, did not change as a function of $[H_2O]$, giving the cited upper limit of $k_{1(Z\text{-})}$. For *E*-CH_3CHOO, the first-order decay rate increased linearly with $[H_2O]$, and the cited value for $k_{1(E\text{-})}$ was obtained by fitting to linear plots.

(c) CH_3CHOO prepared by PLP (266 nm) of CH_3CHI_2 in O_2/N_2 mixtures, mainly at 500 Torr pressure. The kinetics of CH_3CHOO removal were monitored by UV absorption at 368 nm as a

function of [H_2O]. Taking account of the relative cross-sections of the conformers at this wavelength ($\sigma_{(E\text{-})}/\sigma_{(Z\text{-})} \approx 3$), and their relative formation (*Z*-/*E*- ≈ 3), *E*- and *Z*- CH_3CHOO are expected to make comparable contributions to the absorption signal. Accordingly, the observed kinetics could be interpreted in terms of a combination of fast and slow decays (attributed to *E*- and *Z*-CH_3CHOO, respectively). The values of $k_{1(E\text{-})}$ and $k_{2(E\text{-})}$ tabulated above were extracted from the pseudo-first order decay constants for the fast component and the concentrations of [H_2O] and [$(H_2O)_2$], with reaction (1) dominating at low relative humidity and reaction (2) at high relative humidity. The results were consistent with a very strong negative temperature dependence of reaction (2) over the studied range (E_a = -50.9 ± 2.8 kJ mol^{-1}), but an insignificant temperature dependence of reaction (1). Analysis of the slow component resulted in a value of $k_{1(Z\text{-})} \approx 2.4 \times 10^{-16}$ cm^3 $molecule^{-1}$ s^{-1} across the studied temperature range. However, this was reported to be subject to significant uncertainty, and consistent with the upper limit of $k_{1(Z\text{-})} < 2 \times 10^{-16}$ cm^3 $molecule^{-1}$ s^{-1} reported by Sheps et al. (2014).

(d) CH_3CHOO prepared by the O_3 + *trans*-2-butene reaction in the presence of SO_2 in a flow system, equipped with CIMS for detection of H_2SO_4, using NO_3^- as reagent ion. Total pressure = 1 bar. Propane was also present to scavenge HO radicals. The effect of [H_2O] on yield of H_2SO_4 allowed determination of rate coefficient ratio $k(CH_3CHOO + H_2O)/k(CH_3CHOO + SO_2) = (8.8 \pm 0.4) \times 10^{-5}$ where *k* refers to the effective value for both conformers reacting. A refined analysis was conducted using a 'two conformer' model where distinction is made between *Z*- and *E*- conformers of different reactivity, which gave an improved fit to the [H_2SO_4] data. Assuming that *Z*-CH_3CHOO has negligible reactivity with H_2O compared to the *E*- conformer, as indicated by theoretical calculations (e.g. Ryzhkov and Ariya, 2004; Kuwata et al., 2010), their analysis gave $k_{1(E\text{-})}(CH_3CHOO + H_2O)/k_{(E\text{-})}(CH_3CHOO + SO_2) = 1.4 \times 10^{-4}$. The tabulated value uses $k_{(E\text{-})}(CH_3CHOO + SO_2) = 1.4 \times 10^{-10}$ cm^3molecule s^{-1} (IUPAC, current recommendation).

(e) The removal of SO_2 in the presence of but-2-ene/ozone systems was measured as a function of humidity in EUPHORE simulation chamber, under atmospheric boundary layer conditions. Cyclohexane was also present to scavenge HO radicals. SO_2 and O_3 abundance were measured using conventional fluorescence and UV absorption monitors, respectively; alkene abundance was determined via FTIR spectroscopy. SO_2 removal decreased with relative humidity (1.5 – 21%) confirming a significant reaction for CH_3CHOO with H_2O. The best fit to the data was obtained using a two-conformer model applied to data from both *cis*- and *trans*-2-butene isomers. The observed SO_2 removal kinetics are consistent with $k_{1(E\text{-})}(CH_3CHOO + H_2O)/k_{(E\text{-})}(CH_3CHOO + SO_2) = (3.5 \pm 3.1) \times 10^{-4}$. The cited value uses $k_{(E\text{-})}(CH_3CHOO + SO_2) = 1.4 \times 10^{-10}$ cm^3molecule s^{-1} (IUPAC, current recommendation)

Preferred Values

Parameter	Value	T/K
$k_{1(Z\text{-})}$ /cm^3 $molecule^{-1}$ s^{-1}	$< 2 \times 10^{-16}$	298
$k_{1(E\text{-})}$ /cm^3 $molecule^{-1}$ s^{-1}	1.3×10^{-14}	298
$k_{2(E\text{-})}$ /cm^3 $molecule^{-1}$ s^{-1}	4.4×10^{-11}	298
Reliability		
$\Delta \log k_{1(E\text{-})}$	± 0.3	298
$\Delta \log k_{2(E\text{-})}$	± 0.5	298

Comments on Preferred Values

The results of the direct studies of conformer-specific kinetics show that the *Z*-conformer is substantially less reactive than the *E*- conformer. This is consistent with the theoretical calculations of Anglada et.al. (2011), which predicted a lower reaction barrier for the *E*- form. The relative rate constants for the *E*- conformer reaction with H_2O relative to SO_2 were determined in two studies for CH_3CHOO produced by ozonolysis of *cis*- and/or *trans*-2-butene at 1 bar pressure. The results are consistent with the direct studies at both low pressure (4 to 20 Torr) and high pressure (500 Torr), where CH_3CHOO was produced from the reaction of CH_3CHI with O_2. Overall the results for $k_{1(E\text{-})}$ are consistent but the uncertainties of the relative rate studies are much larger due to possible systematic errors deriving from the analytical procedures.

The preferred upper limit value for $k_{1(Z\text{-})}$ is that determined in the study of Sheps et al. (2014), which was based on a well-defined absence of $[H_2O]$ dependence of $k_{1(Z\text{-})}$. The preferred values for $k_{1(E\text{-})}$ and $k_{2(E\text{-})}$ at 298 K are adopted from the direct UVA study of Lin et al. (2016), with that for $k_{2(E\text{-})}$ being the only reported laboratory determination. However, the preferred value for $k_{1(E\text{-})}$ is also consistent with those reported in the direct PIMS and UVA studies of Taatjes et al. (2013) and Sheps et al. (2014) (which are encompassed by the assigned uncertainty range), and comparable to the mean of the three direct determinations. Lin et al. (2016) also reported a very strong negative temperature dependence for $k_{2(E\text{-})}$, based on measurements over a 40 K temperature range. Although this is in qualitative agreement with theoretical calculations (e.g. Vereecken et al., 2017), the value of the temperature coefficient is substantially higher than predicted. At present, we make no recommendation for the temperature dependence, and await the results of confirmatory studies.

References

Anglada, J.M., Gonzalez, J., and Torrent-Sucarrat, M.: Phys. Chem. Chem. Phys., 13, 13034, 2011.

Berndt, T., Jokinen, T., Sipilä. M., Mauldin III, R.L., Herrmann, H., Stratmann, F., Junninen, H., and Kulmala, M.: Atmos. Environ., 89, 603, 2014.

Lin, L.-C., Chao, W., Chang, C.-H., Takahashi, K. and Lin, J.J.-M: Phys. Chem. Chem. Phys., 18, 28189, 2016.

Newland, M.J., Rickard, A.R., Alam, M.S., Vereecken, L., Munoz, A., Rodenas, M., and Bloss, W.J., Phys. Chem. Chem. Phys., 17, 4076, 2015.

Sheps, L., Scully, A. M. and Au, K.: Phys. Chem. Chem. Phys., 16, 26701, 2014.

Taatjes, C. A., Welz, O.; Eskola, A. J., Savee, J. D., Scheer, A. M., Shallcross, D. E., Rotavera, B., Lee, E. P. F., Dyke, J. M., Mok, D. K. W., Osborn, D. L., and Percival, C. J.: Science, 340, 171, 2013.

Vereecken, L., Novelli, A. and Taraborrelli, D.: Phys. Chem. Chem. Phys., 19, 31599, doi: 10.1039/c7cp05541b, 2017.

CGI_17: CH_3CHOO (*Z*- and *E*-) + NO_2
Last evaluated: February 2019; Last change in preferred values: February 2019

CH_3CHOO (*Z*- and *E*-) + NO_2 → products

Rate coefficient data

k/cm^3 molecule^{-1} s^{-1}	Temp./K	Reference	Technique/Comments
Absolute Rate Coefficients			
$(2 \pm 1) \times 10^{-12}$	298	Taatjes et al., 2013	PLP-PIMS (a)
$k_{(Z\text{-})} = (2.0 \pm 0.3) \times 10^{-12}$	298		
$k_{(E\text{-})} = (3.1 \pm 1.1) \times 10^{-12}$	298		
$k_{(Z\text{-})} = (1.7 \pm 0.3) \times 10^{-12}$ (20 Torr)	300	Caravan et al., 2017	PLP-PIMS (b)
$k_{(Z\text{-})} = (2.0 \pm 0.3) \times 10^{-12}$ (40 Torr)	300		

Comments

(a) CH_3CHOO was produced by the reaction of $CH_3CHI + O_2$. CH_3CHI was generated by 248 nm laser photolysis of 1,1-diiodoethane, $CH_3CH_2I_2$, at 298 K and 4 Torr, in a large excess of O_2. The reacting mixture was monitored by tunable synchrotron photoionization mass spectrometry, which allowed characterisation of the PIMS. Both *Z*- and *E*-CH_3CHOO are produced, which could be distinguished by the difference in the ionisation energy of the two conformers. The first order decay plots of *Z*- and *E*-CH_3CHOO in the presence of excess known concentrations of NO_2 were used to determine the rate constants. The cited values were given by unweighted fits of the data, with uncertainty limits of 95%; returns from weighted fits gave k values lower by 30% but also indicated a slightly larger value for *E*- conformer. Although a small (statistically significant at 1σ level) conformer dependence was reported, their preferred recommendation is $k = (2 \pm 1) \times 10^{-12}$ cm^3 molecule^{-1} s^{-1}, for both conformers.

(b) CH_3CHOO was produced by the reaction of $CH_3CHI + O_2$. CH_3CHI was generated by 248-nm pulsed laser photolysis of 1,1-diiodoethane, $CH_3CH_2I_2$, at 300 K and pressures of 20 and 40 Torr, in a large excess of O_2. The reacting mixture was monitored by PIMS at 10.5 eV, which allowed kinetic decay attributed to the *Z*- conformer of CH_3CHOO to be monitored. The first order decay plots in the presence of excess NO_2 (0 – 6.5 molecule cm^{-3}) were used to determine the rate constants. Products were investigated using multiplexed photoionization mass spectrometry.

Preferred Values

Parameter	Value	T/K
$k_{(Z\text{-})}$/cm^3 molecule^{-1} s^{-1}	2.0×10^{-12}	298
$k_{(E\text{-})}$/cm^3 molecule^{-1} s^{-1}	2.0×10^{-12}	298
Reliability		
$\Delta \log k_{(Z\text{-})}$	± 0.15	298
$\Delta \log k_{(E\text{-})}$	± 0.3	298

Comments on Preferred Values

The reported measurements on the overall rate coefficient for the reaction of *Z*- and *E*-CH_3CHOO with NO_2 from the two studies show good agreement. In the study of Taatjes et al. (2013) a slightly faster reaction with the *E*- conformer (statistically significant at 1σ confidence interval) was reported. However, the experiments suffered from low signal quality, and the conformer dependence was not well defined. The Caravan et al. (2017) kinetic measurements were confined predominantly to the *Z*-conformer of CH_3CHOO, and reported a barely significant pressure dependence over the range 20–40 Torr.

Earlier efforts to characterize the yield of NO_3 from this and other sCI + NO_2 reactions have been inconclusive. Many studies have failed to detect NO_3, including Caravan et al. (2017) over a pressure range of 4–40 Torr. However, a temporally resolved and [NO_2]-dependent signal was observed at the mass of the Criegee-NO_2 adduct for both the CH_2OO and CH_3CHOO systems, and the structure of this adduct was explored through *ab initio* calculations. Its origin from a direct CI reaction was demonstrated by observation of its efficient scavenging by SO_2. It is postulated that this adduct is the major reaction product and, based on the acetaldehyde signal, an upper limit of < 30 % is placed on the NO_3 + acetaldehyde yield. The fate of these Criegee-NO_2 adducts requires further investigation to fully understand the impact of this reaction on tropospheric NO_x.

References

Caravan, R. L., Khan, M. A. H., Rotavera, B., Papajak, E., Antonov, I. O., Chen, M.-W., Au, K., Chao, W., Osborn, D. L., Lin, J. J.-M., Percival, C. J., Shallcross, D. E., and C. A. Taatjes: Faraday Discuss., 200, 313, 2017.

Taatjes, C. A., Welz, O.; Eskola, A. J., Savee, J. D., Scheer, A. M., Shallcross, D. E., Rotavera, B., Lee, E. P. F., Dyke, J. M., Mok, D. K. W., Osborn, D. L., and Percival, C. J.: Science, 340, 171, 2013.

CGI_26: CH_3CHOO (*Z*- and *E*-) + HC(O)OH
Last evaluated: May 2020; Last change in preferred values: May 2020

CH_3CHOO (*Z*- and *E*-) + HC(O)OH → products

Rate coefficient data

k/cm^3 molecule^{-1} s^{-1}	Temp./K	Reference	Technique/Comments
Absolute Rate Coefficients			
$k_{(Z\text{-})} = (2.5 \pm 0.3) \times 10^{-10}$	298	Welz et al., 2014	PLP-PIMS (a)
$k_{(E\text{-})} = (5 \pm 3) \times 10^{-10}$	298		

Comments

(a) CH_3CHOO (acetaldehyde oxide) was produced by the reaction of $CH_3CHI + O_2$. CH_3CHI was generated by 248-nm laser photolysis of 1,1-diiodoethane, $CH_3CH_2I_2$, at 298 K and 4 Torr, in a large excess of O_2. Time resolved detection of CH_2OO following its formation was monitored using multiplexed synchrotron photoionization mass spectrometry (MPIMS). The decay constant of each of *Z*- and *E*-CH_3CHOO was determined by fitting a single exponential to the decay curves for each acid concentration, and a linear dependence of the decay constant on [HCOOH] was observed, yielding the bimolecular rate coefficient. The uncertainty limits are 95%, based on unweighted linear fit to decay lifetime plots.

Preferred Values

Parameter	Value	T/K
$k_{(Z\text{-})}$/cm^3 molecule^{-1} s^{-1}	2.5×10^{-10}	298
$k_{(E\text{-})}$/cm^3 molecule^{-1} s^{-1}	5.0×10^{-10}	298
Reliability		
$\Delta \log k_{(Z\text{-})}$	± 0.1	298
$\Delta \log k_{(E\text{-})}$	± 0.3	298

Comments on Preferred Values

The results of the direct studies of conformer-specific kinetics show that the *Z*- conformer of CH_3CHOO is less reactive than the *E*- conformer. This is consistent with the theoretical calculations, which generally predict a lower reaction barrier for the *E*- form. The preferred values of $k_{(Z\text{-})}$ and $k_{(E\text{-})}$ are based on the determinations reported in the sole kinetics study of Welz et al. (2014), and are consistent with the rapid reaction of CH_2OO with HC(O)OH, as also observed by Welz et al. (2014) and by Chhantyal-Pun et al. (2018).

The extremely rapid rates of the reactions of sCIs with organic acids have been interpreted using a dipole-capture model, with the results for a number of sCI-acid combinations being used to formulate a structure-activity relationship, SAR (Chhantyal-Pun et al., 2018). *k* is expected to be only very weakly dependent on temperature. Based on product measurements for the $CH_2OO + CF_3C(O)OH$ reaction (using PIMS), the reactions are believed to proceed via an insertion reaction to form hydroperoxyl-esters, consistent with the results of theoretical studies (e.g. Aplincourt and Ruiz-Lopez, 2000).

References

Aplincourt, P. and Ruiz-Lopez, M. F.: J. Phys. Chem., A,104, 380, 2000.

Chhantyal-Pun, R., Rotavera, B., McGillen, M. R., Khan, M. A. H., Eskola, A. J., Caravan, R. L., Blacker, L., Tew, D. P., Osborn, D. L., Percival, C. J., Shallcross, D. E. and Orr-Ewing A. J.: ACS Earth Space Chem., 2, 833, 2018.

Welz, O, Eskola, A. J., Sheps, L., Rotavera, B., Savee, J. D., Scheer, M., D. Osborn, D. L., Lowe, D., Booth, M., Xiao, P., Khan, M. A. H., Percival, C. J., Shallcross, D. E. and Taatjes, C. A.: Angew. Chemie Int. Ed., 53, 4347, 2014.

CGI_27: CH_3CHOO (*Z*- and *E*-) + $CH_3C(O)OH$
Last evaluated: May 2020; Last change in preferred values: May 2020

CH_3CHOO (*Z*- and *E*-) + $CH_3C(O)OH \rightarrow$ products

Rate coefficient data

k/cm^3 molecule^{-1} s^{-1}	Temp./K	Reference	Technique/Comments
Absolute Rate Coefficients			
$k_{(Z\text{-})} = (1.7 \pm 0.5) \times 10^{-10}$	298	Welz et al., 2014	PLP-PIMS (a)
$k_{(E\text{-})} = (2.5 \pm 0.6) \times 10^{-10}$	298		

Comments

(a) CH_3CHOO (acetaldehyde oxide) was produced by the reaction of $CH_3CHI + O_2$. CH_3CHI was generated by 248-nm laser photolysis of 1,1-diiodoethane, $CH_3CH_2I_2$, at 298 K and 4 Torr, in a large excess of O_2. Time resolved detection of CH_2OO following its formation was monitored using multiplexed synchrotron photoionization mass spectrometry (MPIMS). The decay constant of each of *Z*- and *E*-CH_3CHOO was determined by fitting a single exponential to the decay curves for each acid concentration, and a linear dependence of the decay constant on [$CH_3C(O)OH$] was observed, yielding the bimolecular rate coefficient. The uncertainty limits are 95%, based on unweighted linear fit to decay lifetime plots.

Preferred Values

Parameter	Value	T/K
$k_{(Z\text{-})}$/cm^3 molecule^{-1} s^{-1}	1.7×10^{-10}	298
$k_{(E\text{-})}$/cm^3 molecule^{-1} s^{-1}	2.5×10^{-10}	298
Reliability		
$\Delta \log k_{(Z\text{-})}$	± 0.15	298
$\Delta \log k_{(E\text{-})}$	± 0.15	298

Comments on Preferred Values

The results of the direct studies of conformer-specific kinetics show that the *Z*- conformer of CH_3CHOO is less reactive than the *E*- conformer. This is consistent with the theoretical calculations, which generally predict a lower reaction barrier for the *E*- form. The preferred values of $k_{(Z\text{-})}$ and $k_{(E\text{-})}$ are based on the determinations reported in the sole kinetics study of Welz et al. (2014), and are consistent with the rapid reaction of the CH_3CHOO conformers with HC(O)OH, as also observed by Welz et al. (2014).

The extremely rapid rates of the reactions of sCIs with organic acids have been interpreted using a dipole-capture model, with the results for a number of sCI-acid combinations being used to formulate a structure-activity relationship, SAR (Chhantyal-Pun et al., 2018). *k* is expected to be only very weakly dependent on temperature. Based on product measurements for the $CH_2OO + CF_3C(O)OH$ reaction (using PIMS), the reactions are believed to proceed via an insertion reaction to form hydroperoxyl-esters, consistent with the results of theoretical studies (e.g. Aplincourt and Ruiz-Lopez, 2000).

References

Aplincourt, P. and Ruiz-Lopez, M. F.: J. Phys. Chem., A,104, 380, 2000.

Chhantyal-Pun, R., Rotavera, B., McGillen, M. R., Khan, M. A. H., Eskola, A. J., Caravan, R. L., Blacker, L., Tew, D. P., Osborn, D. L., Percival, C. J., Shallcross, D. E. and Orr-Ewing A. J.: ACS Earth Space Chem., 2, 833, 2018.

Welz, O, Eskola, A. J., Sheps, L., Rotavera, B., Savee, J. D., Scheer, M., D. Osborn, D. L., Lowe, D., Booth, M., Xiao, P., Khan, M. A. H., Percival, C. J., Shallcross, D. E. and Taatjes, C. A.: Angew. Chemie Int. Ed., 53, 4347, 2014.

CGI_13: CH_3CHOO (*Z*- and *E*-) + M
Last evaluated: May 2020; Last change in preferred values: May 2020

CH_3CHOO (*Z*- and *E*-) + M → products

Rate coefficient data

k/ s^{-1}	P/mbar	Temp./K	Reference	Technique/Comments
Absolute Rate Coefficients				
$k_{(Z\text{-})}$, $k_{(E\text{-})} < 250$	5.3	298	Taatjes et al., 2013	PLP-PIMS (a)
$k_{(Z\text{-})} < 160 \pm 25$	6.7-27	298	Sheps et al., 2014	CE-UVA (b)
$k_{(E\text{-})} < 240$	6.7-27	298		
$3 < k_{(Z\text{-})} < 30$	133	293	Novelli et al., 2014	LIF (HO product) (c)
$k_{(Z\text{-})}$, $k_{(E\text{-})} < 150$	2.7 (He)	295	Howes et al., 2018	PLP-PIMS (d)
$k_{(Z\text{-})} = (182 \pm 66)$	33-133	298	Zhou et al., 2019	PLP-LIF (HO product) (e)
$k_{(Z\text{-})} = (67 \pm 15)$	400	278	Li et al., 2020	PLP-UVA (f)
$k_{(Z\text{-})} = (146 \pm 31)$	400	298		
$k_{(Z\text{-})} = (288 \pm 81)$	400	318		
Relative Rate Coefficients				
$76\ ^{+150}_{-50}$	1000*	298*	Fenske et al., 2000	(g)
$k_{(Z\text{-})} = 86 \pm 13$ $k_{(E\text{-})} = 38 \pm 24$	1000*	293	Berndt et al., 2014	(h)
$k_{(Z\text{-})} = 310 \pm 290$	1000*	296-302	Newland et al., 2015	(i)

Comments

(a) CH_3CHOO was produced by the reaction of $CH_3CHI + O_2$. CH_3CHI was generated by 248-nm laser photolysis of 1,1-diiodoethane, CH_3CHI_2, at 293 K and 4 Torr, in a large excess of O_2. The reacting mixture was monitored by PIMS from a synchrotron light source. Both *Z*- and *E*-conformers of CH_3CHOO are produced, which could be distinguished by the difference in their ionisation energies. The upper limit for k is assumed to be represented by the decay in the absence of added reagents to the gas mixtures, and was approximately the same for both conformers.

(b) CH_3CHOO prepared by PLP (266 nm) of CH_3CHI_2 in O_2/Ar mixtures at 5 - 20 Torr pressure. CH_3CHOO kinetics observed by recording the time-resolved UV absorption spectrum in the region 300 – 450 nm, corresponding to the $\tilde{B}$ (1A′) ← $\tilde{X}$(1A′) electronic transition. IO (formed from secondary chemistry) was also detected. Absorption features due to *Z*- and *E*- conformers of CH_3CHOO could be distinguished by their differing reactivities, reflected in their characteristic time dependences, allowing conformer-specific rate coefficients to be determined. The pseudo-first order decay plots in the absence of added H_2O gave the cited upper limit values of $k_{(Z\text{-})}$ and $k_{(E\text{-})}$ for *Z*- and *E*-CH_3CHOO.

(c) Observation of the time dependence of HO formation and removal (LIF) during the ozonolysis of propene or *cis*-but-2-ene in flow-tube experiments at 100 Torr pressure. k was calculated by assuming that the observed formation of HO, over timescales of up to about 30 ms, is due to the thermal decomposition of *Z*-CH_3CHOO. The analysis required simulations using a detailed chemical mechanism which also took account of HO removal reactions, primarily reaction with the precursor alkene.

(d) CH_3CHOO produced from 248 nm laser photolysis of CH_3CHI_2 in the presence of O_2, at 295 K at 2 Torr (He). The PIMS system used in this study was unable to differentiate between the reactivity of *Z*- and *E*-conformers of CH_3CHOO, but earlier work of Taatjes et al. (2013) and Sheps et al.

(2014) suggests that the *Z*- conformer is dominant. The reported upper limit for *k* was expected to include losses due to wall removal and self-reaction.

(e) CH_3CHOO produced from 248 nm laser photolysis of CH_3CHI_2 in the presence of O_2, at 298 K at pressures in the range 10-100 Torr (Ar). The decay kinetics of *Z*-CH_3CHOO ($k_{(Z-)}$) were monitored using HO as a marker species (LIF), making the assumption that the observed formation of HO is due to the thermal decomposition of *Z*-CH_3CHOO, with [HO] controlled by its rapid removal in the system (e.g. via reaction with CH_3CHI_2). Corrections for other loss processes for *Z*-CH_3CHOO under the experimental conditions (e.g. reaction with I atoms) were also made. The value of $k_{(Z-)}$ was reported to be insensitive to variation of pressure above 25 Torr, but was observed to decrease at lower pressure with a value of about 70 s^{-1} determined at 10 Torr.

(f) CH_3CHOO produced from 248 nm laser photolysis of CH_3CHI_2 in the presence of 10 Torr O_2, at 298 K. Measurements were made at pressures in the range 100-700 Torr (balance N_2 and H_2O). H_2O was present at concentrations of about 2×10^{17} molecule cm^{-3} or higher to remove *E*-CH_3CHOO via its rapid reactions with H_2O and (H_2O). *Z*-CH_3CHOO was monitored at 340 nm, and the observed decay constant, k_{obs}, was obtained as a function of the initial concentration, [*Z*-$CH_3CHOO]_0$. Values of $k_{(Z-)}$ were determined from the intercepts of k_{obs} vs. [*Z*-$CH_3CHOO]_0$ plots, following correction for the slow reaction of *Z*-CH_3CHOO with H_2O. Most experiments were carried out at 300 Torr total pressure, leading to the reported rate coefficients tabulated above. A weak dependence of $k_{(Z-)}$ on pressure was observed over the range 100-700 Torr at 298 K.

(g) Reaction studied in an atmospheric pressure flow-tube at room temperature, with CH_3CHOO produced from the ozonolysis of *trans*-but-2-ene. Excess acetaldehyde was added to the reaction mixture to allow thermalised CH_3CHOO to be converted to the corresponding secondary ozonide (SOZ). The SOZ was detected using FTIR. Numerical analysis of the observed SOZ formation at various time points along the tube allowed determination of k/k(CH_3CHOO + acetaldehyde) and an estimate of k(CH_3CHOO + acetaldehyde) = 1.0×10^{-12} cm^3molecule $^{-1}s^{-1}$; allowing the tabulated value of *k* to be reported. The *E*- and *Z*- conformers could not be resolved by the method, so that the reported parameters are bulk observations for their combined population.

(h) *Z*- and *E*-CH_3CHOO prepared by the O_3 + *trans*-2-butene reaction in the presence of SO_2 in an atmospheric pressure flow system, equipped with CIMS for detection of H_2SO_4, using NO_3^- as the reagent ion. Experiments performed as a function of [SO_2] allowed decomposition rates to be determined relative to the rate of reaction with SO_2. An expanded analysis using a two sCI model yielded the rate coefficient ratios $k_{(E-)}/k$(*E*-CH_3CHOO + SO_2) = $(2.7 \pm 1.7) \times 10^{11}$ molecule cm^{-3} and $k_{(Z-)}/k$(*Z*-CH_3CHOO + SO_2) = $(3.3 \pm 0.5) \times 10^{12}$ molecule cm^{-3}, where the former value also required correction for a pseudo-first order contribution to *E*-CH_3CHOO removal resulting from reaction with H_2O. The values of $k_{(E-)}$ and $k_{(Z-)}$ are placed on an absolute basis using k(*E*-CH_3CHOO + SO_2) = 1.4×10^{-10} cm^{-3} $molecule^{-1}$ s^{-1} and k(*Z*-CH_3CHOO + SO_2) = 2.6×10^{-11} cm^{-3} $molecule^{-1}$ s^{-1} (IUPAC, current recommendations).

(i) The removal of SO_2 in the presence of O_3 and either *cis*- or *trans*-but-2-ene was studied as a function of humidity, under atmospheric conditions in the EUPHORE chamber. The relative rate constants for the major competitive reactions, $k_{(Z-)}/k$(*Z*-CH_3CHOO + SO_2) = $(1.2 \pm 1.1) \times 10^{13}$ molecule cm^{-3} and k(*E*-CH_3CHOO + H_2O)/k(*E*-CH_3CHOO + SO_2) = $(3.5 \pm 3.1) \times 10^{-4}$, were determined from experiments performed over a range of [H_2O], allowing explicitly for the differing reactivity for the *Z*- and *E*- conformers. The decomposition rate constant, $k_{(Z-)}$, is placed on an absolute basis here using k(*Z*-CH_3CHOO + SO_2) = 2.6×10^{-11} cm^{-3} $molecule^{-1}$ s^{-1} (IUPAC, current recommendation).

Preferred Values

Parameter	Value	T/K
$k_{(Z\text{-})}$/ s^{-1}	150	298
$k_{(Z\text{-})}$/ s^{-1}	7.4×10^{6} exp(-3220/T)	275-320
$k_{(E\text{-})}$/ s^{-1}	60	298
Reliability		
$\Delta \log k_{(Z\text{-})}$	± 0.3	298
$\Delta \log k_{(E\text{-})}$	± 0.5	298
$\Delta (E_{(Z\text{-})}/R)$	± 700	275-320

Comments on Preferred Values

Measurements of the unimolecular decay rate coefficient for thermal decomposition of CH_3CHOO have been reported in five direct studies, using pulsed photolysis of CH_3CHI_2 as the source, and detection methods which provided a distinction between the *Z*- an *E*- conformers in four of these studies. The studies of Taatjes et al. (2013), Sheps et al. (2013) and Howes et al. (2018), performed at pressures below 30 mbar, provide only upper limit estimates because the observed decay rates are reported to include contributions from other processes, e.g. diffusive loss from the analyzing probe area, wall loss or self-reaction. The more recent studies of Zhou et al. (2019) and Li et al. (2020), performed at higher pressures over the range 33-930 mbar, provide firm measurements of $k_{(Z\text{-})}$, and suggest that the high-pressure limit is reached over this range. However, correction for a number of other loss processes for *Z*-CH_3CHOO were required, introducing a level of uncertainty into the determinations. It is also noted that the measurements of Zhou et al. (2019), using HO as a marker for *Z*-CH_3CHOO (see comment (e)), may also be complicated by other sources of HO in the system, e.g. from decomposition of the vinoxy radical co-product, which has been observed at pressures below about 270 mbar (see data sheet RO_22). The preferred values of $k_{(Z\text{-})}$ are therefore based on those reported as a function of temperature by Li et al. (2020), but with the assigned uncertainty at 298 K encompassing the determination of Zhou et al. (2019).

The relative rate determinations from ozonolysis of *cis*- and/or *trans*-but-2-ene, using reaction of CH_3CHOO with SO_2 as a reference, provide approximate indirect estimates of $k_{(Z\text{-})}$ and $k_{(E\text{-})}$, although the results are all consistent within the reported error limits. Clearly, further studies are required to allow the rates of unimolecular decomposition to be defined with more certainty. In the meantime, the preferred values of $k_{(Z\text{-})}$ and $k_{(E\text{-})}$ are based on those reported by Berndt et al. (2014), following correction to 298 K using the temperature dependences of the likely dominant decomposition reactions (see below) calculated by Vereecken et al. (2017). All of the absolute and relative rate determinations tabulated above are consistent with the preferred values, within the assigned reliability limits.

Theoretical studies predict the dominant decomposition reactions to be 1,4-H atom migration to a vinyl hydroperoxide intermediate for *Z*-CH_3CHOO, and 1,3-cyclisation to a dioxirane intermediate for *E*-CH_3CHOO; and the 298 K rates calculated by Vereecken et al. (2017), $k_{(Z\text{-})}$ = 136 and $k_{(E\text{-})}$ = 53, agree well with the preferred values. Although decomposition of *E*-CH_3CHOO is unlikely to compete with removal by bimolecular reactions under atmospheric conditions, the 1,4-H atom migration of *Z*-CH_3CHOO is estimated to be its major fate. The resultant vinyl hydroperoxide intermediate decomposes to produce HO and the vinoxy radical, and this mechanism more generally is believed to be the most important route to HO radical formation from the ozonolysis of alkenes.

References

Berndt, T., Jokinen, T., Sipilä, M., Mauldin, R. L., Herrmann, H., Stratmann, F., Junninen, H. and Kulmala, M.: Atmos. Environ., 89, 603, 2014.

Fenske, J. D., Hasson, A. S., Ho, A. W. and Paulson, S. E.: J. Phys. Chem. A, 104, 9921, 2000.

Li, Y.-L., Kuo, M-T. and Lin, J.J.-M.: RSC Adv., 10, 8518, 2020.

Newland, M. J., Rickard, A. R., Alam, M. S., Vereecken, L., Muñoz, A., Ródenas, M. and Bloss, W. J.: Phys. Chem. Chem. Phys., 17, 4076, 2015.

Novelli, A., Vereecken, L., Lelieveld, J. and Harder, H.: Phys. Chem. Chem. Phys.,16, 19941, 2014.

Sheps, L., Scully, A. M., and Au, K.: Phys. Chem. Chem. Phys., 16, 19941, 2014.

Taatjes, C. A., Welz, O.; Eskola, A. J., Savee, J. D., Scheer, A. M., Shallcross, D. E., Rotavera, B., Lee, E. P. F., Dyke, J. M., Mok, D. K. W., Osborn, D. L., and Percival, C. J.: Science, 340, 177, 2013.

Vereecken, L., Novelli, A. and Taraborrelli, D.: Phys. Chem. Chem. Phys., 19, 31599, doi: 10.1039/c7cp05541b, 2017.

Zhou, X., Liu, Y., Dong, W. and Yang, X.: J. Phys. Chem. Lett., 10(17), 4817, 2019.

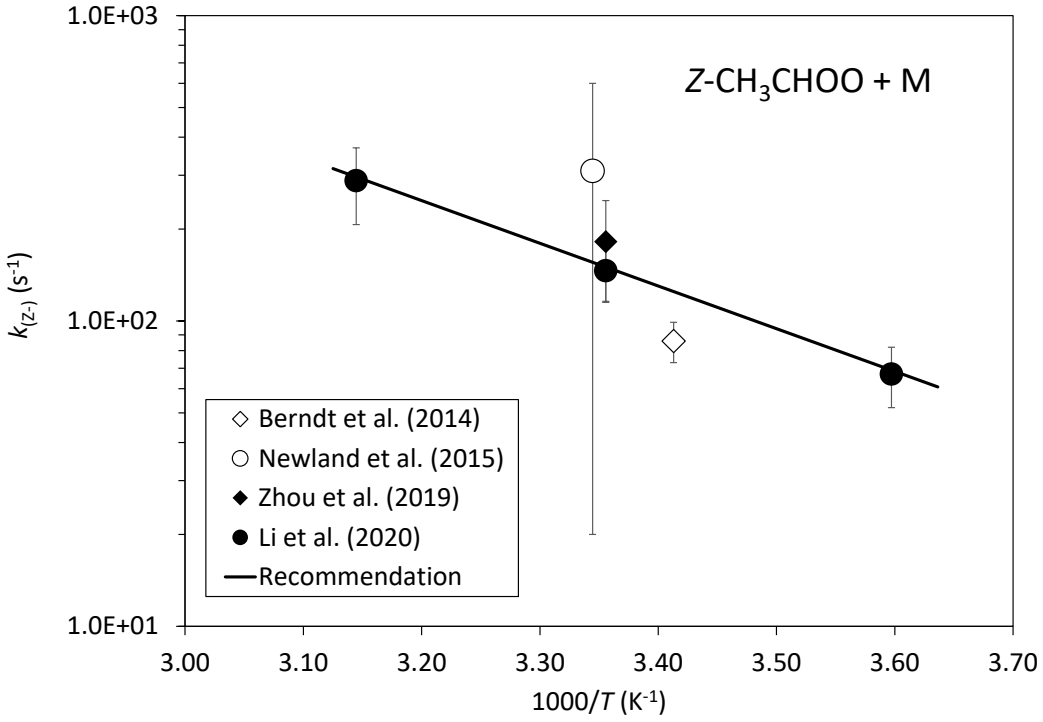

Arrhenius plot of $k_{(Z-)}$. Direct determinations are shown as filled points; relative rate determinations are shown as open points. The displayed errors are the experimental limits cited by the authors (but do not include uncertainty in the reference reaction for the relative rate studies). The line is the IUPAC recommendation, $k_{(Z-)} = 7.4 \times 10^6 \exp(-3220/T)$ s^{-1}.

B3. Data sheets for thermal reactions of C_3 species

CGI_18: $(CH_3)_2COO + SO_2$
Last evaluated: February 2020; Last change in preferred values: February 2020

$(CH_3)_2COO + SO_2 \rightarrow$ products

Rate coefficient data

k/cm^3 molecule^{-1} s^{-1}	P/mbar	Temp./K	Reference	Technique/Comments
Absolute Rate Coefficients				
$k_\infty = (1.32 \pm 0.13) \times 10^{-10}$	>133	298	Huang et al., 2015	PLP-LPUVA (a)
$\frac{(1.32 \pm 0.02) \times 10^{-10}\,[M]}{(4.88 \pm 0.32) \times 10^{17} + [M]}$	13-1030	298		
$k_\infty = (1.90 \pm 0.19) \times 10^{-10}$	400	283	Smith et al., 2016	PLP-LPUVA (b)
$k_\infty = (1.53 \pm 0.15) \times 10^{-10}$	400	293		
$k_\infty = (1.26 \pm 0.13) \times 10^{-10}$	400	303		
$(7.3 \pm 5.0) \times 10^{-11}$	5.3 (He)	298	Chhantyal-Pun et al., 2017	PLP-PIMS (c)
$(1.5 \pm 0.5) \times 10^{-10}$	13 (He)	298		
$k_\infty = (2.2 \pm 0.1) \times 10^{-10}$	67-133	293		PLP-CRDS (c)

Comments

(a) $(CH_3)_2COO$ was generated from pulsed photolysis at 248 nm (KrF excimer laser) of a gaseous mixture consisting of $(CH_3)_2CI_2$, O_2 and buffer gas (N_2). $(CH_3)_2COO$ was monitored by UV absorption in the region 300 – 450 nm, corresponding to the $\tilde{B}$ (1A′) ← $\tilde{X}$(1A′) electronic transition.. $(CH_3)_2COO$ decay kinetics were determined by recording the time-resolved UV absorption spectrum, after correction for other absorbers. IO, which is formed from a second channel of the reaction of iodoalkyl radicals with O_2, was also detected. The dependence of the first-order decay constants on [SO_2] was used to determine k, the values of which were independent of total pressure above 133 mbar (100 Torr). At lower pressures, the rate constant declined with pressure. This was attributed to participation of an unstable adduct formed in the reaction which can be collisionally stabilized. A simple Lindemann-Hinshelwood energy transfer model did not give a good fit to the pressure dependence. The empirical expression cited above, together with the value for the high-pressure limiting rate constant, k_∞, were reported.

(b) $(CH_3)_2COO$ was generated from pulsed photolysis of a gaseous mixture consisting of $(CH_3)_2CI_2$, O_2 and buffer gas (N_2) at 248 nm. Total pressure was 400 mbar, to ensure measurements of k were at the high pressure limit (i.e. k_∞). $(CH_3)_2COO$ was monitored by time-resolved UV absorption at 340 nm, due to the $\tilde{B}$ (1A′) ← $\tilde{X}$(1A′) electronic transition. The amount of $(CH_3)_2COO$ formed was estimated using a cross-section, $\sigma = 1.6 \times 10^{-17}$ cm^2 at 340 nm. Kinetic decays were recorded in the presence of different [SO_2], in the temperature range 283-303 K. The decay kinetics were pseudo-first order, and values of k_∞ were determined from the variation of the first-order decay constants with [SO_2]. The value of k_∞ exhibited a negative temperature dependence, (E/R = -1760 K).

(c) $(CH_3)_2COO$ was formed by laser photolysis of $(CH_3)_2CI_2$ in the presence of O_2, and characterized by synchrotron photoionization mass spectrometry (PIMS) and ultraviolet absorption cavity ringdown spectrometry (CRDS). The cited measurements of k were obtained under pseudo-first

order conditions in He buffer gas, using PIMS. Additional measurements at 293 K and a series of higher pressures (between 13 mbar and 133 mbar in N_2) using CRDS yielded larger rate coefficients, in the range $(1.84 \pm 0.12) \times 10^{-10}$ to $(2.29 \pm 0.08) \times 10^{-10}$ cm^3 molecule^{-1} s^{-1}. The tabulated limiting value at high pressure (k_∞) was reported, based on the measurements between 67 and 133 mbar N_2. The reaction of $(CD_3)_2COO$ with SO_2 was also studied at 4 Torr using PIMS. The results showed an inverse kinetic isotope effect with the deuterated rate coefficient, $(1.37 \pm 0.12) \times 10^{-10}$ cm^3 molecule^{-1} s^{-1}, approximately twice that for the un-deuterated reaction. It was suggested that this could reflect more effective collisional stabilization of the deuterated association complex because of the increased density of vibrational states.

Preferred Values

Parameter	Value	T/K
k_∞/ cm^3 molecule^{-1} s^{-1}	1.55×10^{-10}	298
k_∞/ cm^3 molecule^{-1} s^{-1}	$4.23 \times 10^{-13} \exp(1760/T)$	280-305
Reliability		
$\Delta \log k_\infty$	± 0.15	298
$\Delta (E/R)$	± 500	280-305

Comments on Preferred Values

The preferred values are based on all the tabulated studies, in which the rate coefficients were measured by direct kinetic methods. At pressures above about 133 mbar (100 Torr), k was found to be independent of pressure, and there is reasonable consistency in the results from the three studies. The preferred value of (E/R) is based on the data of Smith et al. (2016). The 298 K preferred value of k_∞ is the average of values reported at or near 298 K in the three studies, corrected for temperature where necessary using the preferred value of (E/R). It is noted that the rate coefficients measured by Chhantyal-Pun et al. (2017) are larger than those reported for similar conditions in the other studies (e.g. by about 40–50 % for k_∞), and this is reflected in the reliability assigned to the 298 K preferred value.

The studies of Huang et al. (2015) and Chhantyal-Pun et al. (2017) demonstrate that the value of k falls off at pressures below about 133 mbar (100 Torr). However, the decrease between 133 mbar and 13 mbar reported by Huang et al. (2015) (about a factor of two) is much greater than that reported by Chhantyal-Pun et al. (2017) (about 20 %). At present, therefore, we make no recommendation for the pressure dependence.

Chhantyal-Pun et al. (2017) also observed the production of SO_3, in experiments at 13 mbar using PIMS. The rise time of SO_3 was found to agree reasonably well with the observed decay of $(CH_3)_2COO$, confirming that SO_3 is a direct product of the reaction. Steady state kinetics studies in which loss of SO_2 (Newland et al., 2015) and formation of H_2SO_4 (Berndt et al., 2014) were measured during the ozonolysis of 2,2-dimethyl-but-2-ene give broadly similar relative rate constants, consistent with SO_3 formation remaining an important pathway at atmospheric pressure.

Quantum chemical studies predict that the reaction of $(CH_3)_2COO$ with SO_2 proceeds via barrierless formation of a chemically-activated cyclic secondary ozonide (Vereecken et al. 2012), and the near gas-kinetic experimental rate coefficient is consistent with this. The pressure dependence arises from the decomposition of the chemically-activated secondary ozonide back to reactants occurring in competition with its collisional stabilization. Decomposition via other routes (e.g. directly to $CH_3C(O)CH_3$ and SO_3) may also compete with collisional stabilization, although stabilization is

calculated to be efficient and dominant under atmospheric conditions. Further studies are required to characterize the reactions of the stabilized secondary ozonide, although the investigations of the ozonolysis of 2,2-dimethyl-but-2-ene at atmospheric pressure (e.g. Berndt et al., 2014; Newland et al., 2015) suggest that this must also form $CH_3C(O)CH_3$ and SO_3, at least partially. Veereecken et al. (2012) speculated that water-catalysed conversion of the longer-lived stabilized secondary ozonide into methyl acetate ($CH_3C(O)OCH_3$) + SO_2 might also be accessible, although further work is clearly required to confirm this. At present, we make no firm recommendations for product channel contributions, and await until additional theoretical and quantitative experimental product channel data.

References

Berndt, T., Jokinen, T., Sipilä, M., Mauldin, R. L., Herrmann, H., Stratmann, F., Junninen, H. and Kulmala, M.: Atmos. Environ., 89, 603, 2014.

Chhantyal-Pun, R., Welz, O., Savee J. D., Eskola, A. J., Lee, E. P. F., Blacker, L., Hill, H. R., Ashcroft, M., Khan, M. A. H., Lloyd-Jones, G. C., Evans, L., Rotavera, B., Rotavera H., Osborn, D. L., Mok, D. K. W., Dyke, J. M., Shallcross, D. E., Percival, C. J., Orr-Ewing, A. J. and Taatjes, C. A.: J. Phys. Chem. A, 121, 4, https://doi.org/10.1021/acs.jpca.6b07810, 2017.

Huang, H.-L., Chao, W. and Lin, J. J.-M.: Proc. Natl. Acad. Sci., 112(35), 10857, doi: 10.1073/pnas.1513149112, 2015.

Smith, M. C., Chao, W., Takahashi, K., Boering, K. A. and J. J.-M.: J. Phys. Chem. A, 120(27), 4789, 2016.

Newland, M. J., Rickard, A. R., Alam, M. S., Vereecken, L., Muñoz, A., Ródenas, M. and Bloss, W. J.: Phys. Chem. Chem. Phys., 17, 4076, 2015.

Vereecken, L., Harder, H. and Novelli, A.: Phys. Chem. Chem. Phys., 14, 14682, 2012.

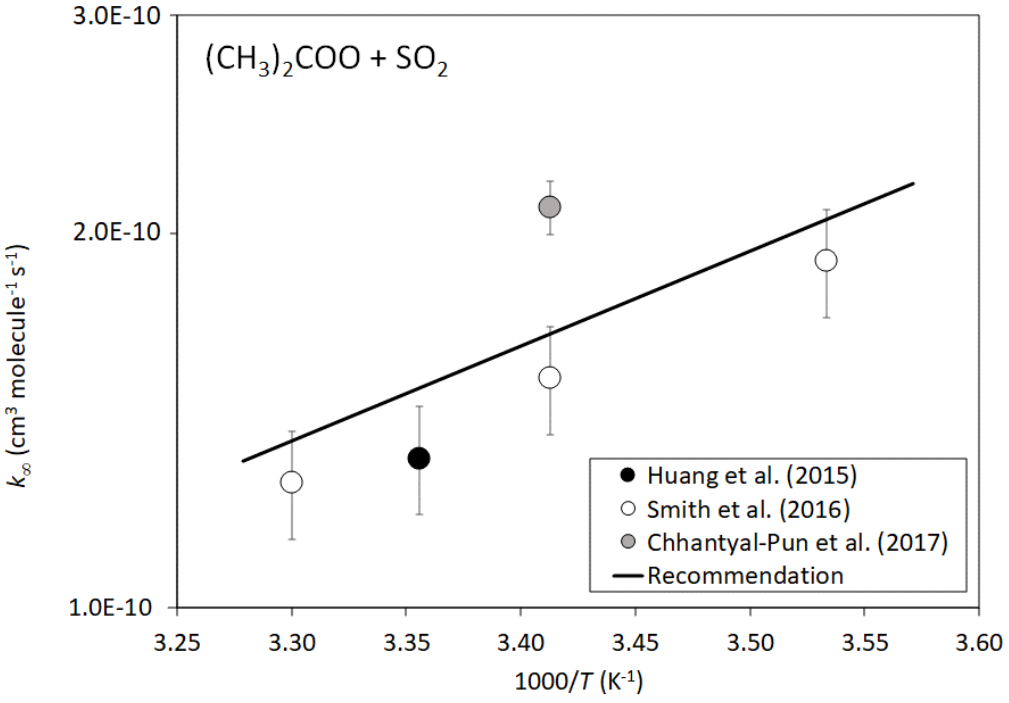

Arrhenius plot of $k_\infty((CH_3)_2COO + SO_2)$. The displayed errors are the experimental limits cited by the authors.

CGI_19: $(CH_3)_2COO + H_2O/(H_2O)_2$
Last evaluated: February 2020; Last change in preferred values: February 2020

$(CH_3)_2COO + H_2O \rightarrow$ products (1)
$(CH_3)_2COO + (H_2O)_2 \rightarrow$ products (2)

Rate coefficient data

k/cm^3 molecule^{-1} s^{-1}	Temp./K	Reference	Technique/Comments
Absolute Rate Coefficients			
$k_1 < 1.5 \times 10^{-16}$	298	Huang et al., 2015	PLP-LPUVA (a)
$k_2 < 1.3 \times 10^{-13}$	298		
Relative Rate Coefficients			
$k_1 = (6.4 \pm 3.4) \times 10^{-14}$	298	Becker et al., 1993	RR-FTIR/ TDLS (b)
$k_1 < 6.9 \times 10^{-16}$	293	Berndt et al., 2014	FT/CI-APi-TOF MS(c)
$k_1 = (1.34 \pm 0.39) \times 10^{-14}$	298-299	Newland et al., 2015	RR-FTIR/UVA/UVF (d)

Comments

(a) $(CH_3)_2COO$ was generated from the 248 nm pulsed photolysis of a gaseous mixture consisting of $(CH_3)_2CI_2$, O_2 and buffer gas (N_2) at 20 - 400 Torr total pressure. $(CH_3)_2COO$ was monitored by UV absorption in the region 300 – 450 nm, corresponding to the $\tilde{B}$ (1A′) ← $\tilde{X}$(1A′) electronic transition (Liu et al., 2014). IO was also detected and is thought to be formed from a second channel of the $(CH_3)_2CI_2 + O_2$ reaction. The $(CH_3)_2COO$ decay showed no dependence on $[H_2O]$ even at high concentrations (90% RH at 298 K), over a wide range of experimental conditions.

(b) Study of the 2,3-dimethyl-but-2-ene + O_3 reaction in the presence of 1 bar of synthetic air with and without added SO_2. Yields of H_2O_2 (a product of the title reaction) were measured by tunable diode laser absorption spectroscopy or by FTIR spectroscopy. The reported rate constant ratio $k_1/k((CH_3)_2COO + SO_2) = (4.1 \pm 2.2) \times 10^{-4}$ was reported. k_1 is placed on an absolute basis using $k((CH_3)_2COO + SO_2) = 1.55 \times 10^{-10}$ cm^3 molecule^{-1} s^{-1} at 298 K (IUPAC, current recommendation).

(c) $(CH_3)_2COO$ prepared by the O_3 + 2,3-dimethyl-but-2-ene reaction in the presence of SO_2 and propane (HO radical scavenger) in a flow system, equipped with CIMS for detection of H_2SO_4 using NO_3^- as reagent ion. Total pressure = 1 bar. The yield of $(CH_3)_2COO$ from the 2,3-dimethyl-but-2-ene + O_3 reaction was reported to be 0.45 ± 0.20. The effect of $[H_2O]$ (RH = 2 – 50%) on yield of H_2SO_4 was very weak and only allowed determination of an upper limit rate coefficient ratio $k_1/k((CH_3)_2COO + SO_2) < 4 \times 10^{-6}$ at 293 K. A distinct temperature dependence of H_2SO_4 formation was observed, attributed to the thermal decomposition of $(CH_3)_2COO$, which is its dominant loss reaction in this system. The cited upper limit value of k_1 uses $k((CH_3)_2COO + SO_2) = 4.23 \times 10^{-13} \exp(1760/T)$ cm^3 molecule^{-1} s^{-1} (IUPAC, current recommendation).

(d) The removal of SO_2 during the ozonolysis of 2,3-dimethyl-but-2-ene was measured as a function of humidity in EUPHORE simulation chamber, under atmospheric boundary layer conditions. Cyclohexane was also present to scavenge HO radicals. The SO_2 and O_3 abundance were measured using conventional fluorescence and UV absorption monitors, respectively; the alkene abundance was determined via FTIR spectroscopy. The yield of $(CH_3)_2COO$ from the 2,3-dimethyl-but-2-ene + O_3 reaction was reported to be 0.32 ± 0.20. The observed SO_2 removal kinetics are consistent with the rate constant ratio: k_1/k $((CH_3)_2COO+SO_2) = (8.7 \pm 2.5) \times 10^{-5}$. k_1 is placed on an absolute

basis using $k((CH_3)_2COO + SO_2) = 4.23 \times 10^{-13} \exp(1760/T)$ cm^3 molecule^{-1} s^{-1} (IUPAC, current recommendation).

Preferred Values

Parameter	Value	T/K
k_1/ cm^3 molecule^{-1} s^{-1}	$< 1.5 \times 10^{-16}$	298
k_2/ cm^3 molecule^{-1} s^{-1}	$< 1.3 \times 10^{-13}$	298

Comments on Preferred Values

All studies point to a slow reaction of $(CH_3)_2COO$ with H_2O. The relative rate determinations from ozonolysis of 2,3-dimethyl-2-butene do not show much consistency, however. The difficulty seems to lie in distinguishing the slow reaction with water from thermal decomposition and other pseudo-first order loss processes, which have similar, system dependent rates. The direct kinetic study of Huang et al. (2015) offers the most definitive picture which shows no dependence of the pseudo-first order decay constant on $[H_2O]$ over a wide range of conditions, which precludes any significant reaction with either monomer or dimer. These data form the basis of the preferred upper limit values for k_1 and k_2.

Quantum chemical studies predict that $(CH_3)_2COO$ is significantly less reactive with H_2O than *E*-CH_3CHOO (Anglada et al., 2011). This is consistent with experimental observations, as reflected in the IUPAC recommended rate coefficients for the two species.

References

Anglada, J.M., Gonzalez, J., and Torrent-Sucarrat, M.: Phys. Chem. Chem. Phys., 13, 13034, 2011.

Becker, K. H., Brockmann, K. J. and Bechara, J.: Atmos. Environ. A, 27(1), 57, 1993.

Berndt, T., Jokinen, T., Sipilä, M., Mauldin, R. L., Herrmann, H., Stratmann, F., Junninen, H. and Kulmala, M.: Atmos. Environ., 89, 603, 2014.

Huang, H.-L., Chao, W. and Lin, J. J.-M.: Proc. Natl. Acad. Sci., 112(35), 10857, doi: 10.1073/pnas.1513149112, 2015.

Newland, M. J., Rickard, A. R., Alam, M. S., Vereecken, L., Muñoz, A., Rodenas, M. and Bloss, W. J.: Phys. Chem. Chem. Phys., 17, 4076, 2015.

CGI_20: $(CH_3)_2COO + NO_2$
Last evaluated: March 2017; Last change in preferred values: March 2017

$(CH_3)_2COO + NO_2 \rightarrow$ products

Rate coefficient data

k/cm^3 molecule^{-1} s^{-1}	Temp./K	Reference	Technique/Comments
Absolute Rate Coefficients			
$(2.3 \pm 2.5) \times 10^{-12}$	293	Chhantyal-Pun et al., 2017	PLP-PIMS (c)
$(2.1 \pm 0.3) \times 10^{-12}$ ($(CD_3)_2COO$)	293		

Comments

(a) $(CH_3)_2COO$ was generated by 248 nm laser photolysis of $(CH_3)_2CI_2$ at 293 K and 4 Torr, in a large excess of O_2. Tunable synchrotron PIMS was used to measure time-dependence of [$(CH_3)_2COO$] in the gas phase. A large background signal at m/z = 74 prevented reliable measurement of the rate coefficient. The cited result, $(2.3 \pm 2.5) \times 10^{-12}$ cm^3 molecule^{-1} s^{-1}, should therefore be interpreted as an upper limit value of $k \leq 5 \times 10^{-12}$ cm^3 molecule^{-1} s^{-1}. However, in the case of $(CD_3)_2COO$ the background had a negligible effect, allowing accurate measurement of its rate coefficient for reaction with NO_2, as tabulated above.

Preferred Values

Parameter	Value	T/K
k/ cm^3 molecule^{-1} s^{-1}	2.1×10^{-12}	298
Reliability		
$\Delta \log k$	± 0.3	298

Comments on Preferred Values

The reported measurement of k for the reaction of $(CH_3)_2COO$ with NO_2 suffers from interference from a background signal. However, that for the deuterated form, $(CD_3)_2COO$, is similar to those for CH_2OO and both *Z*- and *E*-CH_3CHOO reacting with NO_2 (see data sheets CGI_2 and CGI_17). The overall body of data therefore appears to show that all Criegee intermediates react with NO_2 with similar rates, with k close to 2×10^{-12} cm^3 molecule^{-1} s^{-1}.

Attempts to measure NO_3 from the reaction of $(CD_3)_2COO$ with NO_2 failed (Chhantyal-Pun et al., 2017), as have similar attempts for other sCI reactions with NO_2 (Taatjes et al., 2013; Caravan et al., 2017). However, there are several possible association channels leading to addition complexes, and nitrate production observed in ozonolysis experiments may result from further reaction of these complexes. Caravan et al (2017) have shown conclusively that a stable addition product accounts for the major fraction of the products of the reaction of *Z*-CH_3CHOO with NO_2.

References

Caravan, R. L., Khan, M. A. H., Rotavera, B., Papajak, E., Antonov, I. O., Chen, M.-W., Au, K., Chao, W., Osborn, D. L., Lin, J. J.-M., Percival, C. J., Shallcross, D. E. and C. A. Taatjes: Faraday

Discuss., 200, 313, 2017.
Chhantyal-Pun, R., Welz, O., Savee J. D., Eskola, A. J., Lee, E. P. F., Blacker, L., Hill, H. R., Ashcroft, M., Khan, M. A. H., Lloyd-Jones, G. C., Evans, L., Rotavera, B., Rotavera H., Osborn, D. L., Mok, D. K. W., Dyke, J. M., Shallcross, D. E., Percival, C. J., Orr-Ewing, A. J. and Taatjes, C. A.: J. Phys. Chem. A, 121, 4, https://doi.org/10.1021/acs.jpca.6b07810, 2017.
Stone, D., Blitz, M., Daubney, L., Howes, N. U. M. and Seakins, P.: Phys. Chem. Chem. Phys., 16, 1139, 2014.
Taatjes, C. A., Welz, O.; Eskola, A. J., Savee, J. D., Scheer, A. M., Shallcross, D. E., Rotavera, B., Lee, E. P. F., Dyke, J. M., Mok, D. K. W., Osborn, D. L., and Percival, C. J.: Science, 340, 171, 2013.
Welz, O, Savee, J. D. Osborn, D. L., Vasu, S. S., Percival, C. J., Shallcross, D. E. and Taatjes, C. A.: Science, 335, 204, 2012.

CGI_28: $(CH_3)_2COO$ + HC(O)OH
Last evaluated: May 2020; Last change in preferred values: May 2020

$(CH_3)_2COO$ + HC(O)OH → products

Rate coefficient data

k/cm^3 molecule^{-1} s^{-1}	Temp./K	Reference	Technique/Comments
Absolute Rate Coefficients			
$(3.1 \pm 0.2) \times 10^{-10}$	293	Chhantyal-Pun et al., 2018	PLP-CRDS (a)

Comments

(a) $(CH_3)_2COO$ was produced by 355 nm laser photolysis of 2,2-diiodopropane in the presence of HC(O)OH, O_2 and N_2 at a total pressure of 13 mbar; and characterized by cavity ringdown ultraviolet absorption spectroscopy. Experiments were carried out under pseudo-first order conditions, with excess concentrations of HC(O)OH, and k was derived from the linear dependence of the decay constant on [HC(O)OH].

Preferred Values

Parameter	Value	T/K
k /cm^3 molecule^{-1} s^{-1}	3.1×10^{-10}	298
Reliability		
$\Delta \log k$	± 0.1	298

Comments on Preferred Values

The preferred value of k at 298 K is based on the determination reported in the sole kinetics study of Chhantyal-Pun et al. (2018). The extremely rapid rates of the reactions of sCIs with organic acids have been interpreted using a dipole-capture model, with the results for a number of sCI-acid combinations being used to formulate a structure-activity relationship, SAR (Chhantyal-Pun et al., 2018). The temperature dependence in k is expected to be weak. Based on product measurements for the CH_2OO + $CF_3C(O)OH$ reaction (using PIMS), the reactions are believed to proceed via an insertion reaction to form hydroperoxyl-esters, consistent with the results of theoretical studies (e.g. Aplincourt and Ruiz-Lopez, 2000).

References

Aplincourt, P. and Ruiz-Lopez, M. F.: J. Phys. Chem., A,104, 380, 2000.

Chhantyal-Pun, R., Rotavera, B., McGillen, M. R., Khan, M. A. H., Eskola, A. J., Caravan, R. L., Blacker, L., Tew, D. P., Osborn, D. L., Percival, C. J., Shallcross, D. E. and Orr-Ewing A. J.: ACS Earth Space Chem., 2, 833, 2018.

CGI_29: $(CH_3)_2COO + CH_3C(O)OH$
Last evaluated: May 2020; Last change in preferred values: May 2020

$(CH_3)_2COO + CH_3C(O)OH \rightarrow$ products

Rate coefficient data

k/cm^3 molecule^{-1} s^{-1}	Temp./K	Reference	Technique/Comments
Absolute Rate Coefficients			
$(3.1 \pm 0.2) \times 10^{-10}$	293	Chhantyal-Pun et al., 2018	PLP-CRDS (a)

Comments

(a) $(CH_3)_2COO$ was produced by 355 nm laser photolysis of 2,2-diiodopropane in the presence of $CH_3C(O)OH$, O_2 and N_2 at a total pressure of 13 mbar; and characterized by cavity ringdown ultraviolet absorption spectroscopy. Experiments were carried out under pseudo-first order conditions, with excess concentrations of $CH_3C(O)OH$, and k was derived from the linear dependence of the decay constant on $[CH_3C(O)OH]$.

Preferred Values

Parameter	Value	T/K
k /cm^3 molecule^{-1} s^{-1}	3.1×10^{-10}	298
Reliability		
$\Delta \log k$	± 0.1	298

Comments on Preferred Values

The preferred value of k at 298 K is based on the determination reported in the sole kinetics study of Chhantyal-Pun et al. (2018). The extremely rapid rates of the reactions of sCIs with organic acids have been interpreted using a dipole-capture model, with the results for a number of sCI-acid combinations being used to formulate a structure-activity relationship, SAR (Chhantyal-Pun et al., 2018). The temperature dependence in k is expected to be weak. Based on product measurements for the $CH_2OO + CF_3C(O)OH$ reaction (using PIMS), the reactions are believed to proceed via an insertion reaction to form hydroperoxyl-esters, consistent with the results of theoretical studies (e.g. Aplincourt and Ruiz-Lopez, 2000).

References

Aplincourt, P. and Ruiz-Lopez, M. F.: J. Phys. Chem., A,104, 380, 2000.

Chhantyal-Pun, R., Rotavera, B., McGillen, M. R., Khan, M. A. H., Eskola, A. J., Caravan, R. L., Blacker, L., Tew, D. P., Osborn, D. L., Percival, C. J., Shallcross, D. E. and Orr-Ewing A. J.: ACS Earth Space Chem., 2, 833, 2018.

CGI_24: $(CH_3)_2COO + CF_3C(O)OH$
Last evaluated: July 2017; Last change in preferred values: July 2017

$(CH_3)_2COO + CF_3C(O)OH \rightarrow$ products

Rate coefficient data

k/cm^3 molecule^{-1} s^{-1}	Temp./K	Reference	Technique/Comments
Absolute Rate Coefficients			
$(6.1 \pm 0.2) \times 10^{-10}$	294	Chhantyal-Pun et al., 2017	PLP-PIMS (c)
$4.9 \times 10^{-18}\ T^2 \exp[(1620 \pm 230)/T) + 5.2 \times 10^{-10}$	259-313		

Comments

(a) $(CH_3)_2COO$ was produced by the reaction of $(CH_3)_2CI + O_2$. $(CH_3)_2CI$ was generated by 248-nm laser photolysis of $(CH_3)_2CI_2$. Time-resolved direct detection of $(CH_3)_2COO$ by cavity ring-down spectroscopy at 355nm. $(CH_3)_2COO$ concentrations were ~2×10^{12} molecule cm^{-3}, deduced using previously published absorption cross sections. The measured decay constant of $(CH_3)_2COO$, which was linearly dependent on (excess) concentrations of $CF_3C(O)OH$ (up to 3.6×10^{14} molecule cm^{-3}), was used to determine the rate coefficient. The rate coefficients were independent of pressure over the range 13 – 130 mbar and H/D substitution had no effect on k at all temperatures in the range studied. The expression for the temperature dependence is based on a model involving competitive stabilization of a pre-reactive complex.

Preferred Values

Parameter	Value	T/K
k/ cm^3 molecule^{-1} s^{-1}	6.2×10^{-10}	298
k/ cm^3 molecule^{-1} s^{-1}	$4.9 \times 10^{-18}\ T^2 \exp(1620/T) + 5.2 \times 10^{-10}$	260-315
Reliability		
$\Delta \log k$	± 0.2	298
$\Delta (E/R)$	± 500 K	260-315

Comments on Preferred Values

There has only been one study of the reaction of $(CH_3)_2COO$ with trifluoroacetic acid (Chhantyal-Pun et al., 2017). The reaction is extremely rapid at 294 K, as found for reaction of CH_2OO with carboxylic acids (see IUPAC data sheets CGI_10, CGI_11 and CGI_23). The rate coefficient is independent of pressure and exceeds the estimates for collision-limited values, suggesting rate enhancement by capture mechanisms attributable to the large permanent dipole moments of the two reactants. The observed temperature dependence was best represented by a model involving competitive stabilization of a pre-reactive complex (Long et al., 2009), which predicts an overall T-dependence of the form,

$$k = AT^2 \exp\left(\frac{\Delta H}{RT}\right) + k_d$$

where the first term describes the complex-forming reaction, and k_d is the rate coefficient for the direct (non complex-forming) reaction, approximated to be temperature-independent. The recommended parameters are based on a fit of the experimental data using this model, as reported by Chhantyal-Pun et al. (2017).

References

Chhantyal-Pun, R., McGillen, M. R., Beames, J. M., Khan, M. A. H., Percival, C. J., Shallcross, D. E., and Orr-Ewing, A. J.: Angew. Chem. Int. Ed., 56, 9044, 2017.

Long, B., Cheng, J. R., Tan, X. F., Zhang,.W. J.: J. Mol. Struct. Theochem., 916, 159, 2009.

CGI_14: $(CH_3)_2COO + M$
Last evaluated: February 2020; Last change in preferred values: February 2020

$(CH_3)_2COO + M \rightarrow$ products

Rate coefficient data

k/ s^{-1}	Temp./K	Reference	Technique/Comments
Absolute Rate Coefficients			
370 ± 34	298	Huang et al., 2015	PLP-LPUVA (a)
269 ± 82	283	Smith et al., 2016	PLP-Slow Flow-LPUVA (b)
361 ± 49	298		
628 ± 60	310		
916 ± 56	323		
305 ± 70	293	Chhantyal-Pun et al., 2017	PLP- PIMS/CRDS (c)
Relative Rate Coefficients			
605 ± 109	293	Berndt et al., 2012	RR-FTIR/ TDLS (d)
416 ± 121	278	Berndt et al., 2014	FT/CI-APi-TOF MS (e)
722 ± 52	293		
2449 ± 865	323		
4280 ± 544	343		
929 ± 220	298-299	Newland et al., 2015	RR-FTIR/UVA/UVF (f)

Comments

(a) $(CH_3)_2COO$ was generated from 248 nm pulsed photolysis of a gaseous mixture consisting of 2,2-diiodopropane ($(CH_3)_2CI_2$), O_2 and buffer gas (N_2), $(CH_3)_2CI_2 + h\nu \rightarrow (CH_3)_2CI + I$, at about 13 – 1030 mbar (10 - 770 Torr) total pressure and 298 K. $(CH_3)_2COO$ was monitored by UV absorption in the region 300 – 450 nm. IO was also detected, which is formed from the second channel, $(CH_3)_2CI + O_2 \rightarrow (CH_3)_2COO + IO$. First order decay rate constants decreased with total $[(CH_3)_2COO]$ to a limiting value at low initial radical concentration, when influence of radical-CI reactions is minimal. We infer this limiting value to be due to thermal decomposition. The cited value of k was obtained by linear extrapolation of a plot of the pseudo-first order rate constants at 267 mbar (200 Torr) to the limit at zero absorption from $(CH_3)_2COO$.

(b) $(CH_3)_2COO$ was generated from pulsed photolysis of a gaseous mixture consisting of 2,2-diiodopropane, $(CH_3)_2CI_2$, O_2, and buffer gas (N_2) at 248 nm, $(CH_3)_2CI_2 + h\nu \rightarrow (CH_3)_2CI + I$, at a total pressure of 200 Torr. $(CH_3)_2COO$ was monitored by time-resolved UV absorption due to the $\tilde{B}\,(1A') \leftarrow \tilde{X}(1A')$ electronic transition. The amount of $(CH_3)_2COO$ formed was estimated using a cross-section $\sigma = 1.6 \times 10^{-17}$ cm^2 at 340 nm. Kinetic decays were recorded in the temperature range 283-323 K. The decay kinetics exhibited a complex mixed first and second order form, due to thermal decomposition, self-reaction and reaction of $(CH_3)_2COO$ with other radical species produced following photolysis. k was determined by numerical simulation, making use of an optimized value of the second order component (mainly due to self-reaction), which was well defined in experiments at the highest initial concentrations. The values of k increased significantly with temperature. The results are consistent with $k = 7.25 \times 10^6 \exp[-(2919 \pm 604)/T)]$. $(CD_3)_2COO$ kinetics were also investigated using the precursor $(CD_3)_2CI_2$. k for $(CD_3)_2COO$ at 298 K was estimated to be <100 s^{-1}, with no significant T dependence.

(c) $(CH_3)_2COO$ was formed by laser photolysis of $(CH_3)_2CI_2$ in the presence of O_2 and characterized by synchrotron photoionization mass spectrometry; and also by cavity ringdown ultraviolet

absorption spectroscopy. Cavity ringdown measurements of $(CH_3)_2COO$ loss without added reagents display a combination of first- and second-order decay kinetics, which were deconvolved to derive values for both the $(CH_3)_2COO$ self-reaction rate constant, and the unimolecular thermal decay constant, *k*. The cited value is a mean of four determinations of *k* over the pressure range 13 - 131 mbar. Both *k* and the self-reaction rate constant were independent of pressure in this range.

(d) Study of the 2,3-dimethyl-but-2-ene + O_3 reaction in the presence of 1 bar of synthetic air with and without added SO_2, in a flow system, at 1 bar pressure and 50 % RH. Either propane or butane were also present to scavenge HO radicals. Formation of H_2SO_4 from the reaction of $(CH_3)_2COO$ with SO_2 was monitored with CIMS, using NO_3^- as reagent ion. The time dependence of H_2SO_4 production after addition of different $[SO_2]$ allowed estimation of k_{loss} = (3.0 ± 0.4) s^{-1} for $(CH_3)_2COO$, and a rate constant ratio $k_{loss}/k((CH_3)_2COO + SO_2) = (3.9 \pm 0.7) \times 10^{12}$ molecule cm^{-3}; where k_{loss} is the total first-order loss rate due to decomposition and reaction with H_2O. Because the (slow) reaction of $(CH_3)_2COO$ with H_2O can be neglected as a significant removal process for $(CH_3)_2COO$ under the experimental conditions, we infer that of $k_{loss} = k$. The tabulated value of *k* is based on the rate constant ratio, which agrees well with that reported in a subsequent study (Berndt et al., 2014). *k* is placed on an absolute basis using $k((CH_3)_2COO + SO_2) = 4.23 \times 10^{-13} \exp(1760/T)$ cm^3 $molecule^{-1}$ s^{-1} (IUPAC, current recommendation); although it is noted that the resultant value is not in good agreement with their reported absolute estimate.

(e) $(CH_3)_2COO$ prepared by O_3 + 2,3-dimethyl-but-2-ene reaction in the presence of SO_2 and propane (HO radical scavenger) in a flow system, equipped with CIMS for detection of H_2SO_4 using NO_3^- as reagent ion. Total pressure = 1 bar. The effect of $[H_2O]$ (RH = 2 – 50%) on yield of H_2SO_4 was negligible, and it was deduced that thermal decomposition was the dominant reaction competing with $(CH_3)_2COO + SO_2$ reaction. A distinct temperature dependence of H_2SO_4 formation was observed over the studied range (278–343 K), attributed mainly to the thermal decomposition of $(CH_3)_2COO$. The reported values of $k/k((CH_3)_2COO + SO_2)$ were placed on an absolute basis using $k((CH_3)_2COO + SO_2) = 4.23 \times 10^{-13} \exp(1760/T)$ cm^3 $molecule^{-1}$ s^{-1} (IUPAC, current recommendation). An Arrhenius plot of the resultant values of *k* vs. 1/*T*, is linear, yielding a value of $E_a \approx 29$ kJ mol^{-1}.

(f) The removal of SO_2 in the presence of 2,3-dimethyl-but-2-ene/ozone systems was measured as a function of humidity in the EUPHORE simulation chamber, under atmospheric boundary layer conditions. Cyclohexane was also present to scavenge HO radicals. SO_2 and O_3 concentrations were measured using conventional fluorescence and UV absorption monitors, respectively; the alkene concentration was determined via FTIR spectroscopy. The yield of $(CH_3)_2COO$ from the 2,3-dimethyl-but-2-ene + O_3 reaction was reported to be (0.32 ± 0.20). The observed SO_2 removal kinetics are consistent with the rate constant ratio: $k/k((CH_3)_2COO + SO_2) = (6.3 \pm 1.4) \times 10^{12}$ molecule cm^{-3}. The tabulated value of *k* was placed on an absolute basis using $k((CH_3)_2COO + SO_2) = 4.23 \times 10^{-13} \exp(1760/T)$ cm^3 $molecule^{-1}$ s^{-1} (IUPAC, current recommendation).

Preferred Values

Parameter	Value	T/K
k/ s^{-1}	400	298
k/ s^{-1}	7.2×10^6 exp(-2920/T)	280-330
Reliability		
$\Delta \log k$	± 0.2	298
$\Delta (E/R)$	± 700	280-330

Comments on Preferred Values

k has been determined in three direct studies; by Huang et al. (2015) at 298 K, by Smith et al. (2016), who also reported a temperature dependence study over the range 283–323 K, and by Chhantyal-Pun et al. (2017) at 293 K. The results at near ambient temperatures from these studies are all consistent, and the absence of pressure dependence over the range 13-130 mbar (Chhantyal-Pun et al., 2017) indicates the measurements were made at the high-pressure limit. The decomposition rate constant shows a substantial increase with temperature. The preferred values of *k* are based on a fit to all the direct data, with *E*/*R* constrained to a value of 2920 K, based on the activation energy reported by Smith et al. (2016).

The relative rate determinations from ozonolysis of 2,3-dimethyl-but-2-ene, using reaction of $(CH_3)_2COO$ with SO_2 as a reference, are also in good agreement; but consistently give values of *k* over a factor of 2 higher than the direct measurements at room temperature. The temperature dependence of *k* inferred from the data of Berndt et al. (2014) (see comment (e)) supports the direct measurements of Smith et al. (2016), and gives a comparable, but slightly higher, activation energy. An analysis of the indirect data alone provides a value $k = 1.11 \times 10^8$ exp(-3500/T) s^{-1}, with a value 880 s^{-1} at 298 K. The origins of this consistent discrepancy between the direct and relative rate determinations are currently unclear, although it is noted that the mechanism and products of the reference $(CH_3)_2COO + SO_2$ reaction are not fully characterized at atmospheric pressure (see data sheet CGI_18).

The preferred value of *k* at 298 K is in good agreement with the value of 369 s^{-1} calculated by Liu et al. (2014), using master-equation calculations and RRKM theory. Smith et al. (2016) reported theoretical calculations for $(CH_3)_2COO$ and $(CD_3)_2COO$ which show a strong temperature dependence in *k*, with Arrhenius activation energies of 35.5 and 56.4 kJ mol^{-1} respectively. The theoretical and experimental temperature dependences are consistent for $(CH_3)_2COO$, and the experimentally observed slower decomposition of $(CD_3)_2COO$ is predicted.

The quantum chemical studies predict that decomposition of $(CH_3)_2COO$ occurs via a 1,4 H-atom transfer to form the vinyl hydroperoxide intermediate, 2-hydroperoxypropene. This process is exothermic, and HO is produced from its subsequent decomposition. UV depletion studies coupled with photoionization mass spectrometry have shown relative yields of the HO radical to be greater from $(CH_3)_2COO$ than from CH_2OO (Fang et al. 2016). These observations confirm that the facile 1,4 intramolecular hydrogen transfer leads to much faster unimolecular decomposition rate for $(CH_3)_2COO$ compared with CH_2OO, for which the mechanism is unavailable.

References

Berndt, T., Jokinen, T., Mauldin, R. L., Petäjä, T.: Herrmann, H., Junninen, H., Paasonen, P., Worsnop, D. R. and Sipilä, M.: J. Phys. Chem. Lett., 3, 2892, dx.doi.org/10.1021/jz301158u, 2012.

Berndt, T., Jokinen, T., Sipilä, M., Mauldin, R. L., Herrmann, H., Stratmann, F., Junninen, H. and Kulmala, M.: Atmos. Environ., 89, 603, 2014.

Chhantyal-Pun, R., Welz, O., Savee J. D., Eskola, A. J., Lee, E. P. F., Blacker, L., Hill, H. R., Ashcroft, M., Khan, M. A. H., Lloyd-Jones, G. C., Evans, L., Rotavera, B., Rotavera H., Osborn, D. L., Mok, D. K. W., Dyke, J. M., Shallcross, D. E., Percival, C. J., Orr-Ewing, A. J. and Taatjes, C. A.: J. Phys. Chem. A, 121, 4, https://doi.org/10.1021/acs.jpca.6b07810, 2017.

Fang, Y., Liu, F., Barber, V. P., Klippenstein, S. J., McCoy, A. B. and Lester, M. I.: J. Chem. Phys., 144(6), 061102, doi: 10.1063/1.4941768, 2016.

Liu, F., Beames, J. M., Green, A. M., Lester, M. I.: J. Phys. Chem. A, 118(12), 2298, (2014).

Huang, H.-L., Chao, W. and Lin, J. J.-M.: Proc. Natl. Acad. Sci., 112(35), 10857, doi: 10.1073/pnas.1513149112, 2015.

Smith, M. C., Chao, W., Takahashi, K., Boering, K. A. and J. J.-M.: J. Phys. Chem. A, 120(27), 4789, 2016.

Newland, M. J., Rickard, A. R., Alam, M. S., Vereecken, L., Muñoz, A., Ródenas, M. and Bloss, W. J.: Phys. Chem. Chem. Phys., 17, 4076, 2015.

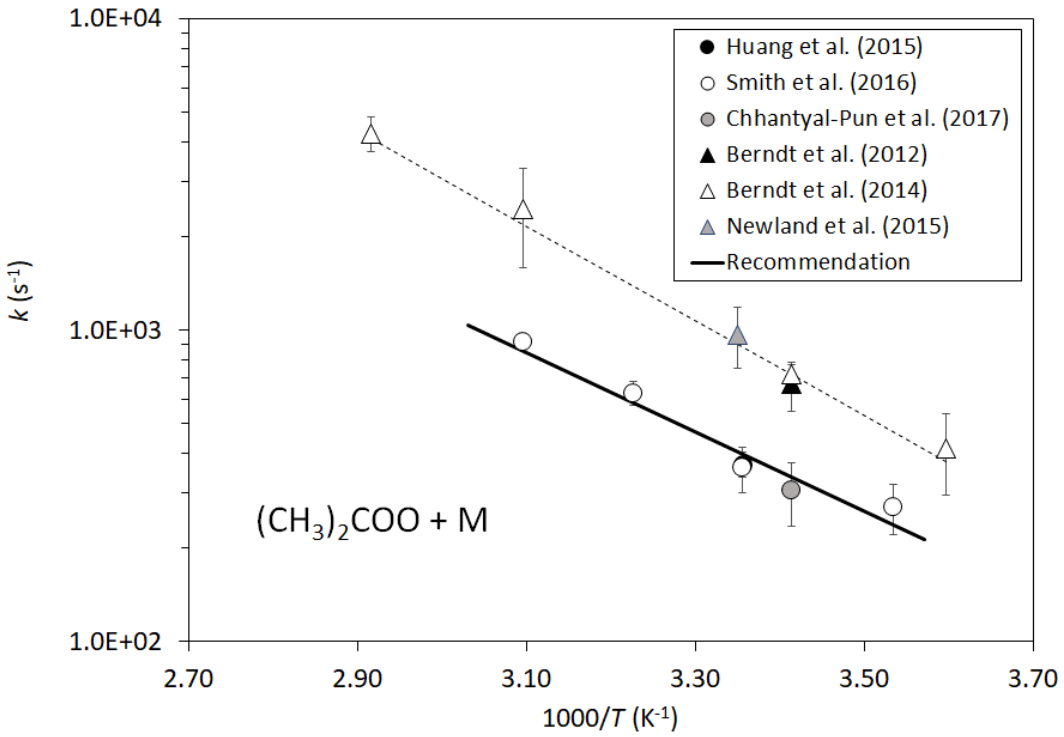

Arrhenius plot of $k((CH_3)_2COO + M)$. Direct determinations are shown as circlular points; relative rate determinations are shown as triangular points. The displayed errors are the experimental limits cited by the authors (but do not include uncertainty in the reference reaction for the relative rate studies). The full line is the IUPAC recommendation, $k = 7.2 \times 10^6 \exp(-2920/T)$ s^{-1}. The broken line is a fit to the relative rate data, $k = 1.11 \times 10^8 \exp(-3500/T)$ s^{-1}.

B4. Data sheets for thermal reactions of isoprene-derived C_4 species

CGI_21: Reactions with SO_2, H_2O, $(H_2O)_2$ and thermal decomposition

Last evaluated: March 2020; Last change in preferred values: March 2020

$(CH=CH_2)(CH_3)COO$ (*Z*- and *E*-), $(C(CH_3)=CH_2)CHOO$ (*Z*- and *E*-)
Reactions with SO_2, H_2O, $(H_2O)_2$ and thermal decomposition

Kinetics studies

Reference	Temp./K	Technique/Comments
Relative Rate Studies		
Sipilä et al., 2014	293	CIMS (a)
Newland et al., 2015	287-302	FTIR/UVF (b)
Nguyen et al., 2016	295	Multi-instrumented (c)

Comments

(a) H_2SO_4 formation from SO_2 oxidation in the presence of isoprene and ozone was studied as a function of $[SO_2]$ and relative humidity in a flow of synthetic air at 1 bar and 293 K. Propane was also present in the mixtures to scavenge HO radicals. NO_3^- chemical-ionization-atmospheric pressure interface-time-of-flight mass spectrometry (CI-APi-TOF MS) was used for the detection of sulfuric acid. Plots of H_2SO_4 formation rate vs. $[SO_2]$ were fitted to determine the yield of sCIs produced from isoprene ozonolysis, where the sCIs comprise CH_2OO and the C_4 species identified above. The total yield was determined from $[H_2SO_4]_{max}/\Delta$[isoprene]. $[H_2SO_4]_{max}$ was the concentration measured at the high end of the applied $[SO_2]$ range (2.4×10^{14} molecule cm^{-3}), and the loss of isoprene, Δ[isoprene], was determined from initial $[O_3]$, [isoprene], the rate coefficient for the O_3 + isoprene reaction, and the residence time in the flow tube (39.5 s). This results in a total sCI yield of 0.66 ± 0.29, based on $k(O_3 + \text{isoprene}) = 1.05 \times 10^{-14} \exp(-2000/T)$ (IUPAC current recommendation). The results were used to determine values of $k_{loss}/k(\text{sCI} + SO_2)$ at 10 % and 50 % RH. k_{loss} is the effective pseudo-first order loss rate of sCI, including thermal decomposition and the reaction with water vapour, given by $k_{loss} = k(\text{sCI} + M) + (k(\text{sCI}+H_2O) \times [H_2O])$. Measured values therefore represent weighted average rate constant ratios for the population of isoprene-derived sCIs. Values of $k_{loss}/k(\text{sCI} + SO_2) = (2.5 \pm 0.1) \times 10^{12}$ cm^{-3} at 10 % RH and $k_{loss}/k(\text{sCI} + SO_2) = (2.1 \pm 0.5) \times 10^{13}$ cm^{-3} at 50 % RH were determined, assuming a single sCI species model, although this did not provide a good description of the data obtained at 50 % RH. An expanded analysis, using a two sCI species model, provided a better description of the data at 50 % RH, with the two species accounting for 85 % and 15 % of the total. The corresponding rate coefficient ratios at 50 % RH, $k_{loss}/k(\text{sCI} + SO_2)$, were 3.3×10^{13} cm^{-3} for species 1 and 2.6×10^{11} cm^{-3} for species 2, consistent with substantially differing reactivities for the component sCIs. It was suggested that the much stronger $[H_2O]$ dependence for species 1 could be consistent with it being CH_2OO.

(b) SO_2 removal in the presence of isoprene and ozone, was measured as a function of humidity under atmospheric boundary layer conditions in a 200 m^3 static chamber (EUPHORE) at 1 bar and 287-302 K. Cyclohexane was also present in the mixtures to scavenge HO radicals. Detection was by FTIR for organic species, and UV fluorescence for SO_2 and O_3. The SO_2 removal rate was observed to display a systematic dependence on $[H_2O]$ over the range $0.4 – 21 \times 10^{16}$ molecule cm^{-3}. This confirmed significant reaction for at least some of the isoprene-derived sCIs with H_2O, as is expected in the case of CH_2OO. Under excess SO_2 conditions ($[SO_2] \approx 2.5 \times 10^{13}$ molecule cm^{-3}), the total isoprene ozonolysis sCI yield was calculated to be 0.56 ± 0.03. The data were analysed using a linear regression of the quantity $[SO_2] \times ((1/f) - 1)$ vs $[H_2O]$, where f is the fraction of the sCIs produced that react with SO_2. This gave the rate constant ratio

k(sCI + H_2O)/k(sCI + SO_2) = (3.1 ± 0.5) × 10^{-5} from the slope, and an estimate of k(sCI + M)/k(sCI + SO_2) = (3.0 ± 3.2) × 10^{11} molecule cm^{-3} from the intercept, where these values represent weighted average rate constant ratios for the population of isoprene-derived sCIs.

(c) The product distribution from the reaction of O_3 with isoprene was investigated in the multi-instrumented Caltech dual 24 m^3 Teflon chamber at 1 bar and ~295 K. In most experiments, cyclohexane was also present in the mixtures to scavenge HO radicals. Experiments were carried out as a function of RH over the range 4 % to 76 %, in the absence or presence of SO_2. The development of the system was monitored using GC-FID and FTIR for isoprene, methacrolein and methyl vinyl ketone, aerosol time-of-flight MS for H_2SO_4, and commercial analysers for O_3 and trace NO and NO_2. HCHO, HO and HO_2 were measured using LIF, and gas phase peroxides (e.g. H_2O_2, $HOCH_2OOH$, CH_3OOH), acidic compounds (e.g. SO_2, HC(O)OH) and other polar organics (e.g. hydroxycarbonyls) using CIMS. The results obtained as a function of RH suggest that CH_2OO is the only sCI to react bimolecularly under the experimental conditions, and a yield of 0.61 ± 0.09 was determined. The yields of methacrolein (0.42 ± 0.06) and methyl vinyl ketone (0.18 ± 0.06) were relatively insensitive to humidity, suggesting that the C_4 CIs either have a low stabilization fraction, or that the C_4 sCIs produced decompose rapidly. A yield of 0.28 ± 0.05 was also determined for HO radicals. The results as a function of [SO_2] yielded the rate coefficient ratio, k(sCI + SO_2)/k(sCI + $(H_2O)_{n=1,2}$) ≈ (2.2 ± 0.3) × 10^4. A comprehensive reaction mechanism was proposed which reproduces laboratory data over the wide range of relative humidity. The observations for $HOCH_2OOH$, HCHO, HC(O)OH and H_2O_2 were used to determine branching ratios for the reactions of CH_2OO with H_2O and $(H_2O)_2$ (see data sheet CGI_4).

Preferred Values

Parameter	$k_{298\ K}$	$k(T)$	Note
k(sCI + SO_2)/cm^3 $molecule^{-1}$ s^{-1}			
Z-(CH=CH_2)(CH_3)COO	1.55 × 10^{-10}	4.23 × 10^{-13} exp(1760/T)	(a)
E-(CH=CH_2)(CH_3)COO	1.55 × 10^{-10}	4.23 × 10^{-13} exp(1760/T)	(a)
Z-(C(CH_3)=CH_2)CHOO	2.6 × 10^{-11}		(b)
E-(C(CH_3)=CH_2)CHOO	1.4 × 10^{-10}		(c)
k(sCI + H_2O)/cm^3 $molecule^{-1}$ s^{-1}			
Z-(CH=CH_2)(CH_3)COO	1.79 × 10^{-18}	2.21 × 10^{-21} $T^{2.27}$ exp(-1858/T)	(d)
E-(CH=CH_2)(CH_3)COO	7.89 × 10^{-20}	7.07 × 10^{-19} $T^{1.46}$ exp(-3132/T)	(d)
Z-(C(CH_3)=CH_2)CHOO	1.19 × 10^{-19}	2.24 × 10^{-19} $T^{1.65}$ exp(-2989/T)	(d)
E-(C(CH_3)=CH_2)CHOO	1.43 × 10^{-16}	2.93 × 10^{-19} $T^{1.66}$ exp(-973/T)	(d)
k(sCI + $(H_2O)_2$)/cm^3 $molecule^{-1}$ s^{-1}			
Z-(CH=CH_2)(CH_3)COO	4.87 × 10^{-15}	2.25 × 10^{-21} $T^{2.27}$ exp(493/T)	(d)
E-(CH=CH_2)(CH_3)COO	3.06 × 10^{-16}	7.63 × 10^{-19} $T^{1.45}$ exp(-675/T)	(d)
Z-(C(CH_3)=CH_2)CHOO	4.39 × 10^{-16}	2.42 × 10^{-19} $T^{1.64}$ exp(-548/T)	(d)
E-(C(CH_3)=CH_2)CHOO	2.79 × 10^{-13}	3.24 × 10^{-19} $T^{1.65}$ exp(1271/T)	(d)
k(sCI + M)/s^{-1} (thermal decomposition)			
Z-(CH=CH_2)(CH_3)OO	1.36 × 10^4	9.75 × 10^8 $T^{1.03}$ exp(-5081/T)	(d),(e)
E-(CH=CH_2)(CH_3)OO	5.13 × 10^1	4.36 × 10^{-67} $T^{25.9}$ exp(2737/T)	(d)
Z-(C(CH_3)=CH_2)CHOO	1.40 × 10^4	2.58 × 10^9 $T^{0.87}$ exp(-5090/T)	(d)
E-(C(CH_3)=CH_2)CHOO	3.02 × 10^1	1.68 × 10^{10} $T^{1.02}$ exp(-7732/T)	(d)

Notes: [a] Based on IUPAC recommendation for $(CH_3)_2COO$ (see data sheet CGI_18); [b] Based on the 298 K IUPAC recommendation for *Z*-CH_3CHOO (see data sheet CGI_15), assumed here to be temperature independent over the range 287-302 K; [c] Based on the 298 K IUPAC recommendation for *E*-CH_3CHOO (see data sheet CGI_15), assumed here to be temperature independent over the range 287-302 K; [d] Adopted from the theoretical/SAR methods reported by Vereecken et al. (2017), as presented in Supplement Tables 31, 35 and 40 of that paper; [e] Exponent of pre-exponential factor changed from 9 to 8 for consistency with 298 K rate coefficient reported by Vereecken et al. (2017).

Comments on Preferred Values

The reaction of O_3 with isoprene results in the formation CH_2OO and the C_4 species, *Z*-(CH=CH_2)(CH_3)COO, *E*-(CH=CH_2)(CH_3)COO, *Z*-(C(CH_3)=CH_2)CHOO and *E*-(C(CH_3)=CH_2)CHOO. The rate coefficient ratios reported in the studies of Sipilä et al. (2014), Newland et al. (2015) and Nguyen et al. (2016) (see comments (a)-(c)) are therefore weighted averages for the population of sCIs under the studied conditions. The three studies demonstrate that the chemistry of the system is strongly dependent on both [SO_2] and [H_2O]. This confirms significant reaction for at least some of the isoprene-derived sCIs with SO_2 and H_2O (and/or $(H_2O)_2$); as indeed is well established from direct kinetics studies in the case of CH_2OO (see data sheets CGI_1 and CGI_4). However, the results of Sipilä et al. (2014) at 50 % relative humidity and theoretical predictions (e.g. Vereecken et al., 2017) indicate that the reactivity of the set of C_1 and C_4 sCIs likely varies considerably from one species to another, such that the system cannot be interpreted consistently in terms of bulk or averaged rate parameters. In addition, the results suggest that the sCI population is dominated by CH_2OO, precluding reliable analytical extraction of kinetic data for the C_4 isomers. An explicit appraisal of the system has therefore been carried out, using parameters either inferred from those for the simpler C_2 and C_3 sCIs, or adopted from theoretical studies. This analysis forms the basis of the preferred values tabulated above, and is explained and justified in the following paragraphs.

The initial formation mechanism for the excited Criegee intermediates (CIs) is shown in the schematic below, with their resultant yields (Y_{CI}) also given in the table below. The contributions assigned to the channels are taken from Nguyen et al. (2016), and are based on a combination of their results and information from the literature. The CIs either decompose promptly, or are stabilized to form the corresponding sCIs. The fractional stabilization (F_{stab}) applied to the CIs is based on the species-dependent values calculated for atmospheric pressure in the theoretical study of Zhang et al. (2002), resulting in the sCI yields (Y_{sCI}) shown in the table below.

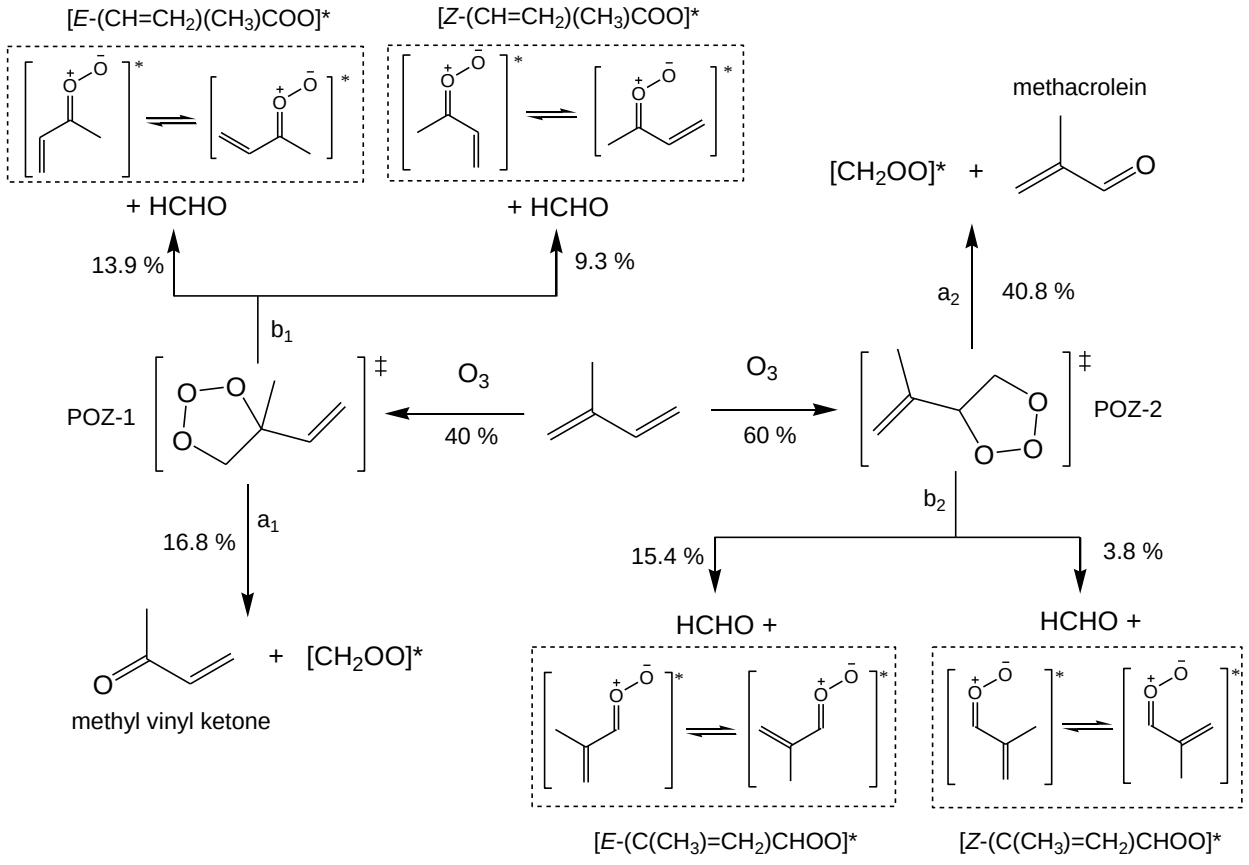

sCI	Y_{CI}	F_{stab}	Y_{sCI}
CH_2OO	0.576	0.95	0.547
Z-$(CH{=}CH_2)(CH_3)COO$	0.093	0.34	0.032
E-$(CH{=}CH_2)(CH_3)COO$	0.139	0.54	0.075
Z-$(C(CH_3){=}CH_2)CHOO$	0.038	0.37	0.014
E-$(C(CH_3){=}CH_2)CHOO$	0.154	0.20	0.031

The resultant total sCI yield, 0.70, is higher than those reported by Sipilä et al. (2014) and Newland et al. (2015). However, *Z*-$(CH{=}CH_2)(CH_3)COO$ and *Z*-$(C(CH_3){=}CH_2)CHOO$ are calculated to decompose very rapidly (Vereecken et al., 2017), such that they are barely scavenged over the reported range of experimental conditions in most studies. The total yield of the remaining sCIs (which likely contribute to the bimolecular reactivity of the system) is about 0.65. This is in acceptable agreement with the adjusted yield of 0.66 ± 0.29, based on the results of Sipilä et al. (2014) (see comment (a)), and 0.56 ± 0.03, reported by Newland et al. (2015). The calculated yield of CH_2OO is about 0.55, which also agrees with the Nguyen et al. (2016) value of 0.61 ± 0.09. Based on this information, we recommend a total sCI yield of 0.65 ± 0.10.

In the following analysis, the rate coefficients shown above in the table of preferred values were applied to the C_4 sCI isomers, along with the IUPAC recommendations for CH_2OO given in data sheets CGI_1, CGI_4 and CGI_13. Those for the C_4 sCI + SO_2 reactions were inferred from the IUPAC recommendations for $(CH_3)_2COO$, in the cases of the di-substituted isomers *Z*- and *E*-$(CH{=}CH_2)(CH_3)COO$; and from the recommendations for *Z*- and *E*-CH_3CHOO, in the cases of the mono-substituted isomers *Z*- and *E*-$(C(CH_3){=}CH_2)CHOO$. The reactions were assumed to proceed via a single channel in each case, producing SO_3 and either methyl vinyl ketone or methacrolein. The rate coefficients for unimolecular decomposition of the C_4 sCIs and their reactions with H_2O and $(H_2O)_2$ were adopted from the theoretical/SAR study of Vereecken et al. (2017). The concentrations of $(H_2O)_2$ were calculated using the equilibrium constants reported by Ruscic (2013). The aim of this analysis is to show that the results reported by Sipilä et al. (2014), Newland et al. (2015) and Nguyen et al. (2016) as a function of $[SO_2]$ and $[H_2O]$ can be recreated acceptably using these parameters.

The pathway contributions shown in the above schematic result in primary yields of 40.8 % for methacrolein and 16.8 % for methyl vinyl ketone. These agree well with those reported (e.g. Aschmann and Atkinson, 1994; Grosjean et al., 1993; Rickard et al., 1999; Nguyen et al., 2016), which lie in the range 32-44 % for methacrolein and 13-18 % for methyl vinyl ketone. Nguyen et al. (2016) showed that the yields are relatively insensitive to humidity, consistent with limited secondary formation from the reactions of the C_4 sCIs with H_2O or $(H_2O)_2$. The adjacent plot shows the calculated maximum dependence of the yields on relative humidity at 295 K (lines), compared with the Nguyen et al. (2016) data (points), based on assuming the H_2O and $(H_2O)_2$ reactions form methacrolein or methyl vinyl ketone exclusively. The calculated yield of methyl vinyl ketone is completely insensitive to relative humidity because thermal decomposition of *Z*- and *E*-$(CH{=}CH_2)(CH_3)COO$ dominates over the water reactions under all conditions, as is also the case for *Z*-$(C(CH_3){=}CH_2)CHOO$. The small dependence simulated for methacrolein (leading to a maximum secondary yield of 2.7 % at 76 % relative humidity) results from *E*-$(C(CH_3){=}CH_2)CHOO$ being significantly scavenged by reactions with both H_2O and $(H_2O)_2$.

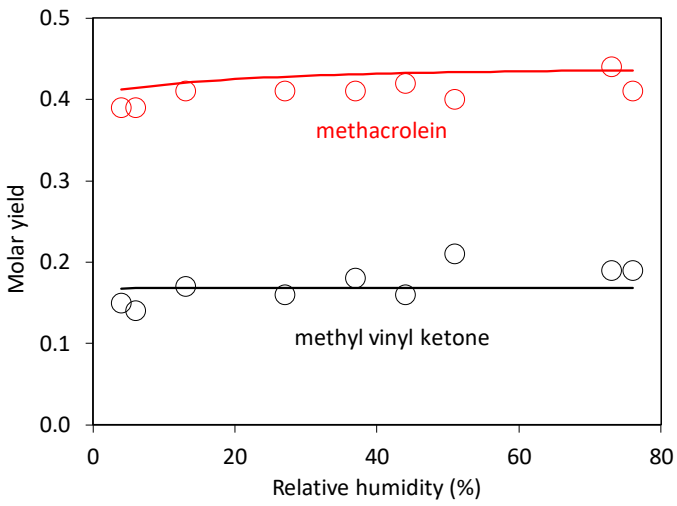

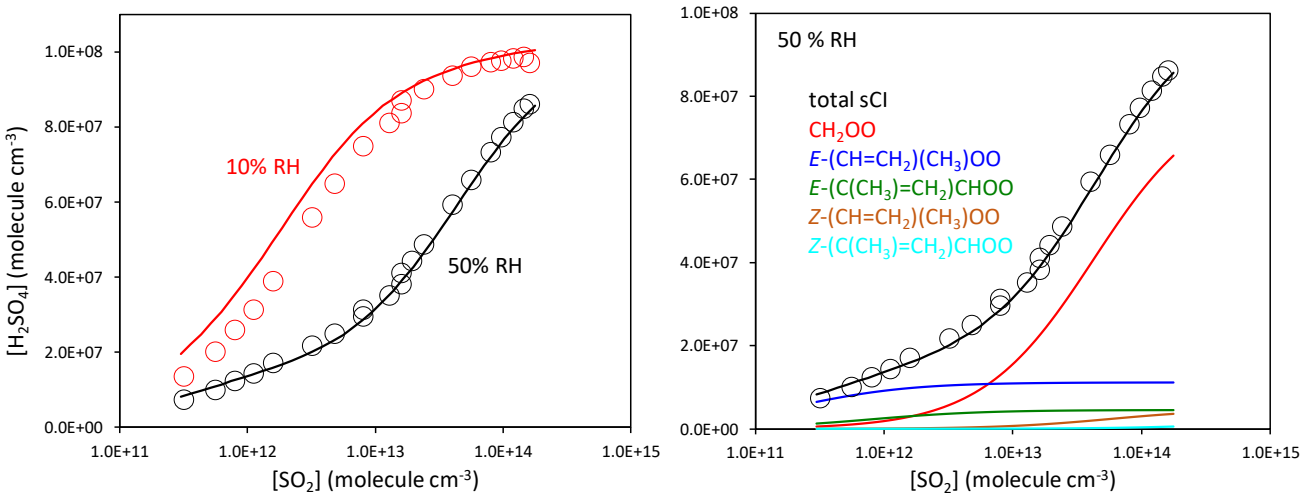

The dependence of H_2SO_4 formation as a function of $[SO_2]$ was calculated for the conditions of the experiments reported by Sipilä et al. (2014), i.e. at 293 K and either 10 % or 50 % relative humidity. The above figure compares the results of the calculations (lines) with the Sipilä et al. (2014) data (points). The observations at 50 % relative humidity are very well recreated, with those at 10 % relative humidity also being reasonably well described, given the uncertainty bounds on the applied parameters. The right-hand panel shows the calculated contributions of the five sCI species to H_2SO_4 formation at 50 % relative humidity. This shows that the total formation is dominated by the contributions from CH_2OO, *E*-$(CH{=}CH_2)(CH_3)COO$ and *E*-$(C(CH_3){=}CH_2)CHOO$ across the $[SO_2]$ range, with *Z*-$(CH{=}CH_2)(CH_3)COO$ also making a contribution at the high end of the range. Of the three main contributors, it is noted that CH_2OO accounts for about 84 % of combined sCI yield of this subset, with *E*-$(CH{=}CH_2)(CH_3)COO$ and *E*-$(C(CH_3){=}CH_2)CHOO$ collectively accounting for the remaining 16 %. This is therefore fully consistent with the two species model of Sipilä et al. (2014), and their differential relative reactivities with SO_2 and H_2O, which was based on 85 % and 15 % contributors (see comment (a)).

The influence of $[H_2O]$ on the removal of SO_2 (initially 50 ppb) was also calculated for conditions representative of those reported by Newland et al. (2015). The experiments were carried out at ambient temperatures, reported to be in the range 287-302 K, such that there was likely temperature variability in this range both between and within experiments. The calculations were therefore performed for the mid-range temperature (294.5 K) and the extreme temperatures. The left-hand panel below shows the calculated $[H_2O]$ dependence of the function *Y* (lines) compared with the Newland et al. (2015) data (points). *Y* is defined as $[SO_2] \times ((1/f) - 1)$ (Newland et al., 2015), where *f* is the fraction of sCIs removed by reaction with SO_2. The observed dependence therefore results from a reduction in *f* as $[H_2O]$ increases. In a single sCI system, and assuming the sCI does not react significantly with $(H_2O)_2$, the plot would be expected to be linear with a slope $k(\text{sCI} + H_2O)/k(\text{sCI} + SO_2)$ and an intercept of $k(\text{sCI} + M)/k(\text{sCI} + SO_2)$, and this was the basis of the Newland et al. (2015) analysis. However, the calculated dependence is not linear, resulting from the differing relative reactivities of the component sCIs with SO_2 and H_2O, and the role of the $(H_2O)_2$ reactions. The initial increase and upward curvature at low $[H_2O]$ in the calculated dependence of *Y* results mainly from the impact of increased loss of CH_2OO via reaction with H_2O and, particularly, $(H_2O)_2$. This is also illustrated in the right-hand panel, which shows that the calculated variation in *f* at low $[H_2O]$ for the set of sCIs is dominated by the decrease in the CH_2OO contribution. By the mid-range $[H_2O]$, less that 20 % of CH_2OO is reacting with SO_2, and $(H_2O)_2$ is its major reaction partner. As a result, the contributions of *E*-$(CH{=}CH_2)(CH_3)COO$ and *E*-$(C(CH_3){=}CH_2)CHOO$ to *f* become increasingly significant. These sCIs both react mainly (70 – 90 %) with SO_2 for the whole range of conditions, such that their contributions show little or no dependence on $[H_2O]$. They therefore have an important influence on the $[H_2O]$

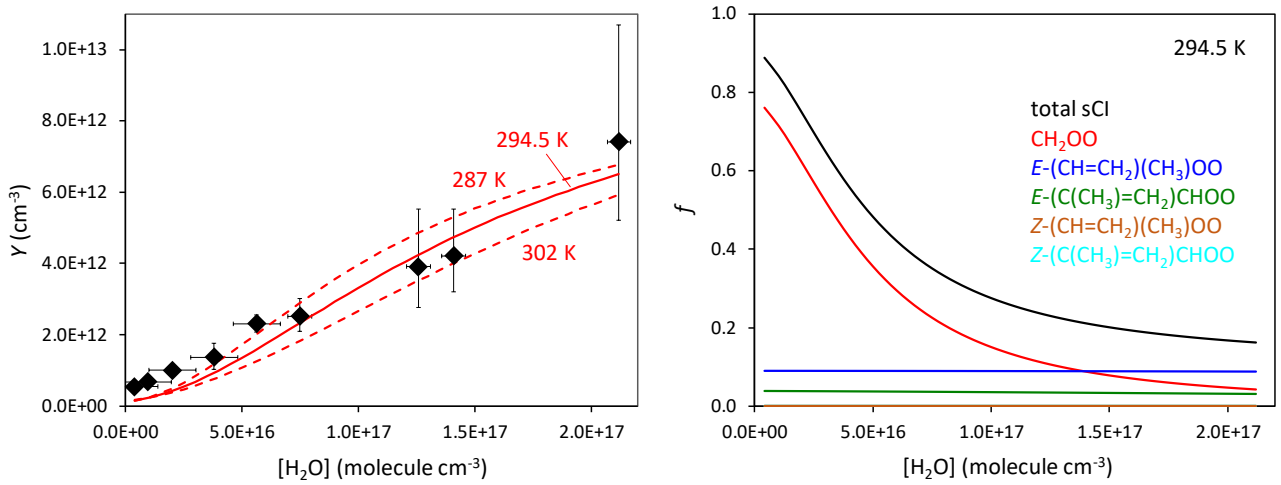

dependence of Y towards the high end of the $[H_2O]$ range, because of their much slower relative reactivity with H_2O and $(H_2O)_2$, compared with CH_2OO. The overall effect of the contributions from CH_2OO, *E*-$(CH{=}CH_2)(CH_3)COO$ and *E*-$(C(CH_3){=}CH_2)CHOO$ is therefore a reduction in the slope of the $[H_2O]$ dependence towards the high end of the studied range.

The calculated dependence of Y on $[H_2O]$ provides an acceptable description of the Newland et al. (2015) data, although the calculated values are systematically below the observations at low $[H_2O]$. It is noted that Newland et al. (2015) applied a correction to account for reaction of sCIs with organic acids formed as products, and also interpreted the intercept of their plot in terms of sCI removal by thermal decomposition and other unaccounted for loss processes. The possible influence of other loss processes (e.g. reaction of sCIs with other reaction products) is not factored into the calculations presented here, and this may explain the small systematic difference that is most apparent at low $[H_2O]$. The sCI population average thermal decomposition rate at the low end of the $[H_2O]$ range is calculated to be about 5 s^{-1}, consistent with the value ≤ 12 ($\pm$ 12) s^{-1}, derived by Newland et al. (2015) from the intercept of their linear regression analysis. This increases to over 50 s^{-1} at the high end of the $[H_2O]$ range, mainly due to the preferential increased removal of CH_2OO (which has a very low decomposition rate) by bimolecular reaction with H_2O and $(H_2O)_2$.

The inferred or adopted parameters recommended here therefore provide an acceptable description of the O_3 + isoprene observations reported by Sipilä et al. (2014), Newland et al. (2015) and Nguyen et al. (2016), although the data can support some tolerance in the absolute and relative parameter values. Measurements of speciated sCI yields, and direct kinetics studies of the rate coefficients and product channels for the reactions of the C_4 sCI isomers, would therefore clearly be valuable. This is particularly important for *E*-$(CH{=}CH_2)(CH_3)COO$ and *E*-$(C(CH_3){=}CH_2)CHOO$, for which bimolecular and unimolecular reactions are calculated to be competitive within the range of reported experimental conditions, and also for some tropospheric conditions. In this respect, Barber et al. (2018) and Vansco et al. (2018; 2019) have characterized the formation and UV-visible spectrum of *Z*- and *E*-$(CH{=}CH_2)(CH_3)COO$ from the photolysis of 1,3-di-iodobut-2-ene, and *Z*- and *E*-$(C(CH_3){=}CH_2)CHOO$ from the photolysis of 1,3-di-iodo-2-methylprop-1-ene, providing possible methods for direct kinetics investigations of these isomers. Barber et al. (2018) also report HO formation from the thermal decomposition of *E*-$(CH{=}CH_2)(CH_3)COO$, compatible with the expected pathway involving 1,4 H-atom transfer from the $-CH_3$ group to form a vinyl hydroperoxide intermediate; and at a rate that is consistent with theory.

References

Aschmann, S. M. and Atkinson, R.: Environ. Sci. Technol., 28, 1539, 1994.

Barber, V. P., Pandit, S., Green, A. M., Trongsiriwat, N., Walsh, P. J., Klippenstein, S. J. and Lester, M. I.: J. Am. Chem. Soc., 140, 10866, https://doi.org/10.1021/jacs.8b06010, 2018.

Grosjean, D., Williams II, E. L. and Grosjean, E.: Environ. Sci. Technol., 27, 830, 1993.

Newland, M. J., Rickard, A. R., Vereecken, L., Muñoz, A., Ródenas, M., and Bloss, W. J.: Atmos. Chem. Phys., 15, 9521, https://doi.org/10.5194/acp-15-9521-2015, 2015.

Nguyen, T. B., Tyndall, G. S., Crounse, J. D., Teng, A. P., Bates, K. H., Schwantes, R. H., Coggon, M. M., Zhang, L., Feiner, P., Millller, D. O., Skog, K. M., Rivera-Rios, J. C., Dorris, M., Olson, K. F., Koss, A., Wild, R. J., Brown, S. S., Goldstein, A. H., de Gouw, J. A., Brune, W. H., Keutsch, F. N., Seinfeld, J, H. and Wennberg, P. O.: Phys. Chem. Chem. Phys., 18, 10241, 2016.

Rickard, A. R., Johnson, D., McGill, C. D. and Marston, G.: J. Phys. Chem. A, 103, 7656, 1999.

Ruscic, B.: J. Phys. Chem. A, 117, 11940, https://doi.org/10.1021/jp403197t, 2013.

Sipilä, M., Jokinen, T., Berndt, T., Richters, S., Makkonen, R., Donahue, N. M., Mauldin III, R. L., Kurtén, T., Paasonen, P., Sarnela, N., Ehn, M., Junninen, H., Rissanen, M. P., Thornton, J., Stratmann, F., Herrmann, H., Worsnop, D. R., Kulmala, M., Kerminen, V.-M., and Petäjä, T.: Atmos. Chem. Phys., 14, 12143, https://doi.org/10.5194/acp-14-12143-2014, 2014.

Vansco, M. F., Marchetti, B. and Lester, M. I.: J. Chem. Phys., 149, 244309, https://doi.org/10.1063/1.5064716, 2018.

Vansco, M. F., Marchetti, B. Trongsiriwat, N., Bhagde, T., Wang, G., Walsh, P. J., Klippenstein, S. J. and Lester, M. I.: J. Am. Chem. Soc., 141 (38), 15058, https://doi.org/10.1021/jacs.9b05193, 2019.

Vereecken, L., Novelli, A. and Taraborrelli, D.: Phys. Chem. Chem. Phys., 19, 31599, 2017.

Zhang, D., Lei, W. and Zhang, R.: Chem. Phys. Lett., 358, 171, 2002.

CGI_25: Reactions with $CF_3C(O)OH$
Last evaluated: August 2017; Last change in preferred values: August 2017

E-$(CH{=}CH_2)(CH_3)COO + CF_3C(O)OH \rightarrow$ products
E-$(C(CH_3){=}CH_2)CHOO + CF_3C(O)OH \rightarrow$ products

Preferred Values

Parameter	Value	T/K
k/ cm^3 molecule^{-1} s^{-1}	7.3×10^{-10}	298
k/ cm^3 molecule^{-1} s^{-1}	$4.9 \times 10^{-18}\ T^2 \exp(1620/T) + 6.3 \times 10^{-10}$	240-340
Reliability		
$\Delta \log k$	± 0.3	298
$\Delta (E/R)$	± 500 K	240-340

Comments on Preferred Values

The preferred value for the rate coefficient for reaction of both E-$(CH{=}CH_2)(CH_3)COO$ and E-$(C(CH_3){=}CH_2)CHOO$ with $CF_3C(O)OH$ is based on the measurements and quantum calculations of Chhaantyal-Pun et al. (2017) for the reaction of other Criegee intermediates with $CF_3C(O)OH$. In particular the rate coefficients for the reactions of CH_2OO and $(CH_3)_2COO$ with $CF_3C(O)OH$, and their temperature dependences, are well described by a model involving a hydrogen-bonded stabilized pre-reaction complex which is sufficiently stable to influence the temperature dependence of k (Long et al., 2009). The computational methodology used in those studies can be applied to the reactions of $CF_3C(O)OH$ with larger Criegee intermediates, such as those formed from the ozonolysis of isoprene. Rate coefficients were calculated at the DF-HF//DF-LCCSD(T)-F12a/aug-cc-pVTZ//B3LYP-6-31+G(d) level of theory by Chaantyal-Pun et al. (2017). This model predicts a T-dependence of the overall reaction of the form,

$$k = AT^2 \exp\left(\frac{\Delta H}{RT}\right) + k_d$$

(Long et al., 2009) where the first term describes the complex-forming reaction, and k_d is the rate coefficient for the direct (non complex-forming) reaction, approximated to be temperature-independent. The recommended parameters are based on the fit to the experimental data for $(CH_3)_2COO$ reported by Chhantyal-Pun et al. (2017) using this model, with the k_d term scaled upward here by about 20 % to account for the larger dipole moment and size of E-$(CH{=}CH_2)(CH_3)COO$ and E-$(C(CH_3){=}CH_2)CHOO$, and the resultant influence on the capture limited rate constants.

References

Chhantyal-Pun, R., McGillen, M. R., Beames, J. M., Khan, M. A. H., Percival, C. J., Shallcross, D. E., and Orr-Ewing, A. J.: Angew. Chem. Int. Ed., 56, 9044, 2017.

Long, B., Cheng, J. R., Tan, X. F. and Zhang, W. J.: J. Mol. Struct. Theochem., 916, 159, 2009.

B5. Photochemical data sheets for $C_1 - C_4$ species

P33: $CH_2OO + h\nu$

Last evaluated: May 2020; Last change in preferred values: June 2017

$CH_2OO + h\nu \rightarrow$ products

Primary photochemical transitions

Reaction		ΔH /kJ·mol^{-1}	$\lambda_{threshold}$/nm
$CH_2OO + h\upsilon \rightarrow CH_2O + O(^3P)$	(1)	185	645
$\rightarrow CH_2O + O(^1D)$	(2)	292	410

Absorption cross-section data

Wavelength range/nm	Reference	Comments
280 – 410	Beames et al., 2012	(a)
300 – 445	Sheps, 2013	(b)
280 – 500	Ting et al., 2014	(c)
375	Buras et al., 2014	(d)
362 – 470	Foreman et al., 2015	(e)

Comments

(a) CH_2OO prepared by PLP (248 nm) of CH_2I_2 in O_2/Ar mixtures in a capillary tube. The photoproducts were cooled in a supersonic expansion and passed to a TOF mass spectrometer where they were ionised with VUV radiation at 118 nm. The signal at *m/z* 46 detected when 248 nm photolysis occurred in the capillary, was attributed to CH_2OO. The UV absorption spectrum was determined from depletion of the *m/z* 46 photo-ionisation signal resulting from excitation of the B $\leftarrow$ X transition in ground state CH_2OO molecules by tunable UV radiation (280 – 420 nm) Nd-YAG laser. The absorption followed a simple Gaussian form with a peak at 335 nm and a breath (fwhm) of 40 nm. The cross section at the maximum of the absorption band at 335 nm was estimated to be approximately 5×10^{-17} cm^2 molecule^{-1}.

(b) CH_2OO prepared by PLP (266 nm) of CH_2I_2 in O_2/Ar mixtures at 5.1 Torr pressure. Absorption of CH_2OO in presence of excess SO_2 was observed by time-resolved UV absorption spectrum. Chemical kinetics measurements of its reactivity establish the identity of the absorbing species as CH_2OO. Separate measurements of the initial CH_2I radical concentration were used to determine the absolute absorption cross section of CH_2OO. The value obtained at the peak of the absorption band, 355 nm, was $\sigma = (3.6 \pm 0.9) \times 10^{-17}$ cm^2 molecule^{-1}. The difference between the absorption and action spectra was attributed to excitation to long-lived $\tilde{B}$ ($^1A'$) vibrational states that may relax to lower electronic states by fluorescence or nonradiative processes. Spectral resolution was ~1 nm.

(c) CH_2OO was prepared by pulsed 248 nm photolysis of CH_2I_2/O_2 mixtures; transient absorption spectra were recorded using a gated intensified CCD camera (1 ms gate width). Spectral

resolution was 2 nm. Decay of CH_2OO by self-reaction and by reaction with SO_2 were utilized to extract the absorption spectrum of CH_2OO, corrected for contributions by other absorbers. The peak cross section is $(1.26 \pm 0.25) \times 10^{-17}$ cm^2 molecule^{-1} at 340 nm, based on the quantum efficiency of CH_2OO production (ϕ_{CH2OO} = 0.86 at 11 Torr, reported by Stone et al. 2013). Absolute absorption cross-sections of CH_2OO were also obtained from laser-depletion measurements in a jet-cooled molecular beam with the laser fluence calibrated using a reference molecule. Values from the laser-depletion measurements, $\sigma = (8.09 \pm 0.90) \times 10^{-18}$ at 308.4 nm and $(1.21 \pm 0.13) \times 10^{-17}$ cm^2 molecule^{-1} at 351.8 nm, are consistent with results from absorption measurements taking into account uncertainties in spectral overlap at different resolution and gas temperature.

(d) CH_2OO was produced by the $CH_2I + O_2 \rightarrow CH_2OO + I$ reaction following 355 nm laser photolysis of CH_2I_2 in a large excess of O_2. CH_2OO kinetics were followed by time resolved absorption at 375 nm in the B $\leftarrow$ X transition and the atomic I co-product followed by probing the 1315.246 nm F = 3 $^2P_{1/2} \leftarrow$ F = 4 $^2P_{3/2}$ atomic transition. $[CH_2OO]_0$ was determined by simultaneous fitting of the decay of [I] and $[CH_2OO]$. The absorption cross section of CH_2OO at the UV probe wavelength (λ = 375 nm) was derived as $(6.2 \pm 2.2) \times 10^{-18}$ cm^2 molecule^{-1}.

(e) CH_2OO was produced by the $CH_2I + O_2 \rightarrow CH_2OO + I$ reaction following the 355 nm laser photolysis of CH_2I_2/O_2 mixtures in 50-70 Torr total pressure of N_2. Absorption spectra of CH_2OO were recorded using two different experimental techniques. First, conventional single-pass absorption spectroscopy using pulsed LED broadband light sources to measure the spectra over the range 362-470 nm. Second, pulsed cavity ring down spectroscopy to record high resolution spectra over the range 417-435 nm. In both systems $[CH_2OO]_0$ was calculated from the CH_2I_2 concentration, CH_2I_2 absorption cross section, laser fluence, and CH_2OO yield in the $CH_2I + O_2$ reaction. Over the wavelength range where the two techniques overlapped there was good agreement in the spectra obtained using the different experimental approaches. The absorption cross section at 375 nm is 6×10^{-18} cm^2 molecule^{-1}.

Preferred Values

Absorption cross-sections at 298 K

λ/nm	$10^{20}\,\sigma$/(cm^2 molecule^{-1})	λ/nm	$10^{20}\,\sigma$/(cm^2 molecule^{-1})	λ/nm	$10^{20}\,\sigma$/(cm^2 molecule^{-1})
280	190	340	1230	400	345
285	290	345	1215	405	190
290	380	350	1200	410	230
295	490	355	1125	415	110
300	551	360	1050	420	120
305	660	365	1004	425	45
310	785	370	844	430	50
315	920	375	767	435	30
320	979	380	720	440	0
325	1075	385	455	445	0
330	1140	390	520	450	0
335	1195	395	300	455	0

$\sigma = (1.23 \pm 0.18) \times 10^{-17}$ cm^2 molecule^{-1} at λ_{max} (340 nm)

Quantum Yields

$\phi_1 = 1.0$ for $280 < \lambda < 420$ nm.

Comments on Preferred Values

All reported studies of UV absorption by the formaldehyde oxide Creigee intermediate show a strong absorption band in the mid UV region attributed to the $\tilde{B}$ (1A′) ← $\tilde{X}$(1A′) electronic transition. However, the results are not all in good agreement, either in absolute magnitude of the cross section at the absorption maximum, or in the overall shape of the spectrum (e.g., see Figure 1 in Foreman et al. 2015 and Figure 4 in Ting et al. 2014). The UV photo-dissociation action spectrum reported by Beames et al. (2012) differs substantially from the absorption spectrum reported by Sheps (2013) with the latter extending to longer wavelengths and exhibiting resolved vibrational structure on its low-energy side. The cross-section estimate of Beames et al. (2012) was based on a laser fluence estimated without correction for beam non-uniformity. Ting et al. (2014) used both multiplex long-path UV absorption and the photo-dissociation action technique, to give improved accuracy to determine cross-sections over a wide range of wavelengths. The shape of the spectra reported by Ting et al. (2014) and Sheps (2013) agree well for $\lambda > 345$ nm but there is clear and unexplained conflict at $\lambda < 345$ nm, where the absorption falls off much more rapidly in the spectrum reported by Sheps (2013). Explanations of the differences in shape based on strong temperature dependence at longer wavelengths (analogy to the Hartley/Huggins bands in iso-electronic O_3 molecule), and a proposed decrease in the dissociation yield at long wavelengths (Sheps, 2013) due to competing processes are not consistent with the body of photophysical information. The single wavelength determination of σ(375) nm of Buras et al. (2014), as part of their kinetic study of the CH_2OO self-reaction, is in good agreement with the results of Ting et al. (2014). Foreman et al. (2015) used both conventional UV absorption spectroscopy and cavity ring down spectroscopy to study the CH_2OO spectrum at 362-470 nm and reported results which are in excellent qualitative and quantitative agreement with those from Ting et al. (2014) and Buras et al. (2013).

There is excellent agreement in the results reported by Buras et al. (2013), Ting et al. (2014), and Foreman et al. (2015). The preferred value of the cross section at the λ_{max} in the B-X transition is based on those measured by Ting et al. (2014), in their jet cooled measurements, i.e. values obtained at 308.4 and 351.8 nm were: $(8.09 \pm 0.90) \times 10^{-18}$ and $(1.21 \pm 0.13) \times 10^{-17}$ cm^2 molecule^{-1} respectively. These values are expected to have very weak temperature dependence by analogy with O_3 Hartley band. The cross-sections at discrete wavelengths over the range 280-500 nm were obtained by Ting et al. (2014), by scaling their absorption data to the above data points near λ_{max}. The IUPAC recommended peak cross section at 340 nm and cross-sections at 5 nm intervals are evaluated by averaging data from their analysis. The error of ±15% includes possible variations arising from the temperature effects. The photodissociation quantum yields of CH_2OO are likely to be close to unity since the product anisotropy measured by Lehman et al. (2013) shows that dissociation occurs faster than rotation of the CH_2OO molecule.

References

Beames, J. M., Liu, Fang Lu, Lu Lu, and Lester, M. I.: J. Amer. Chem. Soc., 134, 20045, 2012.

Buras, Z. J., Elsamra, R. M. I., and Green, W. H: J. Phys. Chem. Lett., 5, 2224, 2014.

Foreman, E. S., Kapnas, K. M., Jou, Y., Kalinowski, J., Feng, D., Gerber, R. B., and Murray, C.: Phys. Chem. Chem. Phys., 17, 32539, 2015.

Lehman, J. H., Li, H., Beames, J. M., and Lester, M. I.: J. Chem. Phys., 139, 141103, 2013.

Sheps, L.: J. Phys. Chem. Lett., 4, 4201, 2013.

Ting, W-L, Chen, Y-H., Chao, W., Smith, M.C., and Lin, J Jr -M.: Phys. Chem. Chem. Phys., 16, 10438, 2014.

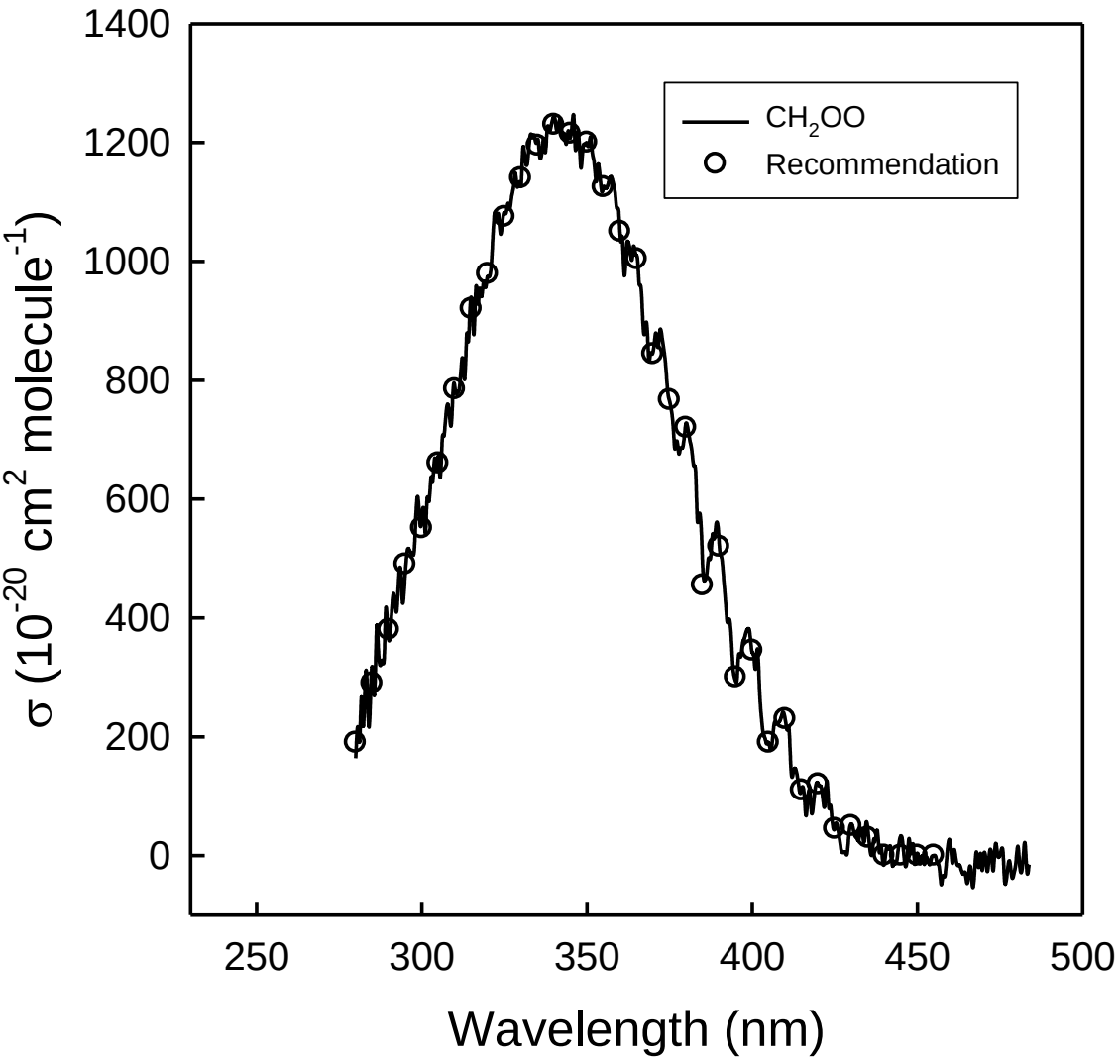

UV absorption cross sections of CH_2OO (using the SO_2 scavenging method) reported by Ting et al. (2014) and recommended values.

P34: CH_3CHOO (*Z*- and *E*-) + hν

Last evaluated: May 2020; Last change in preferred values: June 2017

CH_3CHOO (*Z*- and *E*-) + hν → products

Primary photochemical transitions

Reaction	
$CH_3CHOO + h\upsilon \rightarrow CH_3CHO + O(^3P)$	(1)
$\rightarrow CH_3CHO + O(^1D)$	(2)

Absorption cross-section data

Wavelength range/nm	Reference	Comments
280 – 410	Beames et al., 2013	(a)
300 – 445	Sheps et al., 2014	(b)
280 – 500	Smith et al., 2014	(c)

Comments

(a) CH_3CHOO prepared by PLP (248 nm) of CH_3CHI_2 in O_2/Ar mixtures in a capillary tube. The photoproducts were cooled in a supersonic expansion and passed to a TOF mass spectrometer where they were ionised with VUV radiation at 118 nm. The signal at *m/z* 46 detected when 248 nm photolysis occurred in the capillary, was attributed to CH_3CHOO. Both *Z*- and *E*-conformers of the acetaldehyde oxide species were formed in the process. The UV absorption spectrum was determined from depletion of the *m/z* 46 photo-ionisation signal resulting from excitation of the B ← X transition in ground state CH_3CHOO molecules by tunable UV radiation (280 – 420 nm) from a Nd-YAG laser. The UV-induced depletion approaches 100% near the peak of the simple Gaussian profile at 320 nm, indicating rapid dynamics in the *B* state, and corresponds to a peak absorption cross section of ~5×10^{-17} cm^2 $molecule^{-1}$; the absolute cross section measurements have an uncertainty on the order of a factor of 2.

(b) CH_3CHOO prepared by PLP (266 nm) of CH_3CHI_2 in O_2/Ar mixtures at 5.1 Torr pressure. Absorption of CH_3CHOO in the absence and presence of excess SO_2 or H_2O was observed by time-resolved UV absorption spectrum at 300 – 425 nm. Spectral resolution was ~1 nm. Absorption features due to the B ← X transition in ground state of *Z*- and *E*- conformers of CH_3CHOO could be distinguished by their differing reactivities - reflected in characteristic time dependencies for decay of these absorption features. The absorption band for *Z*-CH_3CHOO peaked at 323 nm, with a 40 nm FWHM. For *E*-CH_3CHOO, FWHM was 35 nm centred at 360 nm. Estimates of the absolute absorption cross sections of the two conformers was based on the value obtained by Smith et al (2014), using the ion depletion method, for *Z*-CH_3CHOO at 308 nm, where only the *Z*- conformer absorbs. The value obtained at the peak of the *Z*-CH_3CHOO absorption band at 323 nm was $\sigma = 1.2 \times 10^{-17}$ cm^2 $molecule^{-1}$, and at the peak of the *E*-CH_3CHOO absorption at 360 nm was $\sigma = 1.2 \times 10^{-17}$ cm^2 $molecule^{-1}$.

(c) CH_3CHOO was prepared by pulsed-248 nm photolysis of CH_3CHI_2/O_2 mixtures. Transient absorption spectra (260 – 500 nm; resolution 1.5 nm) were recorded using a gated iCCD

spectrometer. Decays of CH_3CHOO by self-reaction and by reaction with SO_2 were utilized to extract the absorption spectrum of CH_2OO, corrected for contributions by other absorbers. Absolute absorption cross-sections of CH_3CHOO were obtained from laser-depletion measurements in a jet-cooled molecular beam (as described by Ting et al 2014 for CH_2OO), using EI-MS to monitor $C_2H_4OO^+$ at m/z = 60. The laser fluence at 308 and 352 nm was calibrated directly (from laser beam profiling measurements) and by using the observed laser depletion of CH_3CHI_2 and the literature absorption cross section for CH_3CHI_2 at 308 nm. From the relative laser fluence for the CH_3CHOO and CH_3CHI_2 experiments the cross-section ratio $\sigma(CH_3CHOO)/\sigma(CH_3CHI_2)$, and hence $\sigma(CH_3CHOO)$ at 308 nm was calculated. Consistent results for $\sigma(CH_3CHOO)$ at 308 nm were obtained using the two different calibration methods. The values obtained at 308 and 352 nm were: $(1.06 \pm 0.09) \times 10^{-17}$ and $(9.7 \pm 0.0.6) \times 10^{-17}$ cm^2 $molecule^{-1}$, respectively. These values were consistent with the relative broad band absorption measurements at these wavelengths and were used to calibrate the spectrum to provide absolute cross sections over the range 280 – 480 nm. The peak cross section is $\lambda_{max} = (1.27 \pm 0.11) \times 10^{-17}$ cm^2 $molecule^{-1}$ at 328 nm.

Preferred Values

Absorption cross-sections at 298 K

λ/nm	$10^{20}\,\sigma/(cm^2\ molecule^{-1})$	λ/nm	$10^{20}\,\sigma/(cm^2\ molecule^{-1})$	λ/nm	$10^{20}\,\sigma/\ cm^2\ molecule^{-1})$
280	428	340	1176	400	117
285	528	345	1101	405	83
290	638	350	1008	410	58
295	752	355	902	415	39
300	867	360	788	420	26
305	976	365	673	425	17
310	1074	370	562	430	11
315	1155	375	458	435	7
320	1214	380	365	440	4
325	1247	385	284	445	2
330	1251	390	217	450	1
335	1227	395	161	455	0

Gaussian fit parameters to data of Smith et al. (2014): $\sigma(\lambda) = 1253.16 \times \exp(-0.000460967 \times (328.28 - \lambda)^2)$

Absorption cross-sections at 298 K (conformer resolved)

λ/nm	10^{20} σ (*Z*-)/(cm^2 molecule^{-1})	10^{20} σ (*E*-)/(cm^2 molecule^{-1})
300	847	209
310	1180	287
330	1150	913
350	906	1070
370	318	1200
390	59	965
410	12	652

σ(*Z*-) = (1.20 ± 0.18) × 10^{-17} cm^2 molecule^{-1} at λ_{max} (323 nm)
σ(*E*-) = (1.20 ± 0.18) × 10^{-17} cm^2 molecule^{-1} at λ_{max} (360 nm)

Gaussian fit parameters to data for *Z*-CH_3CHOO: $\sigma(\lambda) = 1253.18 \times 10^{-20} \exp(-0.00060787 \times (324.11 - \lambda)^2)$.
Gaussian fit parameters to data for *E*-CH_3CHOO: $\sigma(\lambda) = 1228.72 \times 10^{-20} \exp(-0.00037271 \times (365.53 - \lambda)^2)$

Quantum Yields

$\phi_1 = 1.0$ for $280 < \lambda < 420$ nm.

Comments on Preferred Values

All reported studies of UV absorption by the acetaldehyde oxide Criegee intermediate show a broad Gaussian band peaking at about 320 nm with weak structure on the long-wavelength side, which is attributed to the $\tilde{B}$ (1A′) ← $\tilde{X}$(1A′) electronic transition. The results from techniques using absorption spectroscopy (Sheps et al., 2013; Smith et al., 2014), and using the UV photo-dissociation action spectrum of CH_3CHOO of Smith et al. (2014), are in good agreement on the overall shape of the spectrum. However, the action spectrum reported by Beames et al. (2013) differs substantially from the other studies in that the band is narrower (FWHM = 37 nm vs 77 nm), and the peak cross section determined from photo-dissociation action spectrum at λ = 320 nm is a factor of 4 higher than by Smith et al. (2014). Smith et al. (2014) also used the photo-dissociation action technique with direct laser fluence measurements to give improved accuracy for $\sigma(CH_3CHOO)$ at 352 nm and 308 nm. They also measured the cross-section ratio $\sigma(CH_3CHOO)/\sigma(CH_3CHI_2)$ at 308 nm, and determined $\sigma(CH_3CHOO)$ based on the known value for $\sigma(CH_3CHI_2)$ at this wavelength. These results agreed and were combined with multiplex long-path UV absorption to determine $\sigma(CH_3CHOO)$ over a wide range of wavelengths. These form the basis of the preferred cross sections in this evaluation. The IUPAC recommended peak cross section at 340 nm and cross-sections at 5 nm intervals are evaluated by averaging data from their analysis. The first figure below shows the values reported by Smith et al. and a Gaussian fit to these data. The error of ±15% includes possible variations arising from the temperature effects.

The source chemistry produces CH_3CHOO in two (stable) conformers: *Z*- and *E*- , which differ in the orientation of the O-O moiety relative to the CH_3- group. Only the study of Sheps et al. (2014) provides cross sections for the individual conformers, by extracting their spectral contributions to the overall absorption band, using their different decay times (175 ± 25 and 2800 ± 300 s^{-1} for *Z*- and *E*- CH_3CHOO, respectively) in the presence of 1×10^{17} cm^{-3} [H_2O]. The sum of absorption components for *Z*- and *E*- CH_3CHOO extrapolated to $t = 0$, agree well with the overall spectra reported by Smith et al. (2014), and are consistent with initial production of ~30% of total CH_3CHOO in the *E*-conformer. The IUPAC preferred cross sections at 5 nm intervals were calculated by fitting a Gaussian to the retrieved conformer-resolved cross-sections (see second figure below). The error of ± 30% on the conformer cross-sections arises mainly from the fitting

procedure used to deconvolute the overlap of the conformer spectra. The UV spectrum of *Z*-CH_3CHOO is centered at 323nm and has FWHM of ~40 nm, whilst the peak cross section of the *E*-conformer is ~360 nm. Both conformers have approximately equal cross-sections at the peak. The spectral features are consistent with theoretical calculations where a combination of ground state stabilization and excited state destabilization shifts the vertical *B*-*X* transition for *Z*-CH_3CHOO (<3.8 eV) to higher energy, and correspondingly shorter wavelength, than those for *E*-CH_3CHOO (<3.5 eV) and CH_2OO (<3.6 eV), in each case starting from the equilibrium configuration.

The photodissociation quantum yields are likely to be close to unity (Lehman et al., 2013). Hydroxyl radicals produced concurrently with the generation of the Criegee intermediates (from the reactions of CH_3CHI and CH_2I with O_2) were measured in the experiments of Beames et al. (2013), where they were detected by 1+1′ resonance enhanced multiphoton ionization. The OH yield observed with CH_3CHOO is 4-fold larger than that from CH_2OO, consistent with prior studies of OH generation from alkene ozonolysis.

References

Beames, J. M., Liu, F., Lu L., and Lester, M. I.: J. Chem. Phys. 138, 244307, 2013.

Lehman, J. H., Li, H., Beames, J. M., and Lester, M. I.: J. Chem. Phys., 139, 141103, 2013.

Sheps, L., Scully, A.M., and Au, K.: Phys. Chem. Chem. Phys. 16, 26701, 2014.

Smith, M.C., Ting, W-L., Chang, C-H., Takahashi, K., Boering, K.A., and Lin, J. Jr -M.: J. Chem. Phys., 141, 074302, 2014.

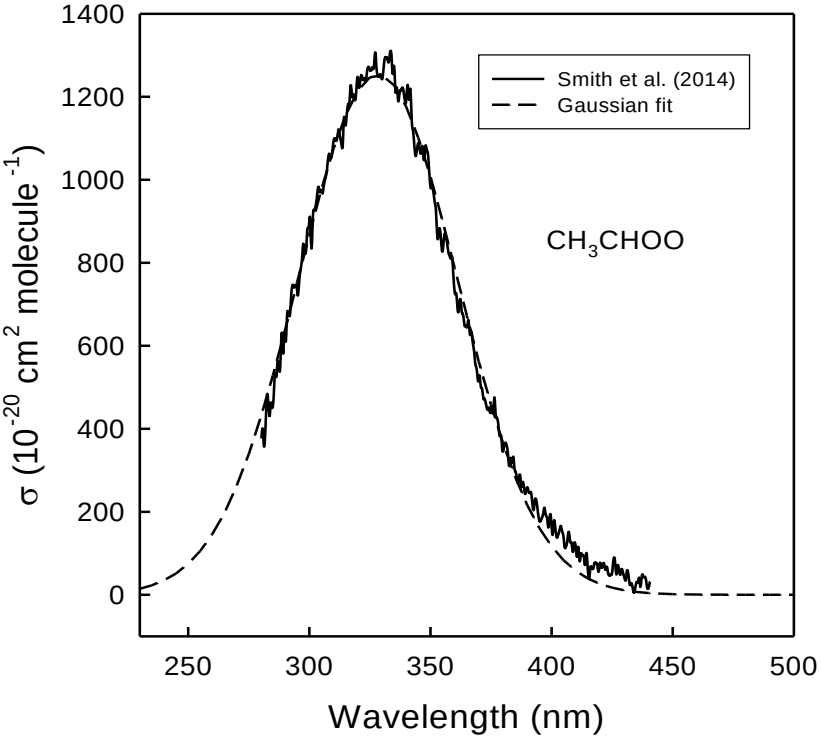

Absorption spectrum of CH_3CHOO, *Z*- and *E*- conformers not resolved; Gaussian fit to experimental data (from Smith et al., 2014) shown as dashed line.

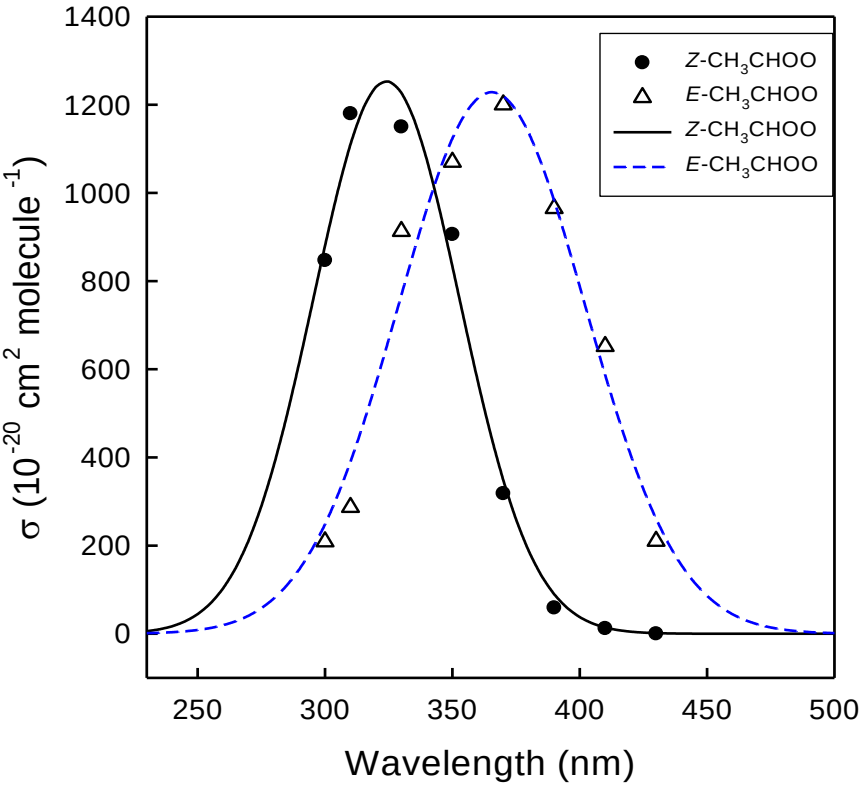

Absorption spectrum of CH_3CHOO, *Z*- and *E*- conformers resolved (shown as circles and triangles, respectively); Gaussian fits to experimental data (from Sheps et al., 2014) shown as dotted lines.

P35: $(CH_3)_2COO + h\nu$

Last evaluated: May 2020; Last change in preferred values: June 2017

$(CH_3)_2COO + h\nu \rightarrow$ products

Primary photochemical transitions

Reaction	
$(CH_3)_2COO + h\upsilon \rightarrow (CH_3)_2CO + O(^3P)$	(1)
$\rightarrow (CH_3)_2CO + O(^1D)$	(2)

Absorption cross-section data

Wavelength range/nm	Reference	Comments
280 – 410	Liu et al., 2014	(a)
280 – 420	Huang et al., 2015	(b)
308 – 352	Chang et al., 2016	(c)
355	Chhantyal-Pun et al., 2017	(d)

Comments

(a) $(CH_3)_2COO$ was prepared by PLP (248 nm) of 2,2-diiodopropane, $(CH_3)_2CI_2$ in O_2/Ar mixtures in a capillary tube. The photoproducts were cooled in a supersonic expansion and passed to a TOF mass spectrometer where they were ionised with VUV radiation at 118 nm. The UV absorption spectrum was determined from depletion of the *m/z* =74 photo-ionisation signal resulting from excitation of the B ← X transition in ground state $(CH_3)_2COO$ molecules by tunable UV radiation (280 – 420 nm) from a Nd-YAG laser. The UV-induced depletion approaches 100% near the peak of the simple Gaussian profile at 320 nm, indicating rapid dynamics in the *B* state, and corresponds to a peak absorption cross section of ~4×10^{-17} cm^2 $molecule^{-1}$; the absolute cross section measurements have an uncertainty on the order of a factor of 2.

(b) $(CH_3)_2COO$ was generated from pulsed photolysis of a flowing gaseous mixture consisting of $(CH_3)_2CI_2$, O_2, and buffer gas (N_2) at 248 nm via the reactions: $(CH_3)_2CI_2 + h\nu \rightarrow (CH_3)_2CI + I$; $(CH_3)_2CI + O_2 \rightarrow (CH_3)_2COO + IO$. Time-resolved difference absorption spectra were recorded and corrected for absorption changes due to precursor and other products (e.g. IO) molecules, leaving a residual absorption attributable to $(CH_3)_2COO$.

(c) The absolute absorption cross sections of $(CH_3)_2COO$ under a jet-cooled condition were measured via laser depletion to be $(1.32 \pm 0.10) \times 10^{-17}$ cm^2 $molecule^{-1}$ at 308 nm and $(9.6 \pm 0.8) \times 10^{-18}$ cm^2 $molecule^{-1}$ at 352 nm. Absolute calibration was achieved using laser beam profiling measurements. Control experiments using CH_2I_2 gave an absorption cross section at 308 nm in good agreement with the well-established literature value. The peak UV cross section of $(CH_3)_2COO$ is estimated to be $(1.75 \pm 0.14) \times 10^{-17}$ cm^2 $molecule^{-1}$ at 330 nm by scaling the UV spectrum of $(CH_3)_2COO$ (Huang et al., 2015; note b) to the absolute cross section at 308 nm.

(d) $(CH_3)_2COO$ was formed by laser photolysis of 2,2-diiodopropane in the presence of O_2 and characterized by synchrotron photoionization mass spectrometry and also by cavity ringdown

ultraviolet absorption spectroscopy. Cavity ringdown measurements of the acetone oxide removal without added reagents display a combination of first- and second-order decay kinetics, which were deconvolved to derive rate coefficients for both unimolecular thermal decay, k_{dec}.(see CGI_14), and the self-reaction of $(CH_3)_2COO$. The loss of $(CH_3)_2CI_2$ following photodissociation was used to calibrate the initial $(CH_3)_2COO$ concentration and determine σ (355nm) = (1.45 ± 0.24) × 10^{-17} cm^2 $molecule^{-1}$ and the $(CH_3)_2COO$ self-reaction rate coefficient, k = (6.0 ± 1.1) × 10^{-10} cm^3 $molecule^{-1}$ s^{-1}.

Preferred Values

Absorption cross-sections at 298 K

λ/nm	10^{20} σ/(cm^2 $molecule^{-1}$)	λ/nm	10^{20} σ/(cm^2 $molecule^{-1}$)
280	279	345	1355
285	403	350	1146
290	560	355	929
295	747	360	723
300	955	365	540
305	1171	370	387
310	1379	375	266
315	1557	380	175
320	1687	385	111
325	1754	390	67
330	1750	395	39
335	1675	400	22
340	1538	405	12

σ = (1.75 ± 0.53) × 10^{-17} cm^2 $molecule^{-1}$ at λ_{max} (330 nm);

Gaussian fit parameters to extracted data from the absorption spectrum for the range 280 - 390 nm reported by Chang et al. (2016): $\sigma(\lambda) = 1747 \times 10^{-20} \exp(-0.5 \times ((\lambda - 327.2)/24.58)^2)$

Quantum Yields

ϕ_1 = 1.0 for 280 < λ < 380 nm.

Comments on Preferred Values

The first UV absorption spectrum of $(CH_3)_2COO$ was reported by Liu et al. (2014), using UV photo-dissociation action technique. The results show a Gaussian band peaking at 330 nm with no resolved structure, which is attributed to the $\tilde{B}$ (1A′) ← $\tilde{X}$(1A′) electronic transition. Huang et al. (2015) used conventional absorption spectroscopy and reported a spectrum for $(CH_3)_2COO$ slightly broader than the jet-cooled spectrum reported by Liu et al. (2014). The contribution of hot bands in the room-temperature spectrum would cause broadening in comparison with the low-temperature spectrum of Liu et al. (2014). The results from the UV action spectra of several Criegee intermediates reported by the University of Pennsylvania group (e.g. CH_2OO and CH_3CHOO, Beames et al., 2012; 2013) differ substantially from spectra recorded subsequently using conventional absorption spectroscopy (e.g. Sheps, 2013; Ting et al, 2014; Smith et al., 2014). The

absorption bands determined using photo-dissociation action spectroscopy by the University of Pennsylvania group are narrower, peak at a shorter wavelength, and the cross sections are up to a factor of 4 higher than those measured using absorption spectroscopy (Sheps et al., 2013; Smith et al., 2014).

Causes for this discrepancy remain unclear, as discussed in Ting et al. (2014) and Chang et al. (2016). The latter study included control experiments which reproduced the well-established absorption cross section for CH_2I_2 at 308 nm. The weight of evidence favours the spectral shape and cross-sections determined by UV absorption and the recommended $(CH_3)_2COO$ spectrum is based upon the work of Huang et al. (2015) and Chang et al. (2016). The figure below shows the experimental values reported by Chang et al. (2014) and a Gaussian fit to those data. The cross-sections listed in the table of preferred values are obtained from the Gaussian fit to the experimental data and are estimated to have an uncertainty of ± 30 %. The photodissociation quantum yields are likely to be close to unity. Hydroxyl radicals produced concurrently with the generation of the Criegee intermediates were measured in the experiments of Liu et al. (2013), where they were detected by 1+1′ resonance enhanced multiphoton ionization. The HO yield observed with CH_3CHOO is 6-fold larger than that from CH_2OO, consistent with prior studies of HO generation from alkene ozonolysis (Kroll et al., 2002).

References

Beames, J. M., Liu, Fang Lu, Lu Lu, and Lester, M. I.: J. Amer. Chem. Soc., 134, 20045, 2012.

Beames, J. M., Liu, Fang Lu, Lu Lu, and Lester, M. I.: J. Chem. Phys. 138, 244307, 2013.

Chang, Y; Chang, C-H., Takahashi, K, Lin, J. J-M.: Chem. Phys. Lett., 653, 155, 2016.

Chhantyal-Pun, R., Welz, O., Savee J. D., Eskola, A. J., Lee, E. P. F., Blacker, L., Hill, H. R., Ashcroft, M., Khan, M. A. H., Lloyd-Jones, G. C., Evans, L., Rotavera, B., Rotavera H., Osborn, D. L., Mok, D. K. W., Dyke, J. M., Shallcross, D. E., Percival, C. J., Orr-Ewing, A. J., and Taatjes, C. A.: J. Phys. Chem. A, 121, 4, 2017.

Huang, H.-L., Chao, W., and Lin, J. J.-M.: Proc. Nat. Acad. Sci., 112, 10857, 2015.

Kroll, J. H., Donahue, N.M., Cee, V.J., Demerjian, K.L., and Anderson, J.G.: J. Am. Chem. Soc., 124, 8518, 2002.

Lehman, J. H., Li, H., Beames, J. M., and Lester, M. I.: J. Chem. Phys., 139, 141103, 2013

Liu, F., Beames, J. M., Green, A. M. and Lester, M. I.: J. Phys. Chem. A, 118, 2298, 2014.

Sheps, L.: J. Phys. Chem. Lett., 4, 4201, 2013.

Sheps, L., Scully, A.M. and Au, K.: Phys. Chem. Chem. Phys., 16, 26701, 2014.

Smith, M.C., Ting, W-L, Chang, C-H., Takahashi, K., Boering, K.A., and Lin, J. Jr -M.: J. Chem. Phys., 141, 074302, 2014.

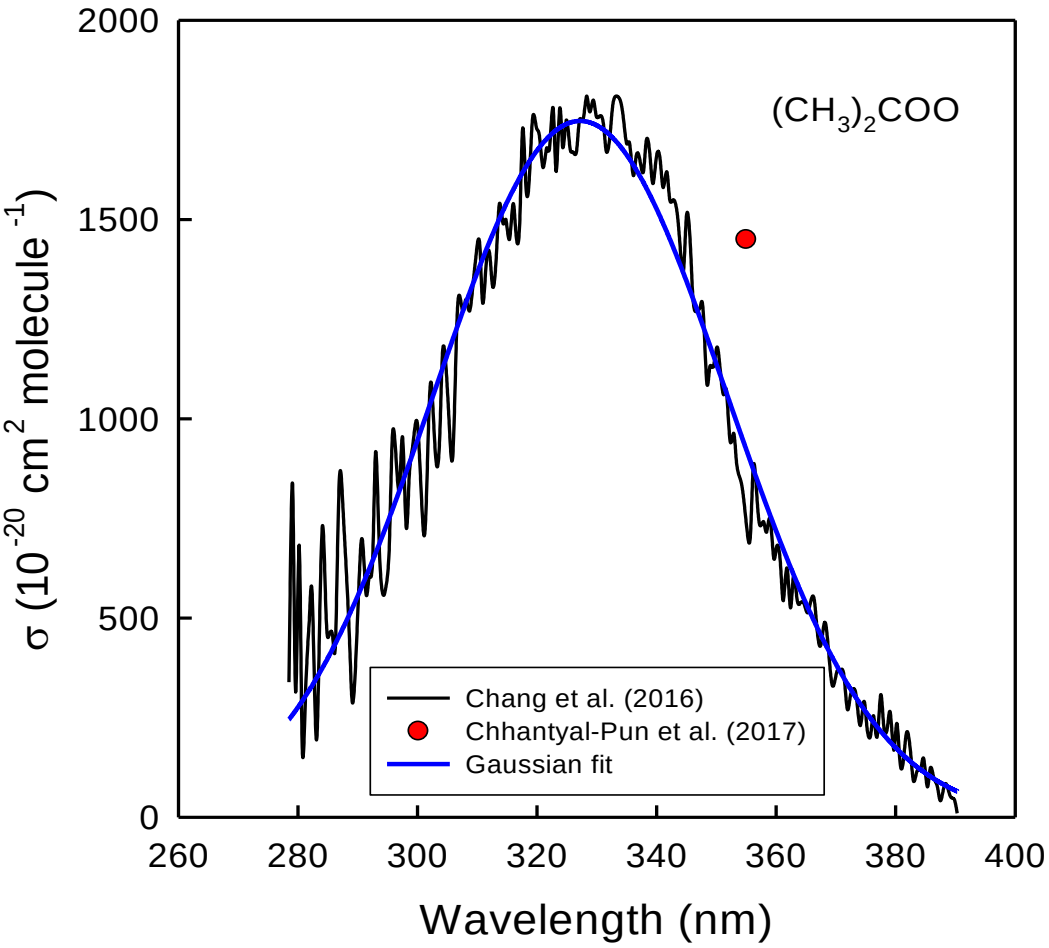

Absorption spectrum of $(CH_3)_2COO$; full line is Gaussian fit to experimental data (filled circles) from Chang et al. (2016). Gaussian fit parameters to data for $(CH_3)_2COO$: $\sigma(\lambda) = 1747 \times 10^{-20} \exp(-0.5 \times ((\lambda - 327.2)/24.58)^2)$

P36: CH_3CH_2CHOO (*Z*- and *E*-) + hν

Last evaluated: May 2020; Last change in preferred values: May 2020

CH_3CH_2CHOO (*Z*- and *E*-) + hν → products

Primary photochemical transitions

Reaction	
$CH_3CH_2COO + h\upsilon \rightarrow CH_3CH_2CO + O(^3P)$	(1)
$\rightarrow CH_3CH_2CO + O(^1D)$	(2)

Absorption cross-section data

Wavelength range/nm	Reference	Comments
280-410	Liu et al., 2014	(a)

Comments

(a) CH_3CH_2CHOO was prepared by PLP (248 nm) of $CH_3CH_2CHI_2$ in O_2/Ar mixtures in a capillary tube. The photoproducts were cooled in a supersonic expansion and passed to a TOF mass spectrometer where they were ionised with VUV radiation at 118 nm. The UV absorption spectrum was determined from depletion of the *m/z* =74 photo-ionisation signal resulting from excitation of the B ← X transition in ground state CH_3CH_2CHOO molecules by tunable UV radiation (280 – 420 nm) from a Nd-YAG laser. The UV-induced depletion approaches 100% near the peak of the simple Gaussian profile at 325 nm, indicating rapid dynamics in the *B* state, and corresponds to a peak absorption cross section of ~3.5×10^{-17} cm^2 $molecule^{-1}$. The absolute cross section measurements have an uncertainty on the order of a factor of 2. The electronic spectrum for CH_3CH_2CHOO is similar to that reported for CH_3CHOO.

Preferred Values

Absorption cross-sections at 298 K relative to value at 320 nm

λ/nm	σ/σ_{320nm}	λ/nm	σ/σ_{320nm}
280	0.145	345	0.548
285	0.224	350	0.411
290	0.328	355	0.292
295	0.454	360	0.196
300	0.594	365	0.124
305	0.735	370	0.075
310	0.862	375	0.043
315	0.954	380	0.023
320	1.000	385	0.012
325	0.991	390	0.006
330	0.929	395	0.003
335	0.824	400	0.001
340	0.691		

Quantum Yields

$\phi_1 = 1.0$ for $280 < \lambda < 380$ nm.

Comments on Preferred Values

The only reported study of the UV absorption spectrum of CH_3CH_2CHOO was obtained by Liu et al. (2014) using the UV photo-dissociation action spectrum technique. CH_3CH_2CHOO can exist in two (stable) conformers, *Z*- and *E*-. The *Z*- form is lower in energy and is expected to be prevalent from the source chemistry employed.

The results show a Gaussian band peaking at 322 nm with no resolved structure, which is attributed to the $\tilde{B}\ (1A') \leftarrow \tilde{X}(1A')$ electronic transition in CH_3CH_2CHOO. No results have been reported for CH_3CH_2CHOO using conventional absorption spectroscopy. The results from the UV action spectra of Criegee intermediates reported by the University of Pennsylvania group (e.g. CH_2OO, CH_3CHOO, and $(CH_3)_2COO$, Beames et al, 2012; 2013 and Liu et al., 2014) are 2-4 times more intense than spectra recorded using conventional absorption spectroscopy (e.g. Sheps, 2013; Sheps et al., 2013; Ting et al, 2014; Smith et al., 2014) and the IUPAC recommendations. Causes for this discrepancy remain unclear, as discussed in Ting et al. (2014) and Chang et al. (2016). The maximum absorption for CH_3CH_2CHOO reported by Liu et al. (2014) of $\sigma_{322nm} \sim 3.5 \times 10^{-17}$ cm^2 molecule^{-1} is approximately a factor of 3 larger than the IUPAC recommended peak absorption for CH_3CHOO. However, theoretical work indicates that elongation of the alkyl radical in RCHOO Criegee intermediates should not lead to substantial changes in the peak wavelength or intensity of their UV spectra (Yin and Takahashi, 2018).

It is likely that there were errors in the calibration procedures and the absorption cross sections reported by Liu et al. (2014) for CH_3CH_2CHOO are approximately a factor of 2-4 too high. The shape of the spectrum is deemed reliable. The relative cross-sections recommended in the table above were obtained from a Gaussian fit to the experimental data for the range 285 - 366 nm extracted from Figure 3 of the paper by Liu et al. (2014) which gives $\sigma(\lambda) = 3500 \times 10^{-20} \exp(-0.5 \times ((\lambda - 321.7)/21.2)^2)$.

The photodissociation quantum yields are likely to be close to unity. Hydroxyl radicals, produced concurrently with the generation of the Criegee intermediates, were measured in the experiments of Liu et al, (2014), where they were detected by 1+1′ resonance enhanced multiphoton ionization. The HO yield observed with CH_3CH_2CHOO is 10-fold larger than that from CH_2OO, and is greater than from prior studies of OH generation from ozonolysis of E-3-hexene (Kroll et al, 2002).

References

Beames, J. M., Liu, F. L., Lu L., and Lester, M.I.: J. Chem. Phys. 138, 244307, 2013.

Kroll, J. H., Donahue, N.M., Cee, V.J., Demerjian, K.L., and Anderson, J.G.: J. Am. Chem. Soc., 124, 8518, 2002.

Lehman, J. H., Li, H., Beames, J. M., and Lester, M. I.: J. Chem. Phys., 139, 141103, 2013.

Liu, F., Beames, J. M., Green, A. M., and Lester, M.I., J. Phys. Chem. A, 118, 2298, 2014.

Sheps, L., J. Phys. Chem. Lett., 4, 4201, 2013.

Sheps, L., Scully, A.M. and Au, K., Phys. Chem. Chem. Phys.: 16, 26701, 2014.

Smith, M.C., Ting, W-L, Chang, C-H., Takahashi, K., Boering, K.A., and Lin, J. Jr -M.: J. Chem. Phys., 141, 074302, 2014.

Ting, W-L, Chen, Y-H., Chao, W., Smith, M.C., and Lin, J. Jr -M.: Phys. Chem. Chem. Phys., 16, 10438, 2014.

Yin, C., Takahashi, K.: Phys. Chem. Chem. Phys., 20, 16247, 2018

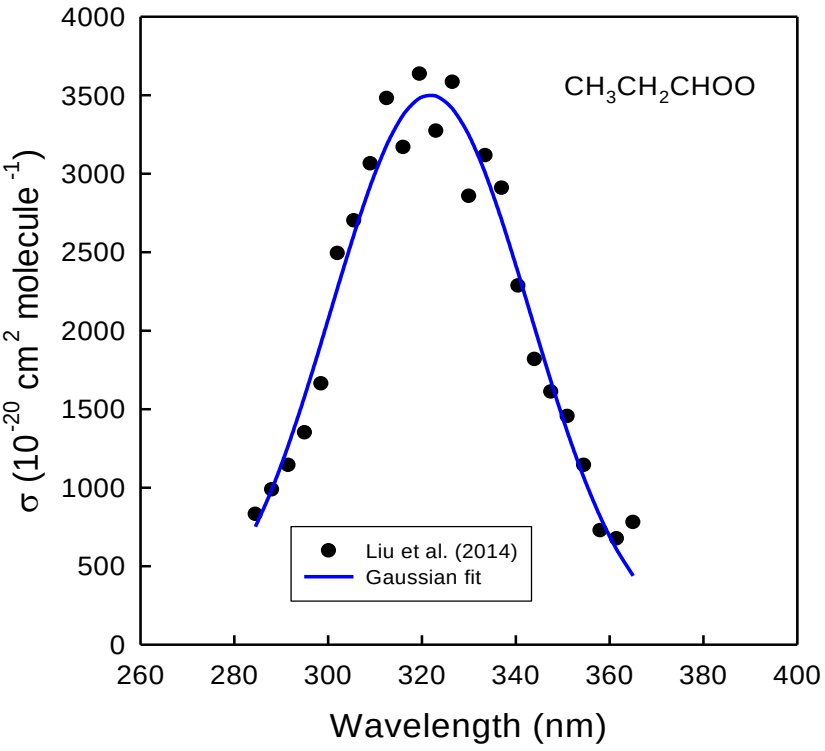

Absorption spectrum of CH_3CH_2CHOO, *Z*- and *E*- conformers not resolved, from Liu et al. (2014) with Gaussian fit.

P38: $(CH=CH_2)(CH_3)COO$ (*Z*- and *E*-) + hν

Last evaluated: May 2020; Last change in preferred values: May 2020

$(CH=CH_2)(CH_3)COO$ (*Z*- and *E*-) + hν → products

Primary photochemical transitions

Reaction
$(CH=CH_2)(CH_3)COO + h\upsilon \rightarrow (CH_2=CH)(CH_3)COO + O(^3P)$ (1)
$\rightarrow (CH_2=CH)(CH_3)COO + O(^1D)$ (2)

Absorption cross-section data

Wavelength range/nm	Reference	Comments
305-480	Vansco et al., 2018	(a)

Comments

(a) Methyl vinyl ketone oxide, $(CH=CH_2)(CH_3)COO$, was prepared by PLP (248 nm) of (*Z*-/*E*)-1,3-diiodobut-2-ene in O_2/Ar mixtures in a capillary tube. The photoproducts were cooled in a supersonic expansion and passed to a TOF mass spectrometer, where they were ionised with VUV radiation at 118 nm. The UV absorption spectrum was determined from depletion of the *m/z* = 86 photo-ionisation signal resulting from excitation of the $\Pi^* \leftarrow \Pi$ transition of ground state $(CH=CH_2)(CH_3)COO$ molecules by tunable UV radiation (305 – 480 nm). The UV-induced depletion increased linearly with UV power and a peak absorption cross section at 388 nm of the order of 10^{-17} cm^2 molecule^{-1} was estimated.

Preferred Values

Absorption cross-sections at 298 K relative to value at 388 nm

λ/nm	σ/σ_{388nm}	λ/nm	σ/σ_{388nm}
310	0.230	390	0.977
320	0.308	400	0.722
330	0.380	410	0.528
340	0.454	420	0.349
350	0.525	430	0.219
360	0.578	440	0.122
370	0.655	450	0.059
380	0.816		
388	1.000		

Quantum Yields

ϕ_1 = 1.0 for 305 < λ <430 nm.

Comments on Preferred Values

The only reported study of UV absorption spectrum of the methyl vinyl ketone oxide Criegee intermediate, $(CH=CH_2)(CH_3)COO$, was obtained by Vansco et al. (2018). The UV photo-dissociation action spectrum technique was used to record the spectrum of a mixture of the four conformers of $(CH=CH_2)(CH_3)COO$ (i.e. two rotamers of each of *Z*- and *E*-$(CH=CH_2)(CH_3)COO$). The spectrum in the range 305-425 nm was broad and unstructured with a maximum at 388 nm which was roughly estimated to be of the order of 10^{-17} cm^2 $molecule^{-1}$. In light of the rough estimate, no recommendation is given for the absolute absorption cross sections but the shape of the spectrum is indicated in the table above. Absorption at λ < 430 nm leads to rapid dissociation to methyl vinyl ketone and $O(^1D)$ which were detected using 2 + 1 REMPI. The photodissociation quantum yields are likely to be close to unity.

References

Vansco, M. F., Marchetti, B. and Lester, M. I.: J. Chem. Phys., 149, 244309, 2018.

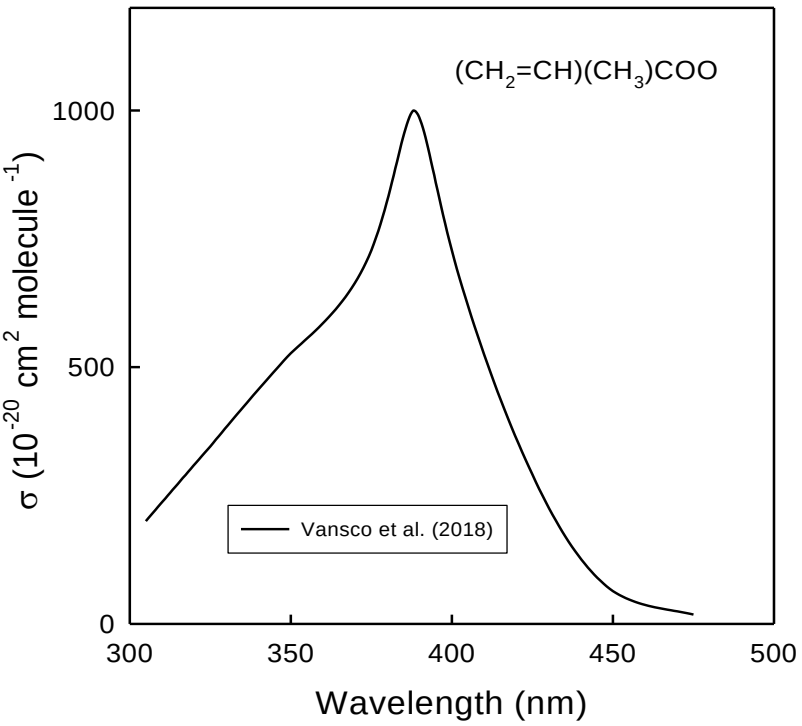

Absorption spectrum of $(CH_2=CH)(CH_3)COO$, *Z*- and *E*- conformers not resolved, from Figure 6 in Vansco et al. (2018).

P39: $(C(CH_3)=CH_2)CHOO$ (*Z*- and *E*-) + hν

Last evaluated: May 2020; Last change in preferred values: May 2020

$(C(CH_3)=CH_2)CHOO$ (*Z*- and *E*-) + hν → products

Primary photochemical transitions

Reaction	
$(C(CH_3)=CH_2)CHOO + h\upsilon$	$\rightarrow CH_2=C(CH_3)CHO + O(^3P)$ (1)
	$\rightarrow CH_2=C(CH_3)CHO + O(^1D)$ (2)

Absorption cross-section data

Wavelength range/nm	Reference	Comments
315-500	Vansco et al., 2019	(a)

Comments

(a) Methacrolein oxide, $(C(CH_3)=CH_2)CHOO$, was prepared by PLP (248 nm) of (*Z*-/*E*)-1,3-diiodobut-2-ene in O_2/Ar mixtures in a capillary tube. The photoproducts were cooled in a supersonic expansion and passed to a TOF mass spectrometer where they were ionised with VUV radiation at 118 nm. The UV absorption spectrum was determined from depletion of the *m/z* = 86 photo-ionisation signal resulting from excitation of the $\Pi^* \leftarrow \Pi$ transition of ground state $(C(CH_3)=CH_2)CHOO$ molecules by tunable UV radiation (305 – 480 nm). The UV-induced depletion increased linearly with UV power and an absorption cross section at 380 nm of approximately 3×10^{-18} cm^2 molecule^{-1} was estimated.

Preferred Values

Absorption cross-sections at 298 K relative to value at 380 nm

λ/nm	σ/σ_{380nm}	λ/nm	σ/σ_{380nm}
320	0.886	410	0.823
330	0.850	420	0.759
340	0.749	430	0.672
350	0.749	440	0.471
360	0.886	450	0.466
370	0.938	460	0.270
380	1.000	470	0.249
390	0.957	480	0.170
400	0.883	490	0.098

Quantum Yields

ϕ_1 = 1.0 for 315 < λ <500 nm.

Comments on Preferred Values

The only reported study of UV absorption spectrum of the methacrolein oxide Criegee intermediate, ($C(CH_3)=CH_2$)CHOO, was obtained by Vansco et al. (2019). The UV photodissociation action spectrum technique was used to record the spectrum of a mixture of the four conformers of ($C(CH_3)=CH_2$)CHOO (i.e. two rotamers of each of *Z*- and *E*-($C(CH_3)=CH_2$)CHOO). The spectrum in the range 315-500 nm was broad with structured at wavelengths > 400 nm with a maximum at 380 nm which was estimated to be approximately 3×10^{-18} cm^2 $molecule^{-1}$. In light of the rough estimate no recommendation is given for the absolute absorption cross sections, but the shape of the spectrum is indicated in the table above. Absorption at λ < 500 nm leads to rapid dissociation to methacrolein and $O(^1D)$ atoms which were detected using 2 + 1 REMPI. The photodissociation quantum yields are likely to be close to unity.

References

Vansco, M. F., Marchetti, B., Trongsiriwat, N., Bhagde, T., Wang, G., Walsh, P. J., Klippenstein, S. J. and Lester, M. I.: J. Am. Chem. Soc., 141, 15058, 2019.

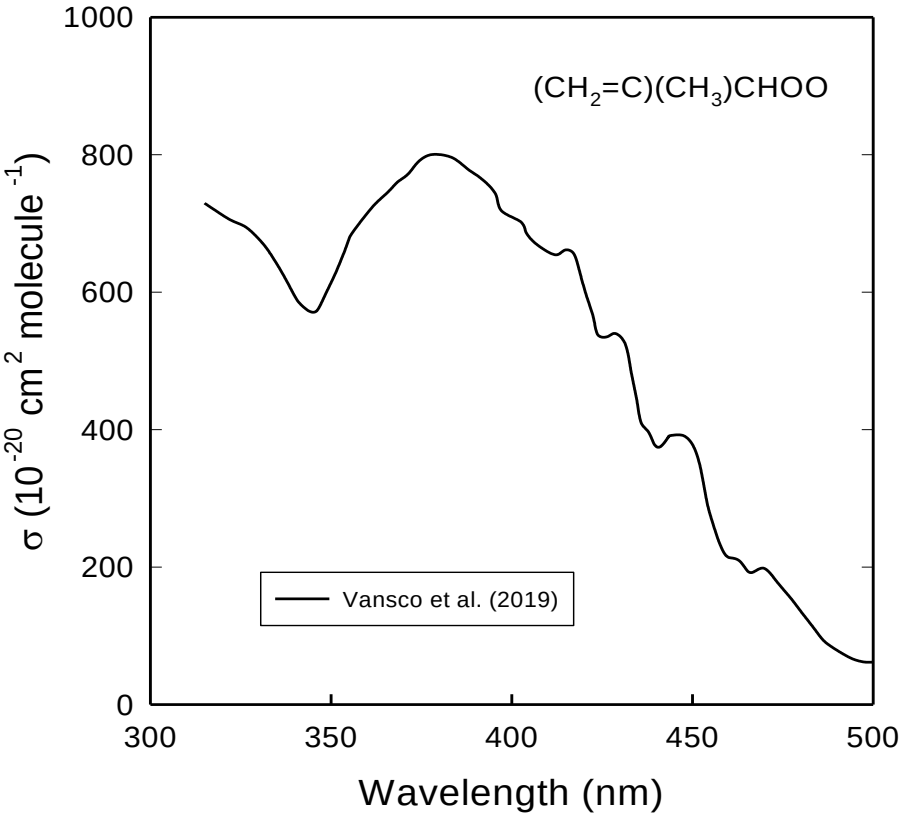

Absorption spectrum of ($C(CH_3)=CH_2$)CHOO, *Z*- and *E*- conformers not resolved, from Figure 4 in Vansco et al. (2019).

B6. Abbreviations used in data sheets

A – absorption

AS – absorption spectroscopy

CCD – charge coupled detector

CIMS – chemical ionization mass spectroscopy/spectrometry

CL – chemiluminescence

CRDS – cavity ring-down spectroscopy

DF – discharge flow

EPR – electron paramagnetic resonance

F – flow system

FP – flash photolysis

FTIR – Fourier transform infrared

FTS – Fourier transform spectroscopy

GC – gas chromatography/gas chromatographic

HPLC – high-performance liquid chromatography

IR – infrared

LIF – laser induced fluorescence

LMR – laser magnetic resonance

LP – laser photolysis

MM – molecular modulation

MS – mass spectrometry/mass spectrometric

P – steady state photolysis

PLP – pulsed laser photolysis

PR – pulse radiolysis

RA – resonance absorption

RF – resonance fluorescence

RR – relative rate

S – static system

TDLS – tunable diode laser spectroscopy

UV – ultraviolet

UVA – ultraviolet absorption

VUVA – vacuum ultraviolet absorption